HEAT SHOCK RESPONSE INHIBITION AND GENE EXPRESSION IN *XENOPUS LAEVIS* CULTURED CELLS

by

Laurie A. Manwell

A thesis
presented to the University of Waterloo
in fulfillment of the
thesis requirement for the degree of
Master in Science
in
Biology

Waterloo, Ontario, Canada, 2006

AUTHOR'S DECLARATION FOR ELECTRONIC SUBMISSON OF A THESIS

I hereby declare that I am the sole author of this thesis. This is a true copy of the thesis, including any required final revisions, as accepted by my examiners.

I understand that my thesis may be made electronically available to the public.

Abstract

Various genes have evolved to protect the cell against stressor-induced damage or death including the heat shock proteins (HSPs). Stressor-induced HSP gene expression involves the activation of heat shock factor (HSF), which binds to the heat shock element (HSE) found in the promoter region of *hsp* genes. Previously, our laboratory has examined the expression and function of *hsp* genes in the South African clawed frog, *Xenopus laevis*. Amphibians are particularly susceptible to adverse environmental conditions, including high temperatures and toxicants. In contrast to the many known inducers of HSF activation in poikilothermic vertebrates, few inhibitors have been either discovered or described in the literature. The present study has compared for the first time the effect of two heat shock response (HSR) inhibitors, quercetin and KNK437, on *hsp* gene expression in *Xenopus* A6 cells, demonstrating their efficacy in poikilotherms. Northern blot and densitometric analysis showed that cells treated with either quercetin or KNK437 decreased the heat shock-induced accumulation of *hsp70, hsp47,* and *hsp30* mRNAs. Additionally, constitutive levels of *hsp47* and *hsc70* mRNAs were reduced. In comparison, neither quercetin nor KNK437 affected the levels of constitutively expressed *ef1α* mRNAs under control or heat shock conditions. Western blot and densitometric analysis in this study showed that under heat shock conditions, exposure to quercetin or KNK437 significantly decreased the accumulation of HSP30, and that KNK437 was more effective in doing so than quercetin. In comparison, levels of actin were not significantly affected by either heat shock or exposure to DMSO, quercetin, or KNK437.

These findings suggest that one mechanism by which quercetin and KNK437 inhibits the HSR in *Xenopus* is through the inhibition of HSF activity.

Results of this study also suggest that KNK437 inhibits the acquisition of thermotolerance in poikilotherms, similar to observations in mammalian systems. In the presence of KNK437, cells given a 2 h heat pretreatment at 33ºC followed by a thermal challenge for 1 h at 37ºC, showed numerous ruffled membrane edges and some aggregates of disrupted stress fibers. In comparison, cells directly challenged for 1 h at 37ºC, showed a marked decrease in HSP30, which was located predominantly at the cellular periphery in conjunction with actin aggregates. These cells showed virtually no intact stress fibers spanning cells and no coherent cell-cell connections. A 3-D analysis of cells given a 1 h thermal challenge at 37ºC (after a prior 2 h heat shock at 33ºC) in the absence of KNK437, showed numerous linear actin bundles transversing the entire cell, even extending into areas of cell-cell contact, and abundant HSP30 concentrated in the perinuclear region surrounding an intact nucleus. However, in the presence of KNK437, there was a significant emergence of membrane ruffles indicating global instability of cellular adhesion. This study has demonstrated that KNK437, which is the more specific and efficient HSR inhibitor, will be an important inhibitor to compare with the well-documented quercetin for future investigations.

Acknowledgements

My thanks must begin with God - everyone could have such an amazing Teacher and loving Father if they so desired. *God loves to have us tug on His skirt,* which is a good thing, because the unanswerably curious child in me must do so each and every day! And He carried me when I needed it most – I've seen His footseps in the sand. Of course, thank you to Dr. John Heikkila for supervising me for the past three + years, of which I'm sure I was a pain-in-the-ass! Thanks for hanging in there John, I finally finished, just like you said I would. Many wonderful thanks to Drs. Bernie Duncker and Mungo Marsden for your valuable insights and unfailing encouragement, especially in pursuring my dream to go to CSHL to study the latest in molecular biotechnology with some of the top experts in the world. I now have the confidence to go after any research goals! Thank you to Julie Gauley also, for if it wasn't for her unflinching determination to figure things out and head off in directions such as CSHL, I never would have known what possibilities to even envison for my career. *I love you, man!* (Sorry, you know I'm terribly sentimental, and thanks for putting up with it all this time!) Thank you to my labmates and dear friends Nikos Hontzeas, Jen (Stearns) Czarny, Anne Mulligan Tuttle, and Angelo Kaldis. Don't worry, I won't tell anyone what went on in the lab 'after hours.' Hell, who would believe us anyway? I owe my family a great debt of gratitude for all of their support – and continual nagging to finish my MSc before my kids started university! My husband Derek, Mom, Dad, and Cara I love you and couldn't have done it without you! To my daughters, Jallaina (Jello) and Sarryvannah (Mouse), thank you for hanging out in mom's lab when I did my crazy experiments, you were great company, asking a million questions, taking care of the froggies, and sneaking candy from my desk!

How Things Change

I used to want brilliant sunshine for all of time.

I used to want sandy beaches with boundless shores.

I used to want winds of romance to carry me away.

I used to want to wander at the whim of a heart's desire.

I used to want to be surrounded by visions of beauty and wealth.

I used to want to hear music only the heavens could acclaim.

I used to want endless joy to befall my family.

I used to want my youth to forever flow…

How things change…

Now I pray for the night to fall upon me.

Now I search for the gutters that lay beyond the beach.

Now I dance in the storms of love.

Now I follow the path of responsibility that leads me home.

Now I look for grace in even the poorest of souls.

Now I know that even the most cherished sounds of love can be silent.

Now I embrace the pain and sorrow that all humanity must bear.

Now I create so that my youth will end…

How things change…

I used to want Paradise,

Now I choose Life.

Laurie A. Manwell

For Sifu Bob Schneider, my Kung Fu Father

1951 – 2006

TABLE OF CONTENTS

LIST OF TABLES

LIST OF FIGURES

1. Introduction

1.1. Cellular Stress Response and Inducible Gene Expression

Various genes have evolved to protect the cell against stressor-induced damage or death, such as those regulating the synthesis of specific proteins required to restore homeostasis. Although heat shock proteins (HSPs) may also be expressed constitutively, they are selectively synthesized in response to almost any stress capable of damaging or denaturing cellular proteins, such as heat or other physiological stresses (Laing and MacCrae, 1997). Induction of the stress response can be environmental (i.e., temperature changes, exposure to heavy metals, ethanol, etc…), pathophysiological (i.e., aging, fever and inflammation due to viral and bacterial infection), or can occur under non-stressful conditions (i.e., cell cycle changes, differentiation, presence of oncogenes) (for reviews, see Macario and Conway de Macario, 2005; Nicholl *et al*., 2006).

Heat shock proteins are essential to cell survival and maintain the integrity of cellular components, often acting as molecular chaperones (Ohtsuka *et al*., 2005). For example, HSPs are involved in protein synthesis and repair, help stabilize unfolded or partially folded target proteins, can prevent misfolding, aggregation, and/or degradation of proteins, and are involved in protein trafficking and transport. HSP induction can confer both thermotolerance to repeated heat stress and cross-tolerance to subsequent stressors (e.g., prior exposure to heat shock can protect against later exposure to chemical agents). In eukaryotes, the heat shock response is mediated by the activation of a preexisting pool of heat shock transcription factors (HSFs) that bind to heat shock elements (HSEs) located in the promoter region of all HSP genes (reviewed in Ohtsuka *et al*., 2005; Macario and Conway de Macario, 2005). HSPs related by sequence are

grouped into families based upon their molecular sizes (in kilodaltons (kDa): the small heat shock proteins (sHSPs) (10-30 kDa) and the higher molecular weight HSP families, HSP40, HSP60, HSP70, HSP90, and HSP100. The different roles of various HSPs are listed in Table 1.

1.2. Heat Shock Protein Gene Regulation

The heat shock response is regulated at several levels, including transcription, mRNA stability, and translational efficiency (Katschinski, 2004). Transcriptional regulation of heat shock protein genes is governed by activation of the HSF-HSE complex. Both the structure and function of HSEs have been highly conserved through evolution and are extraordinarily similar between organisms, from yeast to man. HSEs consist of inverted repeats of the 5 bp motif 5'-nGAAn- 3'. Binding of an HSF molecule requires a minimum of three 5 bp modules (nGAAnnTTCnnGAAn) and HSF binds to inverted repeats in both tail-to tail (← →→) and head-to-head (→ ←←) configurations with equal affinity (reviewed by Lis, 1991). HSFs bind to HSEs cooperatively to facilitate the formation of complexes, thereby increasing affinity and half-life stability. For example, a HSE motif with two trimeric binding sites (six 5 bp units) binds HSF tightly, increasing its half-life to greater than 48 hrs (Xiao *et al*., 1991). HSF DNA-binding activity is induced *in vitro* by many agents that affect the conformation of proteins, such as hydrogen ions, nonionic detergents, urea, and HSF antibodies (Mosser *et al.,* 1990; Zimarino *et al*., 1990). Various other agents that can induce HSF binding to HSE include sodium arsenite, sodium salicylate, dinitrophenol, cadmium, and azetidine (Mosser *et al*., 1988), as well as Ca^{++}, Mn^{++}, and La^{++} (Mosser *et al*., 1990).

Table 1. Conserved HSP Families

HSP Family	Eukaryotes (Prokaryotes)	Function
Small heat shock proteins (sHSPs) (10-30 kDa)	HSP10 (GroES) HSP25 HSP27 HSP30	- co-chaperonin function (HSP10 with HSP60) - suppress aggregation and heat inactivation of proteins - protection of actin filament polymerization upon heat shock
HSP40	HSP40 (DnaJ)	- aids regulation of ATPase activity of HSP70
HSP60 Chaperonin ring family	HSP60 (GroEL)	- mediates the folding of nonnative proteins to native state - can dissolve some protein aggregates - restricted to eubacteria, mitochondria, and chloroplasts
HSP70	HSP70 (DnaK) BiP (GrpE)	- maintain proteins in unfolded and relatively extended conformation by binding to short hydrophobic regions of 6-9 aa - role in negative regulation of HSF activity - folding and assembly of new proteins in the endoplasmic reticulum
HSP90	HSP90 (HtpG)	- role in both stress and nonstress conditions - acts in a developmental or regulatory manner on specific protein targets
HSP100	HSP110 HSP104 [yeast] (ClpB)	- specialized chaperones promoting survival under extreme stress conditions - mediates protein disaggregation after stress

Although yeast & *Drosophila melanogaster* have a single copy of the HSF gene, higher eukaryotes often possess multiple copies (Wu, 1995). The HSF gene family of higher eukaryotes includes HSF1, HSF2, HSF3, and HSF4, which are differentially activated in response to cellular stresses (for review see Morimoto *et al*., 1994). In mammalian species, three HSF family members have been identified, HSF1, HSF2, and HSF4 (Nakai *et al*., 1997; Sarge *et al*., 1991), and in avian species, HSF3 (Inouye *et al*., 2003; Shabtay and Arad, 2006). HSF1, the vertebrate homologue to the single HSF found in lower eukaryotes (such as the yeast and the fly), is activated by heat and other physiological stresses (Holbrook and Udelsman, 1994). HSF2 is activated during embryogenesis, spermatogenesis, and erythroid differentiation. Although similar to the negative regulation of HSF1 and HSF2, HSF3 activation is delayed in a cell-type-dependent manner (Morimoto *et al*., 1994). HSF3 activity has been shown to occur in the absence of stress upon binding to the *c-myb* proto-oncogene product (c-Myb) (Zhu and Mivechi, 1999; Tanikawa et al., 2001). HSF4 is thought to function in the negative regulation of DNA-binding activity of other HSFs (Zhu and Mivechi, 1999). In lower eukaryotes, such as budding yeast, HSFs are found bound to DNA as trimers under both stress and nonstress conditions.

There are two highly conserved regions of HSFs, an amino-terminal DNA-binding domain (~100 aa), and an adjacent trimerization domain with 3 hydrophobic heptad repeats acting as leucine zippers (see Figure 1). In higher eukaryotes, a fourth zipper located near the carboxy-terminus is often observed and is believed to interact with the most amino-terminal leucine zipper, possibly preventing trimerization under non-stress conditions. In *Xenopus laevis*, the isolated cDNA encoding HSF1 (XHSF1)

has additional regions of homology with human HSF1 outside of the DNA binding and trimerization domain, such as the C-terminal hydrophobic domain (Stump *et al*., 1995). Recently, Hilgarth and colleagues (2004) identified a *Xenopus* HSF2 homologue to the transcription factor expressed in humans, chicken, and mouse (Sarge *et al*., 1991; Schuetz *et al.,* 1991; Nakai and Morimoto, 1993). *Xenopus* HSF2 shares the same 3 regions of homology with HSF2 sequences of other species and the sequence previously identified in XHSF1 (Hilgarth *et al*., 2004).

1.3. Heat Shock Factor Activation

Although there are conflicting reports on the localization of HSF1 prior to heat stress, arguing as to whether it is primarily cytoplasmic or nuclear, HSF1 is a nuclear protein prior to and following heat stress in *Drosophila* (Westwood *et al*., 1991; Wu *et al*., 1994; Orosz *et al*., 1996), mammalian cells (Wu *et al*., 1994; Martinez-Balbas *et al.,* 1995), and *Xenopus* (Mercier *et al.*, 1997). HSF1 is regulated mainly at the level of oligomerization and DNA binding, although further posttranslational modifications may be necessary for complete activation of the stress response (Larson *et al.,* 1988). HSPs also play an important role in the negative regulation of HSF1 activity. For example, it is believed that molecular chaperones, such as members of the HSP70 and HSP90 families, exist in complexes with HSF monomers, maintaining its non-DNA-binding state (for review see Morimoto *et al*., 1994; Hu and Mivechi, 2003). It is proposed that during heat shock, as levels of unfolded proteins increase, HSP70 is sequestered away from HSF1, allowing for HSF trimerization and transactivation to occur. In fact, *in vitro* DNA-binding studies show that the addition of exogenous HSP70 blocks the activation of HSF

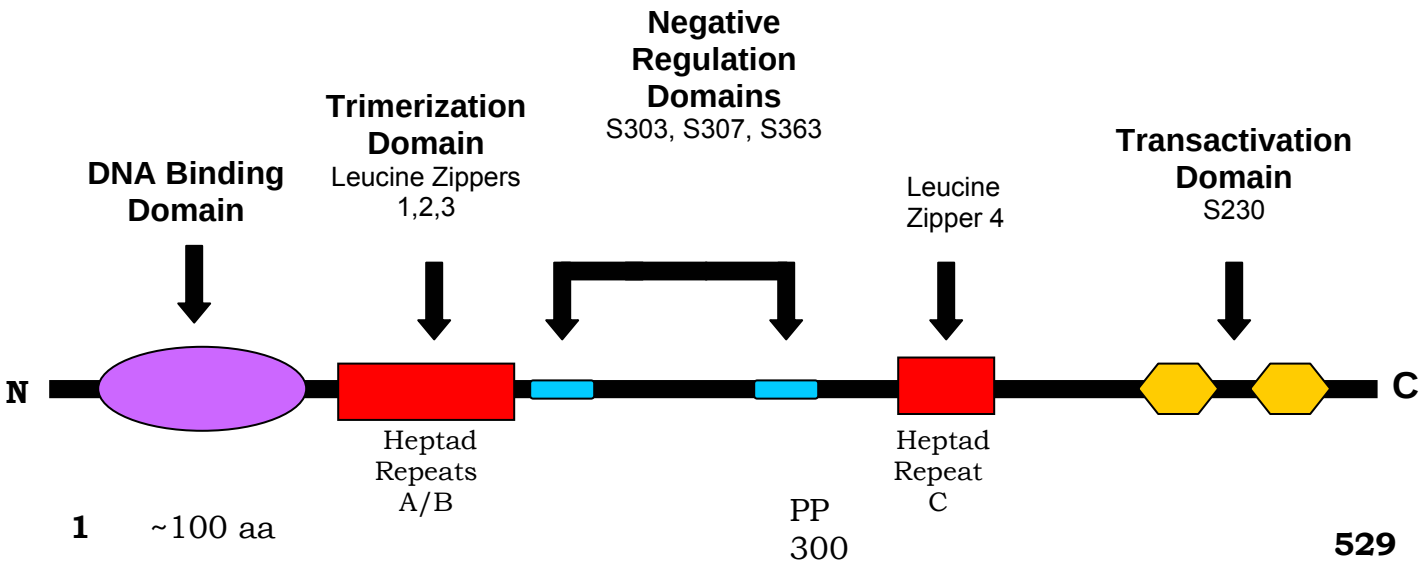

Figure 1. Domains of human HSF1. The functional protein domains of HSF1 are indicated on the molecule, where N and C are the amino and carboxyl termini, respectively. Amino acids are indicated by number and P is a phosphorylation site. Adapted from Knauf *et al.* (1996), Kline and Morimoto (1997), and Locke and Noble (2002).

(Abravaya *et al*., 1992) and HSP90 co-immunoprecipitates with the monomeric form of HSF1 (Ali *et al.,* 1998; Hu and Mivechi, 2003). Thus, the DNA-binding competence of HSF1 appears to be dependent upon a dynamic balance between HSF1 and its negative regulatory molecules.

Under normal growth conditions, HSF1 exists in its inactive monomeric (or dimeric) form (Figure 2). The transactivation of HSF1 upon heat shock includes several key steps allowing for its newly acquired DNA-binding ability. In response to stress, putatively after dissociation from regulatory molecules (e.g., HSP/C70 and/or HSP90) (Bharadwaj *et al.,* 1999), HSF1 monomers (or dimers) coalesce to form homotrimers. HSF1 trimerization is accompanied by hyperphosphorylation. For example, transactivation of human HSF1 appears to be dependant upon the phosphorylation of four serine residues identified to date; S230, S303, S307, and S363 (Knauf *et al*., 1996; Kline and Morimoto, 1997). Under normal growth conditions, the constitutive phosphorylation of S303, S307, and S363 have been shown to repress transcriptional activity of HSF1 (Knauf *et al*., 1996; Kline and Morimoto, 1997). Upon heat shock however, S230 is inducibly phosphorylated, contributing to the transcriptional capacity of HSF1 (Holmberg *et al*., 2001). This transient phosphorylation allows for the colocalization of HSF1 and the small ubiquitin-related modifier 1 protein (SUMO-1) in nuclear stress granules (Hietakangas *et al*., 2003). Posttranslational modification of HSF1 occurs by sumoylation, which is the covalent conjugation of SUMO-1 to one or more lysines of a substrate by isopeptide bonds. In human HSF1, sumoylation occurs at K298, which is located at a site nearby S303 in the regulatory domain (Hietakangas *et al*., 2003). In both

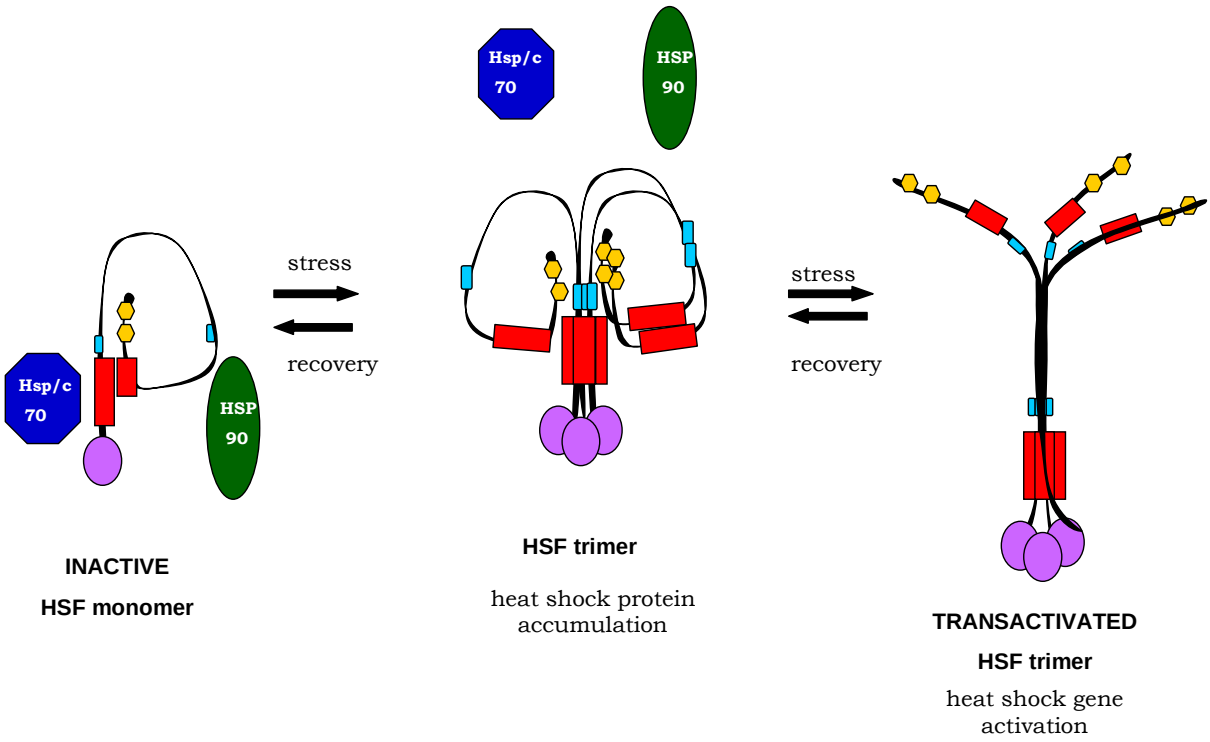

Figure 2. Regulation of HSF1. Model of the stress-inducible activation and deactivation of HSF1. See text for details. Adapted from Locke and Noble (2002).

human and *Xenopus* HSF2, sumoylation occurs at K82 (Goodson *et al*., 2001; Hilgarth *et al.*, 2004).

1.4. HSP Gene Expression in *Xenopus*

The heat shock response (HSR) is developmentally regulated in *Xenopus* (Bienz, 1984a; Heikkila *et al*., 1985). Preexisting HSP70 mRNA can be detected at low levels in non-heat shocked oocytes and levels are not significantly affected by heat shock (Bienz, 1984a/b). In comparison, HSP30 mRNA is not detected, either prior to or after heat shock, in oocytes (Bienz, 1984a). Immediately after fertilization, translation that occurs uses maternal mRNA until the zygotic genome is activated during the mid-blastula transition (MBT) at stage 8.5. Thus, the HSR is not detected until post-MBT when HSPs are synthesized upon exposure to heat and other stressors (Heikkila *et al.*, 1991). There is a developmentally regulated pattern of HSP mRNA accumulation in response to stressors, such as for *hsp70*, *hsp30*, and ubiquitin (Heikkila *et al*., 1991). Detailed studies of the roles of HSPs during early development in *Xenopus* have been conducted for *hsp30* (Ohan and Heikkila, 1995; Tam and Heikkila, 1995; Heikkila *et al*., 1997; Lang *et al*., 1999), *hsp70* (Lang *et al*., 2000), and immunoglobulin heavy chain binding protein (*bip)* (Miskovic and Heikkila, 1999). *Bip* is expressed constitutively during *Xenopus* early development and, only after MBT, also displays a stress-inducible pattern of increased expression in response to endoplasmic reticulum (ER) stressors, including tunicamycin and the calcium ionophore A23187 (Miskovic and Heikkila, 1999).

Concomitantly, HSF1 is both stress-inducible and developmentally regulated in *Xenopus* oocytes (Gordon *et al*., 1997). Although endogenous HSP gene expression may not be induced by heat shock in *Xenopus* oocytes, HSF is present and functional

(Landsberger *et al*., 1995; Mercier *et al*., 1997; Ali *et al*., 1998) and heat shock-induced HSF binding activity is detected at all stages of *Xenopus* development, including unfertilized eggs and cleavage stage embryos (Ovsenek and Heikkila, 1990; Karn *et al*., 1992). A cDNA encoding the *Xenopus laevis* heat shock factor, XHSF1, isolated and sequenced by Stump and colleagues (1995), encodes a 451-amino-acid protein that is similar to other vertebrate HSF proteins. XHSF1 synthesized *in vitro* binds specifically with HSE, as demonstrated by DNA mobility shift assay and DNase I footprinting (Stump *et al*., 1995). Studies with both pre- and post-midblastula stage *Xenopus* embryos showed that the molecular mass of endogenous *Xenopus* HSF was approximately 88 kDa (Karn *et al*., 1992), which is equivalent to HeLa cell HSF (Goldenberg *et al*., 1988). Given that transcriptional activity is absent prior to MBT, it is probably maternal HSF that provides a readily accessible mechanism for HSP mRNA to be transcribed, thus conferring thermotolerance at the earliest possible time after MBT (Parsell and Lindquist, 1993; Morimoto *et al*., 1994).

Although HSF binding activity has not been extensively studied in *Xenopus* A6 kidney epithelial cells, HSP gene expression has been well characterized. For example, in cultured A6 cells, *hsp30* and *hsp70* are reliably induced by heat shock, sodium arsenite, hydrogen peroxide, and herbimycin A (Darasch *et al*., 1988; Briant *et al.,* 1997; Ohan *et al*., 1998a; Phang *et al.,* 1999; Muller *et al.,* 2004), and constitutively expressed ER residents *bip* and *hsp47* are increased upon exposure to heat shock (Miskovic *et al.,* 1997; Hamilton and Heikkila, 2006). However, whereas constitutive *bip* mRNA levels are increased upon exposure to the specific ER stressors tunicamycin and A23187, *hsp47* mRNA levels are unaffected by tunicamycin and inhibited by A23187 in A6 cells

(Miskovic *et al.,* 1997; Hamilton and Heikkila, 2006). Functional studies have shown heat-induced HSP30 to form high molecular weight complexes that are competent molecular chaperones (Ohan *et al.,* 1998a; Fernando and Heikkila, 2000; Abdulle *at al.,* 2002; Fernando *et al.,* 2002), with recent research suggesting that this role of HSP30 occurs primarily in the cytoplasm and perinuclear regions of cells upon heat shock or sodium arsenite treatment (Gellalchew and Heikkila, 2005). For example, immunocytochemistry and laser scanning confocal microscopy (LSCM) revealed a granular or punctuate pattern of HSP30 accumulation in the cytoplasm of heat shocked or sodium arsenite treated cells, suggesting the localization of super-aggregated sHSP structures in response to various stressors (Gellalchew and Heikkila, 2005). The same LSCM images also showed changes in cellular morphology, such as F-actin cytoskeletal disorganization, in response to heat shock and sodium arsenite treatment, and that these regions often coincided with enriched areas of HSP30 accumulation (Gellalchew and Heikkila, 2005). Considering that studies incubating HSP30 antibody with heat shocked cell lysates showed co-immunprecipitation of HSP30 with actin (Fernando *et al.,* 2003), it is possible that stress-inducible HSP30 acts as a molecular chaperone, primarily in the cytoplasm, localizing with the actin cytoskeleton to maintain the integrity of actin filaments under stressful conditions (Gellalchew and Heikkila, 2005).

1.5. Comparison of the Putative Heat Shock Response Inhibitors Quercetin and KNK437

Quercetin (3,3’,4’,5,7-pentahydroxyflavon) is a well known bioflavonoid, one of the many water-soluble polyphenols found in most plants which give them their characteristic pigments. In a synergistic association with Vitamin C, quercetin may act as

an important phytonutrient, boosting immunity, slowing the aging process, and combating a wide range of diseases, from heart disease to cancer (Galisteo *et al.,* 2004; Shackelford, 2005; Conklin *et al.,* 2006; Nair *et al.,* 2006). All of these benefits are based on the dozen or so wide-ranging biological effects of quercetin, from cytoprotective and neuroprotective to antiproliferative, cytotoxic and apoptotic (reviewed in Dajas *et al.*, 2003a/b). Quercetin is also one of the few known inhibitors of the stress response to injury by inhibiting the synthesis of HSPs and other important factors (Hosokawa *et al*., 1992; Hansen, 1997), by interfering with HSF DNA-binding activity (Nagai *et al*., 1995). Although quercetin pretreatment of cells does not affect HSF1 trimer formation, it does result in the reduction of the HSF1-HSE complex, possibly by decreasing levels of HSF1 within the cell (Nagai *et al*., 1995).

Abnormally high expression levels of HSPs in many tumour cells protect them from injurious conditions, resulting in increased resistance to chemotherapy and poor patient prognosis (Wei *et al*., 1994; Creagh *et al*., 2000; Jolly and Morimoto, 2000). Several studies show that quercetin inhibits *hsp* expression and induces apoptosis in various tumour cell lines (Koishi *et al*., 1992; Hosokawa *et al*., 1992; Elia and Santoro, 1994; Wei *et al*., 1994; Nagai *et al.*, 1995; Csokay *et al*., 1997; Fujita *et al.*, 1997; Hansen *et al.*, 1997; Jakubowicz-Gil *et al*., 2002). Induction of apoptosis by quercetin treatment is likely mediated by reduced *hsp* expression, leading to increased tumour cell sensitivity. Interestingly, quercetin's action appears to be cell-type specific, for example in two tumour cells lines, HeLa cells and human breast carcinoma cells (MDA-MB-231). Quercetin inhibits both HSF DNA-binding activity and HSF expression in HeLa cells,

but not HSF DNA-binding activity in MDA-MB-231 cells, only marginally affecting HSF expression (Hansen *et al*., 1997).

Similarly, KNK437, a benzylidene lactam compound, and its metabolite KNK423, have recently been shown to inhibit the heat shock response in mammalian cells and inhibit the acquisition of thermotolerance in a dose-dependent manner (Yokota *et* al., 2000; Koishi *et al*., 2001; Nonaka *et al*., 2003a/b; Ohnishi *et al.,* 2004). However, KNK437 and KNK423 reportedly are less toxic and more effective than quercetin in inhibiting the heat shock response, purportedly not affecting the activities of certain protein kinases (e.g., PKA, PKC, or PTK) and cellular pathways as does quercetin (Yokota *et* al., 2000; Koishi *et al*., 2001).

1.6. Effects of Heat Shock on Cytoskeleton Organization and Dynamics

The cytoskeleton, a network of filamentous elements spread throughout the cytoplasm of cells, organizes and provides structural support for the cytosol and organelles. It extends both into the nuclear compartment and into the plasma membrane, mediating between the cell's internal and external environments. Thus, the cytoskeleton functions in many essential processes, including intra- and inter-cellular communication and transport, membrane stability, adhesion, and motility, protein synthesis, and metabolism (Cervera *et al.,* 1981; Geiger, 1983; Fulton, 1984; Ben-Ze'ev and Amsterdam, 1986; Coss and Linnemans, 1996; Rustom *et al.,* 2004; Sheetz et al., 2006).

The cytoskeleton is composed of three major types of protein filaments: 1) actin microfilaments (or F-actin), which determine the cell's surface shape and locomotive ability; 2) microtubules, which direct intracellular transport, determining the positions of membrane-enclosed organelles; and 3) intermediate filaments, which confer mechanical

strength and shear-stress protection. Microfilaments are double-stranded helical polymers of the protein actin, with a diameter of 5-9 nm, and organized into an assortment of linear bundles, two-dimensional networks, and three-dimensional gels (Alberts *et al.,* 2002). F-actin is most concentrated in the cell cortex, just beneath the plasma membrane, and in active regions of the cell, particularly stress fibers and actin-enriched protrusions at the plasma membrane, such as lamellopodia (membrane "sheets") at the cell periphery, filopodia (membrane "fingers," also called cytoneme-like filopodia (CLFs) when long and thin), membrane ruffles, and shorter and more numerous cell protrusions called microvilli or microspikes (Huot *et al.,* 1998; Demontis, 2004; Rustom *et al.*, 2005; Timpson and Daly, 2005; Zhu *et al.,* 2005). However, actin may also be dispersed throughout the cell as nonfilamentous structures (Spector *et al.,* 1998). Stress fibers are formed when bundles of cross-linked actin filaments extend from the cell surface through the cytosol making secure connections with the substratum in cutured cells. In focal adhesions, the stress fibers attach to the substratum through bound adapter proteins, which are associated with plasma membrane integrins (Alberts *et al.*, 2002). In contrast, the actin-based protrusions are thought to promote long range cell-to-cell signaling, directing cellular migration to specific targets (Demontis, 2004). Various stressors including oxidative stress and heat shock can induce actin-based stress fibers and plasma membrane protrusions in cultured cells.

Cellular functions such as growth, wound healing, intercellular communication, and migration have been shown to be affected by a cell's adhesion to its extracellular matrix (Juliano and Haskill, 1993; Clark and Brugge, 1995; Schwartz *et al.,* 1995; Rustom *et al.,* 2004; Sheetz *et al.,* 2006). Focal adhesions (or contact points), consisting

of bundles of actin filaments (stress fibers) and various adhesion-proteins, act to anchor the cytoskeleton to the extracellular matrix and to transduce environmental signals across the plasma membrane (Jockusch *et al.,* 1995; Schwartz *et al.*, 1995; Burridge and Chrzanowska-Wodnicka, 1996). In addition to the well-documented cellular contacts with the extracellular matrix such as focal complexes and focal adhesions, are fibrillar adhesions, podosomes, and invadopodia, which are gaining recognition as important adhesion contacts and mechanosensors (Linder and Kopp, 2005). Although these various types of adhesion contacts differ on the basis of their unique protein compositions (e.g., enriched in talin, paxillin, and/or vinculin (Zamir and Geiger, 2001), it is thought that they in fact exist as a continuum of fundamental matrix contacts (Linder and Kopp, 2005).

Actin filaments also support cell-cell contacts, for example in epithelial tissue, wherein cytoskeletal elements anchor to the plasma membrane by association with transmembrane cadherin proteins forming adherens junctions (Alberts *et al.,* 2002). Recent research also suggests that other membrane protrusions, such as tunneling nanotubes (TNTs), which are tiny F-actin based cell protrusions, are an important mechanism for cell-to-cell communication wherein the exchange of information occurs via the direct membrane continuity of connected cells (Rustom *et al.,* 2004). Studies of TNTs and the continuity between membranes of connected cells suggest that F-actin is needed for both protrusion biogenesis and organelle transport, and is supported by observations that TNTs can transfer membrane-bound proteins along their axes, which are detected in the receiving cells (Rustom *et al.,* 2004).

The plasma membrane of cells generally conforms to the actin cytoskeleton, thus changes in both membrane and cytoskeleton dynamics promptly affect membrane-cytoskeleton adhesion (see Sheetz *et al.,* 2006 for review). Under conditions wherein gaps in the cytoskeleton arise or there is a loss of adhesion strength, pressure changes within the cell result in separations of the plasma membrane from the cytoskeleton, which is marked by the appearance of membrane blebs. For example, damaged or stressed cells with newly formed blebs must assemble actin on the cytoplasmic surface to restore membrane support and eliminate the rapid diffusion of membrane proteins and lipids (Sheetz *et al.,* 2006). Underlying the plasma membrane, actin filaments in the cell cortex regulate the shape and movement of the cell surface. Correspondingly, actin density is greatest at the cell periphery, where actin filament nucleation occurs most frequently. Changes in the external environment mediate nucleation of actin at the plasma membrane, assisting the cell in its response to its environment by changing its shape and stiffness. Nucleation is catalyzed by actin-related protein (ARP) complexes located at the minus end, which allow rapid elongation of F-actin filament at the plus end, a dynamic process regulated by intracellular signaling molecules and elements at the cytosolic face of the plasma membrane (Alberts *et al.,* 2002). An ARP complex nucleating one actin filament can simultaneously attach to the side of another actin filament, producing in a treelike web formation of filaments growing at 70º angles to one another (Alberts *et al.,* 2002). Actin polymerization and de-polymerization are inhibited by drugs such as cytochalasin B and phalloidin, respectively (Alberts *et al.,* 2002).

Structural reorganization of the actin cytoskeleton can be induced by a wide-range of extracellular signals, which converge inside the cell, activating pivotal monomeric

GTPases that are members of the Rho protein family – *Cdc42, Rac*, and *Rho*. Functioning as molecular switches to regulate cycling between active, GTP-bound states and inactive, GDP-bound states, these Rho proteins can trigger dynamic rearrangements of the actin cytoskeleton. For example, Cdc42 activates actin polymerization and bundling to establish filopodia or microspikes and podosome formation (Alberts *et al.,* 2002; Linder and Aepfelbacher, 2003; Linder and Kopp, 2005). Rac activation induces actin polymerization at the cell periphery forming lamellipodia and membrane ruffles, whereas Rho activation induces actin filament bundling into stress fibers and associated integin clustering to form focal adhesions (Alberts *et al.,* 2002). Stressors that interfere with a cell's ability to construct normal actin-based protrusions such as filopodia and lamellipodia may result in the formation of membrane blebs around the cell periphery (Alberts *et al.,* 2002).

Welch and Suhan (1985) examined the effects of heat shock on three major cytoskeletal networks; actin filaments, vimetin-containing intermediate filaments, and microtubules. Heat shock, which had previously been associated with an increased number of actin stress fibers transversing the cell accompanied by a broad flattening of cells (Thomas *et al.,* 1982), was also shown to result in the collapse and aggregation of intermediate filaments in and around the nucleus without apparent changes in microtubule distribution (Welch and Suhan, 1985). Furthermore, compared to control cells, wherein nucleoli were well-organized and condensed, Welch and Suhan (1985) observed in heat shocked cells a significant unraveling of nucleoli conforming to a less condensed state, accompanied by the appearance of a many "unusual rod-like inclusion bodies that appeared to be packed with thin parallel filaments" (~4-6 nm in diameter)

within these nuclei. Although these structures did not appear to traverse the nuclear membrane into the cytoplasm, numerous filaments were observed to end in close proximity to the nuclear envelope, with further examination confirming an actin-based composition (Welch and Suhan, 1985). Correspondingly, heat shocked cells displayed an increased peri-nuclear localization of mitochondria, postulated to be in response to a collapse and aggregation of intermediate filaments surrounding nucleus (Welch and Suhan, 1985).

Evidence of increased HSP interaction with cytoskeletal components suggests that HSPs are also modulators of cell adhesion and adhesion-mediated signal transduction (Schneider *et al.,* 1998). For example in the mammalian stress response, HSP27 is postulated to function in the regulation of adhesion-mediated growth and differentiation signaling pathways through the stabilization of actin stress fibers and focal adhesions (Schneider *et al.,* 1998). Lavoie *et al.* (1993) found that overexpression of HSP27 in mouse cells is sufficient for the transient acquisition of thermotolerance, possibly by contributing to actin filament stabilization during heat shock. In previous studies, overexpression of HSP27 only after heat shock (i.e., during recovery at normothermic temperatures) did not effectively protect cells, suggesting that to be effective, HSP27 must be present at the time of treatment (Landry *et al.,* 1989). However, the mechanism by which HSP accumulation confers transient thermotolerance to cells is yet to be determined, and a minority of incongruous studies indicate that HSP synthesis is neither sufficient nor necessary for thermotolerance acquisition (Landry and Chretien, 1983; Watson *et al.,* 1984).

Although the molecular targets for the protective action of HSP27 are unknown, it has been shown that overexpressing HSP27 not only protected against treatment with cytochalasin B, but also protected stress fibers in mouse cells against heat shock, leading Lavoie *et al.* (1993) to postulate a direct interaction between HSP27 and actin components. For example, immediately (minutes) after heat shock, HSP27 is phosphorylated, transitions from a nonionic detergent soluble to insoluble cellular compartment, and relocalizes from the cytoplasm to within or around the nucleus (Arrigo *et al*., 1988; Landry *et al.,* 1989; Landry *et al.,* 1991).

Many studies implicate sHSPs in the protection of the actin cytoskeleton by interfering with F-actin fragmentation induced by oxidative stress (Huot *et al.,* 1996), heat shock (Lavoie *et al.,* 1995; Bryantsev, 2002), energy depletion (Loktionova *et al.,* 1998; Van Why *et al.,* 2003), or cytochalasin D (Lavoie *et al.,* 1995; Wang and Spector, 1996; Bryantsev, 2002). For example, various cellular insults induce translocation of sHSPs to the cytoskeleton from the cytosol whereupon they stabilize actin filaments thus protecting actin contacts with the plasma membrane via its associated scaffolding proteins (Lavoie *et al.,* 1995; Bryantsev, 2002, Van Why *et al.,* 2003; Koh and Escobedo, 2004). Recent research argues against the protection of actin from denaturation by sHSPs based on evidence that sHSPs virtually do not interact with intact actin (Pivovarova *et al*., 2005). Alternatively, Pivovarova *et al.* (2005) proposed that since sHSPs do interact with denatured actin, they prevent the aggregation of heat-denatured F-actin, which fragments into short sticky oligomers that, in the absence of sHSPs, would otherwise coalesce into soluble aggregates ultimately entangling intact actin fibers (Pivovarova *et al.,* 2005).

1.7. *Xenopus laevis* as a Model System for Studying Inhibition of the HSR and the Acquisition of Thermotolerance

For the purposes of developmental research, *Xenopus laevis* is an excellent model organism. The South African clawed frog is entirely aquatic, preferring stagnant water pools, and is thus maintained easily and inexpensively. Female frogs can be induced to lay eggs up to 3 times a year, producing large eggs and embryos that develop quickly. Accordingly, *Xenopus laevis* is advantageous for experimental embryology and widely used for microinjections, extracts, and developmental analysis (Sive *et al*., 2000).

To a great extent, the cellular and molecular information obtained from the study of *Xenopus* is applicable to human cells. The associated cultured cell line, A6 kidney epithelial cells, originated from the renal uriniferous tubule of adult *Xenopus* (Rafferty and Sherwin, 1969) and is used as a principal cell model of differentiation and cation (Na^+) reabsorption in culture (Verrey *et al*., 1989). A6 cells display adhesive properties and tight junctions in culture, forming an epithelial monolayer which can function as a permeability barrier, sealing intercellular spaces and limiting the diffusion of proteins and lipids (Gumbiner, 1987). At confluence, the monolayer differentiates into a dome structure as the expressed Na^+ and Cl^- channels on the apical surface take in Na^+ and pump it out through N^+/K^+-adenosine triphosphatase (ATPase) on the lateral surface (Verrey *et al*., 1989; Zeiske *et al*., 1998; Chen *et al*., 1999).

Although it can be difficult to produce permanent vertebrate cell lines, the A6 line is well established (e.g., exceeding 100 cell generations *in vitro*) and does not develop the fibroblastic morphology that many cell lines derived from avian and mammalian organs display (Rafferty, 1968). *Xenopus* A6 cells are extremely hardy and their vigorous growth

allows for minimal time to reach confluence (e.g., 22 h doubling time) (Rafferty, 1968). In many diploid cell lines, growth begins to decline several days before cells reach confluence as contact between cells begins to inhibit mitosis (Rafferty, 1968). In comparison, the A6 line, which is tetraploid, remains in logarithmic growth phase until cells reach confluence and can continue to accumulate in layers if the medium is changed frequently (Rafferty, 1968).

As mentioned previously, HSP regulation is well characterized in A6 cells and many HSPs are inducible in this cell line, including HSP30, HSP47, HSP70, HSP90, and BiP (Ohan and Heikkila, 1995; Tam and Heikkila, 1995; Heikkila *et al*., 1997; Lang *et al*., 1999; Lang *et al*., 2000; and Miskovic and Heikkila, 1999; Hamilton and Heikkila, 2006).

1.8. Objectives

Interest is growing in the role of HSF in the stress response and induction of stress proteins. Our lab is interested in studying inhibition of the HSR and the effect inhibition has on the developmental regulation of HSPs. This study focused on the effects of inhibiting HSF binding activity on the acquisition of thermotolerance. Although there are many widely known inducers of the stress response, there are few known inhibitors. Quercetin and KNK437 have been widely shown to inhibit HSF activity and both are extremely inexpensive to use. In the present study, the effects of quercetin and KNK437 on the relative levels of the heat shock-induced accumulation of several *hsp* mRNAs (e.g., *hsp70, hsp30, hsp47*) and the synthesis of HSPs for which readily accessible and effective antibodies were available (e.g., HSP30).

Specific objectives included:

1) Northern hybridization analysis of the accumulation of *hsp* mRNA transcripts, including *hsp30, hsp47*, and *hsp70,* in response to heat shock in the presence or absence of quercetin and KNK437
2) Western analysis of the accumulation of HSP30 in response to heat shock in the presence or absence of quercetin and KNK437.
3) Immunocytochemistry and LSCM to examine the effects of HSR inhibition on cell morphology, including the cytoskeleton, nucleus, and HSP30 localization, in response to heat shock and the acquisition of thermotolerance.

2. Experimental Procedures

2.1. Culture and treatment of *Xenopus laevis A6* cells

Xenopus A6 kidney epithelial cells [American Type Culture Collection (ATCC), Rockville, Maryland] were cultured in 55% (w/v) Leibovitz L-15 media (Sigma, Oakville, Ontario) supplemented with 10% (v/v) fetal bovine serum (FBS) (Sigma), 100U/ml penicillin (Sigma), and 100µg/ml streptomycin (Sigma) at 22°C in T75cm^2 tissue culture-treated flasks. Upon reaching confluence, cells were washed with 2 ml versene [0.02% (w/v) KCl, 0.8% (w/v) NaCl, 0.02% (w/v) KH_2PO_4, 0.115% (w/v) Na_2HPO_4, 0.02% (w/v) sodium ethylenediaminetetraacetic acid (Na_2EDTA)] for 2 min and then treated with 0.5 ml of 1X trypsin (Sigma) in 100% Hank's balanced salt solution (HBSS; Sigma) until cells began detaching. Non-adherent cells were re-suspended in fresh media and distributed evenly into additional culture flasks. Once cells reached 90-100% confluence, cell treatments were performed, adhering to a minimum of 48 h between cell plating and experimentation.

For RNA and protein accumulation studies, cells were exposed to 100 µM quercetin or KNK437 dissolved in 0.1% dimethylsulphoxide (DMSO; Sigma) for a minimum of 6 h prior to all heat shock treatments. Heat shock treatments, ranging from 1 to 4 h were performed in a 1245PC waterbath (VWR, Cornelius, Oregon) at various temperatures ranging from 33 to 37ºC. For RNA accumulation studies, cells were immediately harvested and total RNA isolated. For protein accumulation studies cells were given a 2 h recovery period at 22ºC. After final treatment, cells were washed with 2 ml of 65% HBSS followed by addition of 1.5 ml of 100% HBSS for gentle scraping and transfer of cells to 1.5 ml microcentrifuge tubes. Cells were pelleted in an Eppendorf 5415D

microcentrifuge (Brinkmann Instruments Ltd, Mississauga, Ontario) for 30 sec at 13,000 rpm. The supernatant was removed and stored at -80ºC.

2.2. Clones from HSP families

2.2.1. Templates used for riboprobe generation

This study evaluated the effect of quercetin and KNK437 upon the heat shock-induced accumulation of a number of mRNAs, including *hsp30, hsp47, hsp70, hsc70,* and *elongation factor 1 alpha (efIα)*. Table 2 lists all clones used, plasmid vectors they were propagated into, restriction endonuclease sites, and cells they were transformed into. Table 2 also lists the specific polymerases required for *in vitro* transcription of DIG-labeled antisense riboprobes from linearized clones.

Previously, the coding region of *hsp30C* genomic DNA in pUC19 (Krone *et al.,* 1992) was isolated by digestion with *Eco*RI and *Bam*HI, DNA polymerase (Klenow fragment) was used to fill in the ends, and the entire sequence was subcloned into the *SmaI* site of the pSP64(polyA) plasmid in both sense (Fig. 3A) and antisense (Fig. 3B) orientations. Antisense riboprobes were created by linearizing the construct with *PvuII* followed by *in vitro* transcription with SP6 RNA polymerase.

Similarly, the coding region of *hsp70* genomic DNA (pXL16P; Bienz, 1984b) was isolated by digestion with *Fsp*I and *Pst*I and subcloned into the *Sma*I and *Pst*I sites of pSP72 (Promega, Madison, WI) (Fig. 4A). Antisense riboprobes were created by linearizing the construct with *Mlu*NI *(Bal*I*)* followed by *in vitro* transcription with SP6 RNA polymerase. The coding region of *hsc70.1* cDNA (Ali *et al*., 1996b) was isolated with *Xba*I and *Xho*I then subcloned into the corresponding sites of pSP72 (Promega) (Fig. 4B). Antisense riboprobes were created by linearizing the construct with *Xho*I followed by *in vitro* transcription with SP6 RNA polymerase. *Hsp47* cDNA subcloned into the

*Not*I and *Sal*I site of pCMV-SPORT6 phagemid vector (ATCC; Hamilton and Heikkila, 2006) (Fig. 5) was isolated by digestion with *Sma*I followed by *in vitro* transcription with T7 RNA polymerase. The coding region of *ef1α* subcloned into the *Not*I and *Sal*I site of pCMV-SPORT6 (ATCC) (Fig. 6) was isolated by digestion with *Sma*I followed by *in vitro* transcription with T7 RNA polymerase.

2.2.2. Isolation of plasmid DNA

Escherichia coli DH5α or DH10B cells carrying plasmid vectors were streaked onto Luria Bertani (LB) agar plates [1% (w/v) tryptone-peptone, 0.5% (w/v) yeast extract, 1% (w/v) NaCl, 1.5% (w/v) bacto-agar, pH7.5] supplemented with 100µg/ml ampicillin (Bioshop, Burlington, Ontario) and incubated overnight at 37ºC. Individual colonies were inoculated into 15 ml Falcon tubes with 5 ml of LB broth [1% (w/v) tryptone-peptone, 0.5% (w/v) yeast extract, 1% (w/v) NaCl, pH7.5] supplemented with 100µg/ml ampicillin and incubated in a shaker waterbath at 37ºC. Cells were pelleted by centrifugation at 5,000 rpm for 10 min at 4ºC in an Eppendorf Centrifuge 5810R (Brinkmann Instruments Ltd) in a swinging-bucket rotor.

Pelleted cells were resuspended in 200 µl of ice-cold solution I [50 mM glucose, 25 mM Tris (pH 8.0), 1 mM EDTA (pH 8.0)], transferred to a microcentrifuge tube, then lysed with 200 µl solution II [0.2 N NaOH, 1% (w/v) SDS], gently mixed and incubated at room temperature for 5 min. Samples were precipitated with 200 µl of ice-cold solution III [3 M potassium acetate, 5 M glacial acetic acid], gently mixed and incubated on ice for 5 min. Samples were centrifuged at 14,000 rpm for 15 min at 4ºC and supernatants transferred to fresh tubes, followed by the addition of 10 µl RNase A (10 mg/ml; Bioshop) and incubated at 37ºC for 2 h to digest any remaining RNA. A solution

Table 2. Clones used for digoxygenin (DIG)-labeled antisense riboprobes.

Cloned DNA used for *in vitro* transcription of DIG-labeled antisense riboprobes are listed, including the plasmid vectors they were propagated into, restriction endonuclease sites, and cells they were transformed into.

Clone	Source	Plasmid Vector	Cell Type	RE Site for Antisense Riboprobe	Polymerase
hsp30C(-)	Heikkila Lab (Lang *et al*., 1999)	pSP64(poly A)-Hsp30C-	DH5α	*Pvu*II	SP6
hsp47	GenBank Accession No. BG360108 (Hamilton and Heikkila, 2006)	pCMV-SPORT6 (A.T.C.C.)	DH10B	*Sma*I	T7
hsp70	Heikkila Lab (Lang *et al*., 2000)	pSP72	DH5α	*Mlu*NI *(Bal*I*)*	SP6
hsc70.1	Heikkila Lab (Ali *et al*., 1996b)	pSP72	DH5α	*Xho*I	SP6
ef1α	GenBank Accession No. BG160504	pCMV-SPORT6	DH10B TonA	*Sma*I	T7

Figure 3. The *hsp30C* cDNA. The coding region of *hsp30C* genomic DNA in pUC19 (Krone *et al.,* 1992) was isolated by digestion with *Eco*RI and *Bam*HI, DNA polymerase (Klenow fragment) was used to fill in the ends, and the entire sequence was subcloned into the *SmaI* site of the pSP64(polyA) plasmid in both sense (Fig. 3A) and antisense (Fig. 3B) orientations. Antisense riboprobes were created by linearizing the construct with *PvuII* followed by *in vitro* transcription with SP6 RNA polymerase.

A

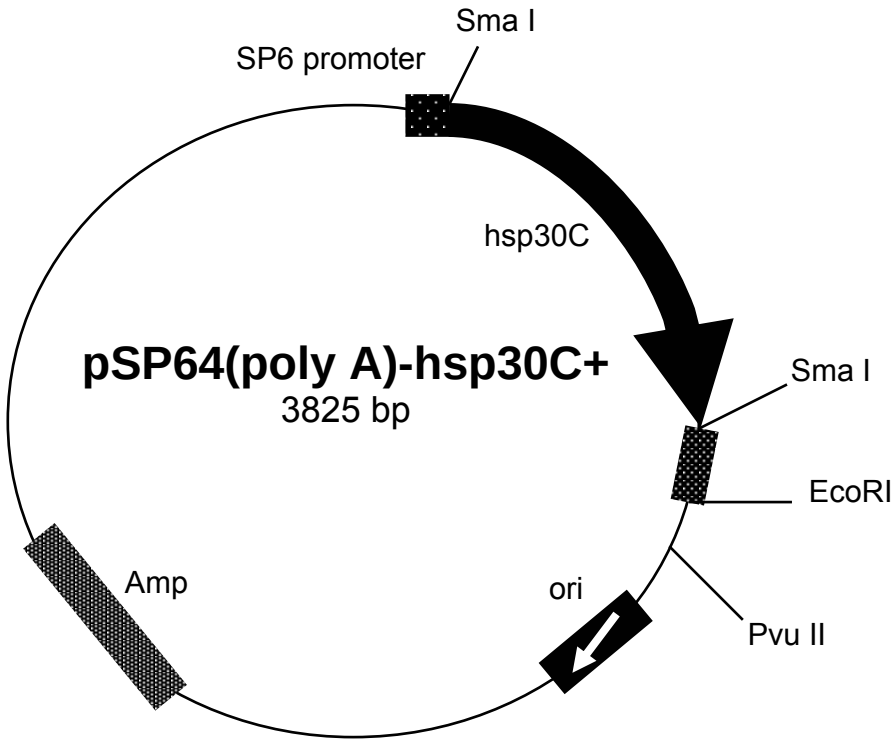
Sma I
SP6 promoter
hsp30C
pSP64(poly A)-hsp30C+
3825 bp
Sma I
EcoRI
Amp
ori
Pvu II

B

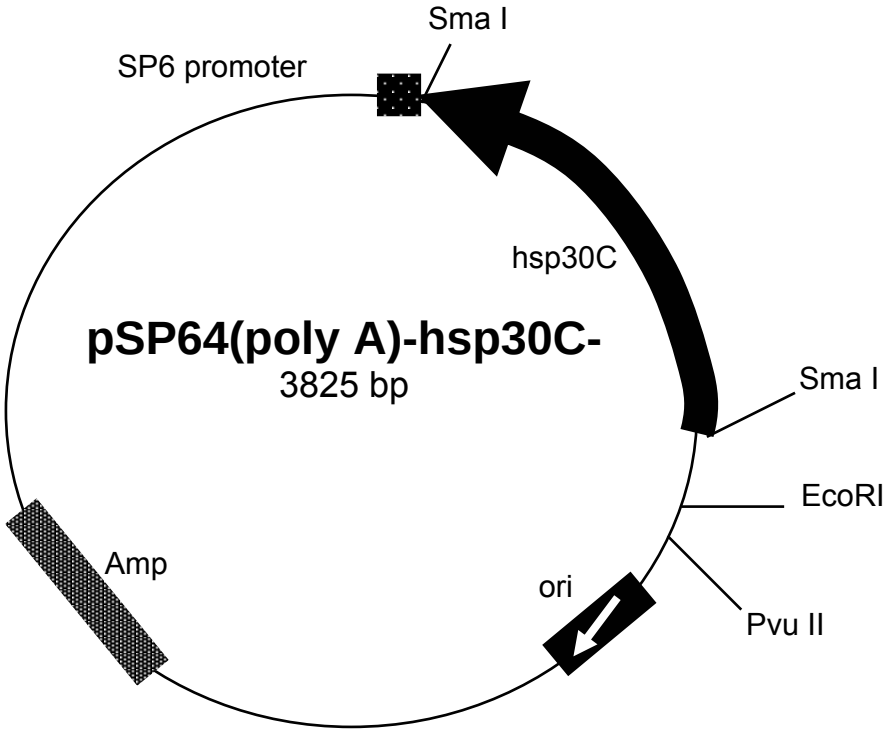
Sma I
SP6 promoter
hsp30C
pSP64(poly A)-hsp30C-
3825 bp
Sma I
EcoRI
Amp
ori
Pvu II

Figure 4. The *hsp70* and *hsc70.1* cDNAs. The coding region of *hsp70* genomic DNA (pXL16P; Bienz, 1984b) was isolated by digestion with *Fsp*I and *Pst*I and subcloned into the *Sma*I and *Pst*I sites of pSP72 (Promega, Madison, WI) (Fig. 4A). Antisense riboprobes were created by linearizing the construct with *Mlu*NI *(Bal*I*)* followed by *in vitro* transcription with SP6 RNA polymerase. The coding region of *hsc70.1* cDNA (Ali *et al*., 1996b) was isolated with *Xba*I and *Xho*I then subcloned into the corresponding sites of pSP72 (Promega) (Fig. 4B). Antisense riboprobes were created by linearizing the construct with *Xho*I followed by *in vitro* transcription with SP6 RNA polymerase.

A

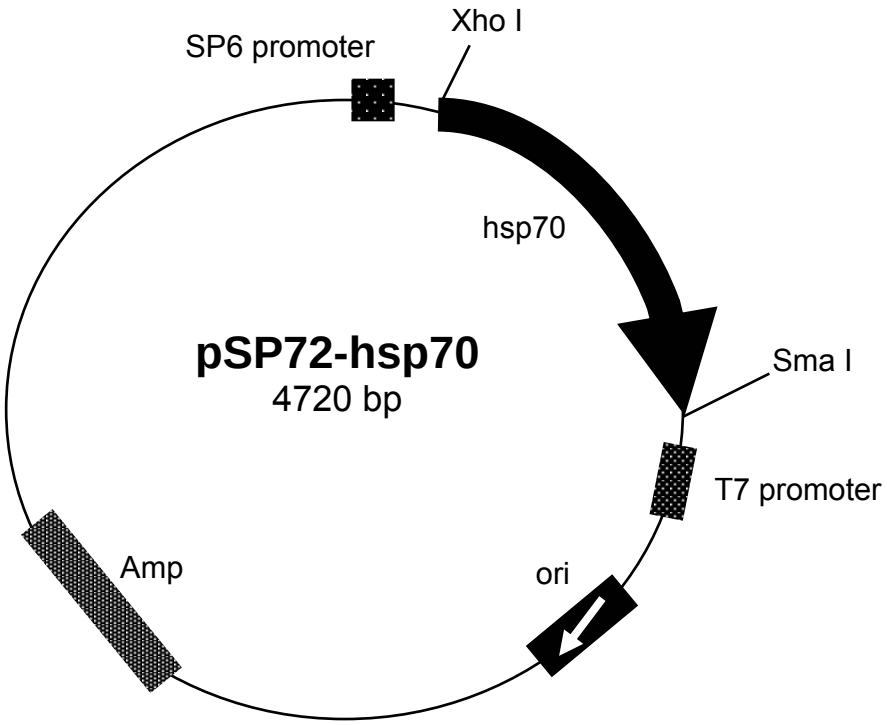
SP6 promoter
Xho I
hsp70
pSP72-hsp70
4720 bp
Sma I
T7 promoter
Amp
ori

B

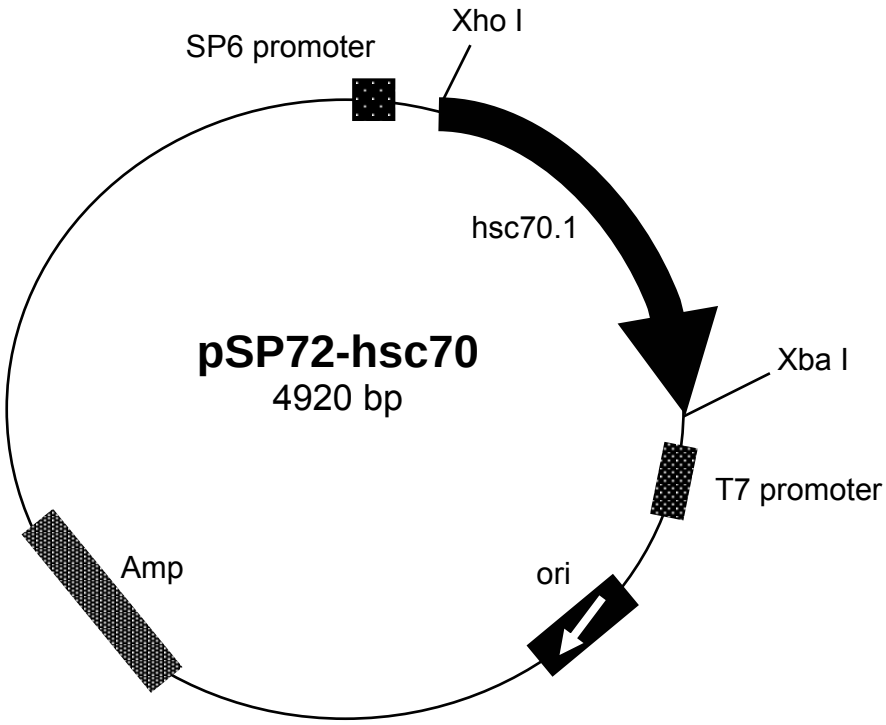
SP6 promoter
Xho I
hsc70.1
pSP72-hsc70
4920 bp
Xba I
T7 promoter
Amp
ori

Figure 5. The *hsp47* cDNA. *Hsp47* cDNA subcloned into the *Not*I and *Sal*I site of pCMV-SPORT6 phagemid vector (ATCC; Hamilton and Heikkila, 2006) (Fig. 5) was isolated by digestion with *Sma*I followed by *in vitro* transcription with T7 RNA polymerase.

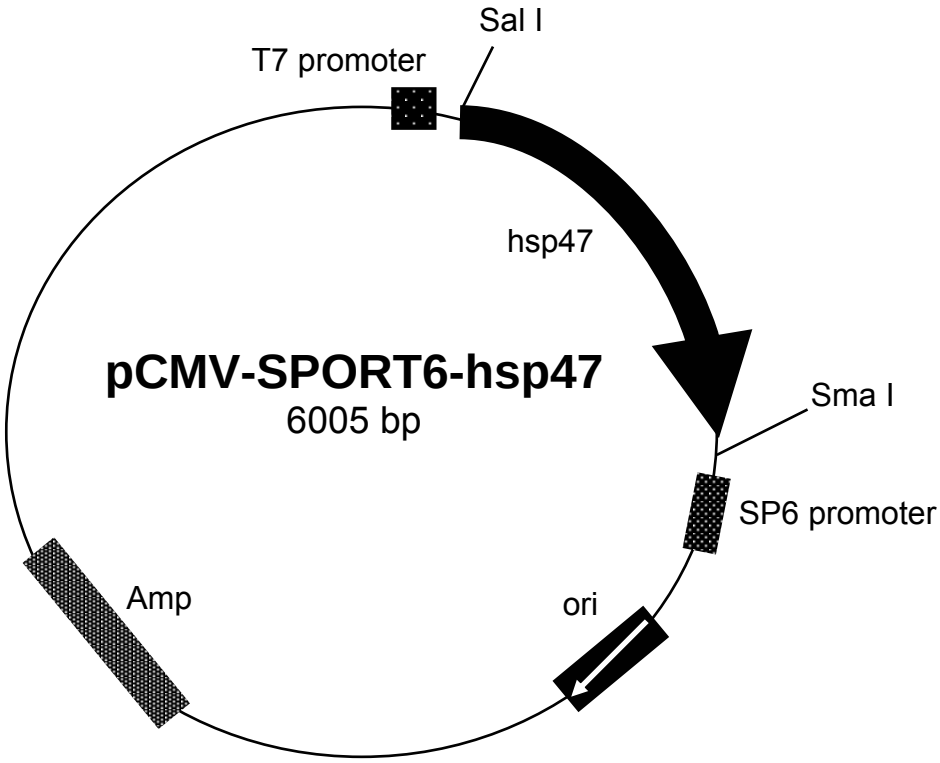
Sal I
T7 promoter
hsp47
pCMV-SPORT6-hsp47
6005 bp
Sma I
SP6 promoter
Amp
ori

Figure 6. The *ef1α* cDNA. The coding region of *ef1α* subcloned into the *Not*I and *Sal*I site of pCMV-SPORT6 (ATCC) (Fig. 6) was isolated by digestion with *Sma*I followed by *in vitro* transcription with T7 RNA polymerase.

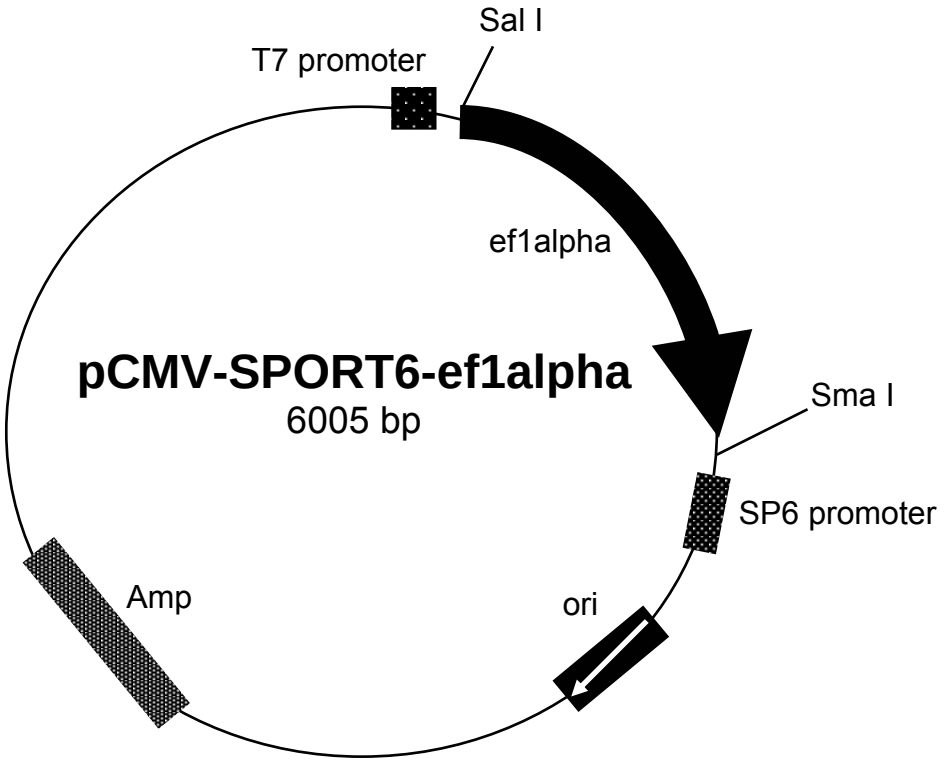
Sal I
T7 promoter
ef1alpha
pCMV-SPORT6-ef1alpha
6005 bp
Sma I
SP6 promoter
Amp
ori

of phenol, chloroform, and isoamyl alcohol (25:24:1) in an equal volume to the supernatant was added (e.g., 500 µl), vortexed for 30 sec and centrifuged at 14,000 rpm for 2 min at 4ºC. The top layer was carefully transferred to a fresh tube and the phenol:cholorform:isoamyl alcohol step repeated several times until the supernatant appeared clear. The supernatant was transferred to a fresh tube and precipitated at −80ºC for 30 min to overnight with (0.1X supernatant volume) 3 M sodium acetate (e.g., 50 µl) and (2.5X supernatant volume) 100% ice-cold ethanol (e.g., 750 µl). Plasmid DNA was pelleted by centrifugation at 14,000 rpm for 15 min at 4ºC, supernatant decanted, and pellet washed 2X with 500 µl of 70% (v/v) ethanol. After pellets were air-dried on ice, they were resuspended in 50 µl of sterile distilled water and stored at −20ºC.

A QIAprep Miniprep Kit (QIAgen, Mississauga, Ontario) was also used to isolate plasmid DNA from bacterial cells according to the QIAprep Spin Miniprep Kit Protocol (2002). Pelleted cells were resuspended in 250 µl Buffer P1 containing RNase A and transferred to a fresh microcentrifuge tube. To lyse cells, Buffer P2 was added to the suspension in an equal volume and mixed by gentle inversion for 1 min, followed by the addition of 350 µl of Buffer N3 and gently mixed again. Samples were centrifuged at room temperature for 10 min at 13,000 rpm in an Eppendorf 5415 D microcentrifuge (Brinkmann Instruments Ltd). Supernatants were added to QIAprep columns, which were centrifuged for 1 min as before, with flow-through discarded. QIAgen spin columns were washed with 500 µl of Buffer PB and centrifuged for 1 min, followed by addition of 750 µl of Buffer PE and centrifuged for 2 min. To elute plasmid DNA, columns were transferred to fresh 1.5 ml microcentrifuge tubes, followed by the addition of 50 µl of

Buffer EB [10 mM Tris-Cl (pH 8.5)]. After a 1 min incubation, samples were centrifuged for 1 min. Isolated plasmids were stored at −20ºC.

2.2.3. Preparation of digoxygenin (DIG)-labelled riboprobes

2.2.4. *In vitro* transcription

In vitro transcription was used to synthesize digoxygenin (DIG)-labelled riboprobes with linearized vectors described in Table 2. Ingredients for each transcription reaction were brought to room temperature (except for RNA polymerase and RNA inhibitors) and mixed in a microcentrifuge tube in the following order: 4 µl of linearized DNA template, 4 µl of rNTP mix [2.5 mM rGTP, 2.5 mM rATP, 2.5mM rCTP, 1.625 mM rUTP (Promega, Nepean, Ontario), 0.875 mM DIG-11-UTP (Roche Molecular Biochemicals, Laval, Quebec], 1.5 µl diethylpyrocarbonate (DEPC)-treated water, 4 µl of 100 mM dithiothreitol (DTT) (final 20 mM; Promega), 4 µl of 5X transcription buffer (final 1X; MBI Fementas), 0.5 µl RNase inhibitor (MBI Fermentas) and 40 IU of the appropriate RNA polymerase [SP6 RNA polymerase (Roche Molecular Biochemicals), T7 RNA polymerase, T3 polymerase (MBI Fermentas)]. Transcription reactions were incubated at 37ºC for 1 h followed by the addition of 2 µl of RNase-free DNase 1 (Roche Molecular Biochemicals) for 10 min at 37ºC to digest any remaining DNA template. Transcripts were precipitated with 10 µl of 3 M sodium acetate (pH 5.2), 80 µl of TES [10 mM Tris-HCl (pH 7.4), 5 mM EDTA (pH 8.0), 1% (w/v) SDS] and 220 µl of ice-cold 100% filtered ethanol combined and incubated at −80ºC for 30 min to overnight. After precipitation, transcribed riboprobes were pelleted by centrifugation at 14,000 rpm at 4ºC in an Eppendorf centrifuge 5810R (Brinkmann Instruments Ltd), supernatant decanted, and the pellet air dried on ice. Pelletted riboprobes were re-suspended in 2 µl of DEPC-

treated water, of which a 1 µl sample was analyzed by electrophoresis to determine transcript integrity. Riboprobes were stored at −80ºC until required for northern blot analysis.

2.3. RNA Isolation and Northern Hybridization

2.3.1 RNA isolation from A6 cells

Total RNA was isolated from A6 cells using the QIAgen RNeasy Mini Kit (QIAgen) as described in the RNeasy Mini Handbook Animal Cell Protocol (2001) at room temperature. Pelleted cells stored at −80ºC were lysed with 600 µl Buffer RLT containing 1% (v/v) β-mercaptoethanol, vortexed, and homogenized by 10 passages of the lysate through a $20^{1}/_{2}$–gauge needle, fitted to a sterile syringe. Filtered 70% ethanol was added to the lysate in an equal volume and mixed by pipetting. Samples were applied in 700 µl aliquots to RNeasy mini columns held in 2 ml collection tubes and centrifuged at 13,200 rpm for 30 sec in an Eppendorf 5415 D microcentrifuge (Brinkmann Instruments Ltd) and flow-through discarded. Buffer RW1 was added to columns in 700 µl aliquots and centrifuged again at 13,200 rpm for 30 sec. Buffer RPE was added to columns in 500 µl aliquots and centrifuged again at 13 200 rpm for 30 sec. The flow-through was discarded and another 500 µl of Buffer RPE was added to columns and centrifuged at 13 200 rpm for 2 min. RNA was eluted into 1.5 ml Eppendorf tubes by the addition of two 40 µl aliquots of DEPC-treated water, directly onto the membrane, followed by centrifugation at 12,000 rpm for 1 min each. RNA was stored at −80ºC.

2.3.2 Quantification of RNA

RNA samples were diluted 1:200 in sterile water and quantified by ultraviolet (UV) spectrophotometry at 260 nm in a Cary 50 Bio UV-visible spectrophotometer

(Varian, Mississauga, Ontario). RNA integrity was assessed by electrophoresis of 1 µg samples on a 1.2% (w/v) formaldehyde/agarose gel [1.2% (w/v) agarose, 10%(v/v) 10X MOPS (pH 7.0; 0.2 M 3-(morpholino) propane sulfonic acid; Bioshop), 50 mM anhydrous sodium acetate, 10 mM EDTA, pH 8.0) and 16% (v/v) formaldehyde]. RNA samples were heat denatured for 10 min at 68ºC in a solution of 1 µl 10X MOPS, 1.6 µl formaldehyde, 2 µl loading dye [0.2% (w/v) bromophenol blue, 1 mM EDTA (pH 8.0) and 50% (v/v) glycerol], 5 µl formamide and 0.5 µg /ml ethidium bromide. After cooling on ice for 5 min, samples were loaded onto the gel and electrophoresed at approximately 90 V for 1-2 h.

2.3.3 Northern blot analysis

Total RNA was analyzed by northern hybridization using the following digoxygenin (DIG)-labeled riboprobes: *hsp70*, *hsc70*, *hsp47, hsp30,* and *ef1α.* For a northern hybridization, 3-15 µg of total RNA was electrophoresed on a 1.2% (w/v) formaldehyde/agarose gel, as described above, except ethidium bromide was not included in the loading buffer and the gel was electrophoresed for 3-4 h at 65 V. After electrophoresis, gels were soaked in 0.05 N NaOH at room temperature for 20 min to ensure RNA denaturation. Gels were rinsed with DEPC-treated water then soaked twice, for 20 min each, in 20X SSC buffer [3 M sodium chloride, 300 mM sodium citrate (pH 7.0)].

RNA was transferred onto a positively charged nylon membrane (Roche Molecular Biochemicals) via capillary transfer for a minimum of 4 h as described below. For transfer, gels were inverted onto a blotting paper (VWR International, West Chester, Pennsylvania) wick, presoaked in 20 X SSC, set on a plexiglass support over a Pyrex®

dish filled with 500 ml 20X SSC. Nylon membrane, cut to fit the gel, was laid directly on the gel and covered with 2 additional pieces of presoaked blotting paper and a 10 cm stack of paper towels and 500 g weight. After transfer, ultraviolet cross-linking was used to attach RNA to the membrane using either a GS-Gene linker (program 'C3' 150 mJ; BioRad Mississauga, Ontario) or an UVC-515 Unltraviolet Multilinker (120,000 μJ/cm^2; UltraLum Inc., Claremont, California).

Equal loading and quality of transfer of the RNA was confirmed by staining the membrane with 1X Reversible Blot Stain (Sigma). The membrane was pre-soaked in 10% (v/v) glacial acetic acid for 5 min prior to addition of the blot stain. The membrane was destained in DEPC-treated water to visualize individual RNA bands and photographed.

The membrane was transferred to a hybridization bag (SealPAK pouches, VWR) and incubated in a Boekel Scientific Shake'N'Bake Hybridization Oven (VWR International) at 65-68^{o}C for 3 to 4 h in 50 ml of pre-hybridization buffer [50% (v/v) formamide, 5X SSC, 0.02% SDS, 0.01% N-lauryl sarcosine, 2% Blocking Reagent (Sigma)]. The membrane was then incubated in fresh pre-hybridization buffer, to which the appropriate DIG-labeled riboprobe was added, and further incubated for a minimum of 8 h.

Excess unbound riboprobe was removed by washing the membrane in decreasing concentrations of SSC stringency solutions. The first two washes in 2X SSC (with 0.1% (w/v) SDS) for 5 min each were at room temperature, followed by a 15 min wash in 0.5X SSC (with 0.1% (w/v) SDS) at hybridization temperature, then a 15 min wash in 0.1X SSC (with 0.1% (w/v) SDS) also at hybridization temperature. The membrane was equilibrated at room temperature for 1 min in washing buffer [100 mM maleic acid, 0.3%

(v/v) Tween 20] and then incubated for 30 to 60 min at room temperature in blocking solution [2% (w/v) blocking reagent, 10% (v/v) maleic acid buffer (pH 7.5)]. The membrane was incubated for another 30 min at room temperature in fresh blocking solution containing 1:800 dilution of anti-DIG-alkaline phosphatase-conjugated Fab fragments antibody (Roche Molecular Biochemicals). To remove excess unbound antibody, the membrane was washed twice for 20 min each in washing buffer at room temperature. The membrane was equilibrated at room temperature for 2 min in detection buffer [0.1 M Tris-HCl (pH 9.5), 0.1 M NaCl]. The membrane was placed in a fresh hybridization bag and CDP-Star (Roche Molecular Biochemicals) was applied evenly across the membrane and allowed to incubate for 10 min while the chemiluminescent reaction developed. A Fluorchem 800 Chemiluminescence and Visible Imaging System (filter position 1; Alpha Innotech Corp, San Leandro, California) was used for signal detection for up to 30 min depending upon strength.

2.4. Protein Isolation and Western Blotting

2.4.1 Protein isolation from A6 cells

A6 cell pellets were lysed on ice with 500 µl of lysis buffer [160 mM sucrose, 1.6 mM ethylene glycol-Bis N,N,N',N'-tetraacetic acid (EGTA; Bioshop), 0.8 mM EDTA, 32 mM NaCl, 24 mM N-Z-hydroxylethylpiperazine-N'-2 ethane sulfonic acid (HEPES; Bioshop), 1% (w/v) SDS, 100 µg/ml phenylmethyl-sufonyl fluoride (PMSF; Bioshop), 1 µg/ml aprotinin, 0.5 µg/ml leupeptin, pH 7.4], vortexed, and homogenized using a Teflon pestle. Samples were sonicated with a Branson Sonifer 250 (15 pulses, duty cycle 65%, output control 4.5; Branson Sonic Power Co., Danbury, CT) then centrifuged at

14,000 rpm for 30 min at 4ºC in an Eppendorf Centrifuge 5810R. Supernatants were removed and stored at −20ºC.

2.4.2 Protein quantification

Protein concentrations were determined via bicinchoninic acid (BCA) protein assay according to the manufacture's instructions (Pierce, Rockford, Illinois) as described. A standard series of bovine serum albumin (BSA; Bioshop) dilutions ranging from 0 to 2 mg/ml were prepared in sterile water from a 2 mg/ml stock. Aliquots of isolated protein samples were also diluted in sterile water 1:2 and 1:4. BSA standards and protein samples were loaded in triplicate into a polystyrene 96 well assay plate in 10 ul aliquots followed by the addition of 80 ul of BCA reagent A and reagent B (50:1; Pierce). Plates were incubated at 37ºC for 30 min and then equilibrated for 10 min at room temperature. Reactions were analyzed with a Versamax Tunable microplate reader (Molecular Devices, Sunnyvale, CA) at 562 nm using a soft max pro program. BSA standards were used to construct a standard curve which was used to determine protein concentrations of each sample.

2.4.3 Western blot analysis

Sodium dodecyl sulfate-polyacrylamide gel electrophoresis (SDS-PAGE) was performed using a Mini Protean II gel apparatus (BioRad, Mississauga, Ontario) according to the manufacturer's instructions. Separating gels [10% (v/v) acrylamide, 0.27% (v/v) n'n'-bis methylene acrylamide, 0.375 M Tris pH 8.8, 0.1% (w/v) SDS, 0.05% (w/v) ammonium persulfate (APS), 0.15% (v/v) n,n,n'n'-tetramethylethylenediamine (TEMED)] were prepared, poured and overlaid with 100% ethanol for 30 min. After polymerization, ethanol was decanted and separating gels were overlaid with stacking

gels [4% (v/v) acrylamide, 0.11% (v/v) n'n'-bis methylene acrylamide 0.125 M Tris pH 6.8, 0.1% (w/v) SDS, 0.05% (w/v) APS, 0.2% (v/v) TEMED].

Protein samples (10 to 40 µg) were prepared in loading buffer [0.0625 M Tris pH 6.8, 10% (v/v) glycerol, 2% (w/v) SDS, 5% (v/v) β-mercaptoethanol, 0.00125% (w/v) bromophenol blue] to a final concentration of 1X. Protein samples and prestained low range molecular size markers (BioRad) were denatured by boiling for 10 min, cooled on ice for 5 min and pulse-centrifuged prior to loading onto polymerized gels. Holding tanks for the gel apparatus were filled with 1X electrophoresis buffer [25 mM Tris, 0.2 M glycine, 1 mM SDS] and the protein samples were electrophoresed at 75 V until samples reached the separating gel, at which time the voltage was turned up to approximately 160-170 V until the dye front reached the bottom of the gel.

While gels were running, a polyvinlyidene fluoride (PVDF) membrane (Millipore Corp., Nepean, Ontario) and 6 blotting papers (VWR) per gel were cut to 5.5 cm X 8.5 cm. Membranes were activated in 10% methanol for 10 sec and then incubated for 30 min in cold transfer buffer [25 mM Tris, 192 mM glycine, 20% (v/v) methanol]. After electrophoresis, gels were soaked in transfer buffer for 10-15 min. Proteins were transferred to the PVDF membrane with a Trans-Blot Semi-dry Transfer Cell (BioRad) at 25 V for 25 min. Following transfer blots were stained for 10 min with Ponceau-S stain [0.19% (w/v) Ponceau-S, 5% (v/v) acetic acid], destained in sterile water for 5 min, and then scanned with a Hewlett Packard ScanJet 3300C. Membranes were then incubated for 1 h at room temperature in Tris Buffered Saline solution plus Tween 20 (TBS-T) [2 mM Tris (pH 7.5), 0.1% Tween 20 (Sigma), 30 mM NaCl] containing 5% (w/v) Nestle® Carnation skim milk powder. Membranes were then incubated, at room temperature for 1

h in fresh blocking solution with appropriate primary antibody added. (e.g., for HSP30 and 1:200 dilution for actin). The antibodies employed were either the polyclonal rabbit anti-HSP30 (1:3000 dilution; Fernando and Heikkila, 2000) or the polyclonal rabbit anti-actin (1:200 dilution; Hamilton and Heikkila, 2006). Excess unbound antibody was removed by rinsing membranes twice with TBS-T, followed by incubation in fresh TBS-T at room temperature for 15 min, and then washed twice for 2 min each in TBS-T. Membranes were incubated, at room temperature for 1 h, in fresh blocking solution with the secondary antibody conjugate added, goat anti-rabbit IgG HRPO (horse radish peroxidase) conjugate (1:3000; BioRad).

Membranes were washed once with fresh TBS-T for 15 min, then twice more for 5 min, and incubated for 5 min in ECL+ Western Blotting Detection System reagent A and B (40:1; Amersham Biosciences, Brockville, Ontario) according to the manufacturer's instructions. A Fluorchem 8000 Chemiluminescent and Visible Imaging System (filter position 1; Alpha Innotech) was used for detecting chemiluminescent signals for up to 5 min depending upon signal, strength.

2.5. Immunocytochemistry and Laser Scanning Confocal Microscopy

2.5.1 A6 cell fixation and fluorescent labeling of HSP30 and F-actin

Immunocytochemical analyses were performed according to protocols described by Spector *et al.* (1998). To enhance cell adhesion to micro-cover glass slips, oil and other debris were removed from cover slips by soaking in a 2:1 nitric acid / HCL (v/v) solution followed by several distilled water rinses, 70% ethanol wash, and flame sterilization. Cover slips were seeded with A6 cells a minimum of 48 h prior to experimentation to relegate effects of stress-induction due to cell culturing procedures.

Upon conclusion of cell treatments, cover slips were washed twice with phosphate buffered saline (PBS; pH 7.4) and fixed with freshly prepared 3.7% paraformaldehyde (PA) (BDH: Inc., Toronto, Ontario) in PBS (pH 7.4) for 20-30 min at room temperature. After removing PA by three 5-min rinses with PBS, cells were permeabilized in 0.3% (v/v) Triton X-100 (ICN Biomedicals Inc, Aurora, Ohio) in PBS for 10 min at room temperature, followed by three 2 min washes in PBS. Reactive groups were blocked with 3.7% (w/v) bovine serum albumin (BSA) fraction V (Boehringer Ingelheim, Burlington, Ontario) in PBS for 1 h in a humid chamber at room temperature. Cells were labeled indirectly with fluorescein-isothiocyanate (FITC) for HSP30 and directly with phalloidin-tetramethylrhodamine (TRITC) for filamentous actin (F-actin) and 4',6-diamidino-2-phenylindole (DAPI) for DNA counterstaining as described below.

For indirect labeling of HSP30, cells were incubated with rabbit anti-HSP30 polyclonal antibody diluted in 3.7% BSA in PBS (1:500) for 1 h. Unreacted primary antibody was removed by three 2 min washes with PBS and then incubated with mouse anti-rabbit IgG (whole molecule) FITC conjugate secondary antibody (Clone RG-16, Sigma) diluted in 3.7% BSA in PBS (1:320) for 30 min. Unreacted secondary antibody-FITC conjugate was removed by three 2 min washes with PBS. For direct labeling of F-actin, cells were incubated with TRITC (300 U of rhodamine phalloidin in 1.5 ml 100% methanol; Molecular Probes, Oregon) diluted in 3.7% BSA in PBS (1:60) for 30 min. Unreacted TRITC was removed by three 2 min washes with PBS. Cover slips were rinsed with double distilled water prior to mounting on 1.2 mm thick glass slides (No.1; VWR) with 25µl of Vectashield mounting medium (Vector Laboratories, Burlingame, California) to preserve fluorescence and protect fluorophores from photobleaching. For

direct labeling of the nucleus, Vectashield mounting medium with DAPI (1.5 μg/ml) was used, which produces blue fluorescence when bound to DNA. Coverslips were sealed to glass slides with clear nail varnish and stored at 4ºC, which promotes fluorescence signal retention for 6 to 12 months.

2.5.2 Visualization of A6 cells with Laser Scanning Confocal Microscopy

Images were acquired with an inverted laser scanning confocal microscope (LSCM) system, Zeiss LSM 510 Meta (Carl Zeiss, Jena, Germany) outfitted with a 4-line argon laser, primary and secondary helium-neon lasers, a 405 laser diode, and a mercury arc lamp. The oil immersion objectives used were a Plan-Neofluar 40x / 1.3 NA (numerical aperture) Oil DIC (differential interference contrast) and a Plan-Apochromat 63x / 1.4 NA Oil DIC, both adjusted for spherical and chromatic aberration. A multi-channel configuration was used to collect emission spectra from three different visible wavelength ranges, including blue for DAPI (411 – 486), green for FITC (505-550 nm), and red for TRITC (550-750 nm). Although a few preliminary images were taken on a single track, to eliminate the possibility of false colocalization in merged images, a multi-channel configuration executed on multiple tracks was used to collect fluorescence from individual wavelengths, minimizing cross-channel contamination of fluorescence emissions (Gingrich *et al.,* 2000). For consistency, the same dichroic beam splitter and filter configuration was maintained across individual channels, whether in single or multiple track mode. All laser light passed through the primary dichroic beam splitter (MBS) HFT 405/488/543, followed by the secondary dichroic beam splitter (DBS1) NFT 545. Fluorescence light stimulated at 543 by the primary Helium-Neon (HeNe1) laser (approx. 0.1 % of 1 mW) was passed through the NFT 545 filter and a glass plate

followed by a 550-750 nm filter, collected in Channel S, and correspondingly labeled red in all images. Light at 488 nm from the Argon laser (approx. 0.1 % of 30 mW) was deflected by the secondary dichroic beam splitter (DBS2) NFT 545, passed through the band pass filter BP 475-525, collected in Channel 3, and correspondingly labeled green in all images. Light at 405 nm from the diode laser (approx. 0.1% of 25mW) was deflected by both the NFT 545 and NFT 490 filters and a mirror, passed through a long pass filter LP 420, collected in Channel 2, and correspondingly labeled blue in all images.

Zeiss LSM 510 Meta software automatically labeled overlapping regions between channels the following colours: yellow for overlap of Channel S (red) and Channel 3 (green); violet for overlap of Channel S (red) and Channel 2 (blue); turquoise for overlap of Channel 2 (blue) and Channel 3 (green); and orange for overlap of all three channels. Differential interference contrast (DIC) images were taken on the same track as Channel 3 and collected in Channel D. DIC images are shown in grayscale.

All images were obtained at the slowest scan speed (e.g., 1) to ensure the lowest interference noise and greatest resolution possible. Individual images were acquired at 12 bits without frame averaging for an area of 512 by 512 pixels (X by Y planes). Post hoc image analysis was performed using Zeiss LSM Image Browser software to create 3-D projections of Z-stack image galleries. Scanning parameters for all images are detailed in Table 3.

Table 3. LSCM image acquisition parameters.

All Images in Figures	11 to 17	18 to 24
Scan Mode:	Plane / Multiple tracks	Plane / Multiple tracks
Objective:	Plan-Neofluar 40x/1.3 Oil DIC Plan-Apochromat 63x/1.4 Oil DIC	Plan-Apochromat 63x/1.4 Oil DIC
Pinhole Diameter (µm) and Airy Unit (AU) per 1 µm slice: Channel S1 Channel 2 Channel 3 Channel D	 NA 127 µm and 1.32 AU 124µm and 1.04 AU coupled to Ch3	 124µm and 1.04 AU 129 µm and 1.57 AU 127 µm and 1.32 AU coupled to Ch 3
Filters: Channel S1 Channel 2 Channel 3	 NA LP 420 LP 505	 BP 550-750 LP 420 LP 505
Beam Splitters: MBS DBS1 DBS2 DBS3	 HFT 488/543 Mirror NFT 545 None	 HFT 405/488/543 NFT 545 NFT 490 Plate
Wavelength: Channel S Channel 2 Channel 3	 NA 488 nm at 0.1% of 30mW 543 nm at 0.1% of 1mW	 543 nm at 0.1% of 1mW 405 nm at 0.1% of 25mW 488 nm at 0.1% of 30mW
Pixel Number:	512 x 512	512 x 512
Bit Size:	12	12
Z-Stack Size:	NA	10 – 200

3. Results

3.1. Effect of Quercetin and KNK437 on *hsp* Gene Expression in *Xenopus* A6 cells

Northern hybridization and western blot analysis were used to examine the effects of quercetin and KNK437 on *hsp* mRNA and protein levels in *Xenopus* A6 cells under control (22^{o}C) and heat shock (33^{o}C) conditions. Densitometric analysis was performed on northern and western blot images using ImageJ (Version 1.24o) software, with resultant values expressed as percentages of the maximum density detected for each set, followed by statistical analysis of the data using SPSS (Version 13.0) software. Figures 7 and 8 show that the relative levels of *hsp30*, *hsp47*, and *hsp70* transcripts were significantly increased upon heat shock in comparison to control conditions. For example, compared to control, *hsp30*, *hsp70,* and *hsp47* mRNA levels increased upon heat shock significantly. Addition of 0.1% DMSO to the media did not affect relative transcript levels in either the control or heat shock samples. However, under heat shock conditions, exposure to 100 μM quercetin or KNK437 (dissolved in 0.1% DMSO) significantly decreased the accumulation of *hsp30*, *hsp70,* and *hsp47* transcripts by approximately 85%, in comparison to DMSO alone ($p < 0.001$). No significant differences in *hsp30, hsp47,* or *hsp70* mRNA levels were found between exposure to quercetin or KNK437 under heat shock conditions. Additionally, under control conditions both quercetin and KNK437 reduced the constitutive levels of *hsp47* mRNA by approximately 50%.

Figures 7 and 8 also show that the relative levels of *hsc70* transcripts were slightly increased upon heat shock in comparison to control conditions by 25%. Addition of 0.1%

DMSO to the media slightly increased relative to transcript levels in both the control and heat shock conditions. However, exposure to quercetin or KNK437 did not produce a significant difference in *hsc70* mRNA levels between control and heat shock conditions. Finally, no significant differences in *hsc70* mRNA levels were found between exposure to quercetin and KNK437 under either control or heat shock conditions.

In comparison to the *hsp* and *hsc* mRNAs, Figures 7 and 8 show that the relative levels of *ef1α* transcript were not elevated upon heat shock compared to control. Addition of 0.1% DMSO to the media did not affect relative transcript levels in either the control or heat shock conditions. Neither exposure to 100μM quercetin nor 100 μM KNK437 affected the accumulation of *ef1α* transcript compared to media or DMSO alone.

Figures 9 and 10 show that the relative levels of HSP30 were significantly increased upon heat shock compared to control. Addition of 0.1% DMSO to the media did not affect relative protein levels in either the control or heat shock conditions. However, compared to 0.1% DMSO alone under heat shock conditions, exposure to 100 μM quercetin and KNK437 significantly decreased the accumulation of HSP30 by 50% and 100%, respectively ($p < 0.001$). In comparison, Figures 9 and 10 also show that levels of actin were not significantly affected by either heat shock or exposure to DMSO, quercetin, or KNK437.

Finally, immunocytochemistry and LSCM were used to examine the morphological effects of heat shock and the HSR inhibitors on A6 cells, as shown in Figures 11 through 20. In these studies, HSP30 accumulation was used to monitor the effect of the HSR inhibitors on *hsp* gene expression. Figure 11 compared the effect of quercetin and KNK437 at 22ºC on HSP30 and F-actin localization in *Xenopus* A6 cells.

Control conditions (Fig. 11, A-F) revealed intact actin stress fibers transversing the entire length of cells in mostly axial bundles with the appearance of few radial bundles at the periphery. Arrows indicate areas where the actin cytoskeleton terminated at distinct and well separated sites of substrate adhesion at the cell periphery. Membrane ruffles were not observed, indicating secure attachment to the substratum across the length of cells. Similarly, exposure to quercetin (Fig. 11, G-I) or KNK437 (Fig. 11, J-L) did not show an observable effect on stress fibers in cells maintained at 22ºC. As expected, immunochemical analysis employing an anti-HSP30 antibody did not show detectable levels of HSP30. In contrast, Figure 12, which compared the effects of a 2 h heat shock at 33ºC (Fig. 12, G-L), showed abundant accumulation of HSP30 throughout the cytoplasm and around the nucleus (Fig. 12, G, I, J, L), without an observable effect on actin stress fibers.

Figure 13 compared the effect on A6 cells of exposure to quercetin and KNK437 during a 2 h heat shock at 33ºC. In contrast to cells maintained at 22ºC treated with either quercetin (Fig. 13, A-C) or KNK437 (Fig. 13, D-F), cells heat shocked at 33ºC showed detectable levels of HSP30 throughout the cytoplasm of some cells when treated with quercetin (Fig. 13, G and I). HSP30 accumulation was not detected in cells treated with KNK437 (Fig. 13, J and L). Although stress fibers were intact after exposure to both HSR inhibitors at 33ºC, a slight disruption in actin stress fibers and possible aggregation of actin at the cell periphery (indicated by arrows) was observed in approximately 1-10% of cells exposed to KNK437 but not quercetin.

Figures 14 and 15 demonstrate the effect of increasing the temperature of heat shock to 35ºC for 2 h and 4 h, respectively. Control conditions at 22ºC revealed the

presence of intact actin stress fibers without detectable levels of HSP30 (Fig 14, A-C). Similar to heat shock at 33ºC, cells heat shocked for 2-4 h at 35ºC still showed intact actin stress fibers transversing the entire length of cells. Under those heat shock conditions, HSP30 levels were abundant throughout the cytoplasm, but became increasingly concentrated in the perinuclear or nuclear region of the cell after 2 h at 35ºC. Interestingly, after 4 h at 35ºC, HSP30 was found primarily in the cytoplasm (Fig. 15, D-F). In contrast, after 2 h at 35ºC, cells treated with quercetin showed fewer actin stress fibers transversing cells accompanied by some actin fiber disruption at the cell periphery (Fig. 14, H and I). After 4 h at 35ºC, changes in the actin cytoskeleton were marked by the appearance of membrane blebs at the cellular periphery (indicated by arrows) (Fig. 15, G-I). Cells treated with quercetin also showed a reduction in detectable levels of HSP30, which was mostly nuclear, after 2 h at 35ºC (Fig. 14, G and I). After 4 h at 35ºC, cells treated with quercetin showed an accumulation in cytoplasmic HSP30, with a marked punctuated pattern of aggregation, particularly in membrane blebs, at the cellular periphery (Fig. 15, G and I). Cytoskeletal collapse around the nucleus was also observed in some cells.

Cells treated with KNK437 and heat shocked at 35ºC for 2 h showed an increase in radially-oriented actin bundles which, rather than spanning the length of the cell, converged at focal points around the cell periphery, giving the cell a diamond-like shape (Fig. 14, K and L). After 4 h at 35ºC, these radial bundles broke down into smaller aggregates of actin at the periphery with the appearance of numerous microspikes (indicated by arrows) in areas where the cell did not have stabilizing cell-cell contacts (Fig. 15, K and L). In general, membrane blebs occurred predominantly in heat shocked

cells treated with quercetin, whereas microspikes were evident in heat shocked cells treated with KNK437.

Figure 16 focuses on an interesting observation of cells treated with quercetin and heat shocked for 4 h at 35ºC. Optical slices were taken through cells, merged into a 3-channel, 3-D projected image, and rotated to show the bottom (Fig. 16, A-C) and top (Fig. 16, C-F) views to show the spatial distribution of HSP30 throughout cells. Arrows indicate the presence of a distinct pattern of HSP30 accumulation, which may be HSP30 supermolecular aggregates. This diffuse punctuate pattern was present throughout the cytoplasm and around the nucleus of cells exposed to quercetin only.

Another important observation was the emergence of actin-based cellular protrusions, similar in appearance to microspikes, CLFs, and TNTs. Figure 17 shows an example of the long actin-based protrusions connecting cells separated by distances of 50 to 100 μm. Under heat shock conditions of 33ºC up to 37ºC, both longer and shorter actin-based protrusions were observed in varying degrees of number and length, including cell-to-cell connections spanning long distances.

Figure 18 shows the effect of a 1 h thermal challenge at 37ºC, with and without a prior 2 h heat shock at 33ºC. Control conditions at 22ºC showed intact actin stress fibers spanning the entire cell, with a few distinct and well separated sites of adhesion, the presence of intact condensed nuclei, and no detectable levels of HSP30 (Fig. 18, A-D). Congruent with images in Figure 13, cells heat shocked for 2 h at 33ºC showed intact actin stress fibers and abundant levels of HSP30 distributed throughout the cytoplasm (Fig. 18, E-H). Cells incubated at 33ºC for 2 h and then further heat shocked for 1 h at 37ºC appeared very similar, showing intact actin stress fibers, distinct focal points, intact

nuclei, and abundant HSP30 throughout the cytoplasm (Fig. 18, I-L). At 37ºC, the appearance of microspikes was also evident (as indicated by arrows) (Fig. 18, L and P). In contrast, cells directly challenged 1 h at 37ºC showed a marked decrease in HSP30 relative to the previous heat shock condition. HSP30 was located predominantly at the cellular periphery in conjunction with apparent actin aggregates at sites of adhesion (Fig. 18, M-P).

Figure 19 shows the effect of treatment of A6 cells with KNK437 after a 1 h thermal challenge at 37ºC, with and without a prior 2 h heat shock at 33ºC. Similar to Figure 13, cells exposed to KNK437 at 22ºC showed intact actin stress fibers, the presence of intact condensed nucleus, and no detectable levels of HSP30 (Fig. 19, A-D). Cells heat shocked for 2 h at 33ºC still showed intact stress fibers spanning cells, but at the cellular periphery displayed ruffled edges in areas of cell-cell contact (Fig. 19, E-H). Cells further heat shocked for 1 h at 37ºC showed increased ruffling at edges and some aggregates of disrupted actin fibers (indicated by arrows) (Fig. 19, I-L). In contrast, cells without a prior heat shock exposure at 33ºC and directly challenged for 1 h at 37ºC showed virtually no intact stress fibers spanning cells without any coherent cell-cell connections as actin fibers are almost entirely degenerated into a myriad of aggregates (Fig. 19, M-P).

Figure 20 shows the results of an in depth 3-D analysis of A6 cells given a 1 h thermal challenge at 37ºC, after a prior 2 h heat shock at 33ºC, in the presence or absence of KNK437. Optical slices were taken through the cells, merged into a 3-channel, 3-D projected image, and rotated to show top (Fig. 20, A and C) and bottom (Fig. 20, B and D) views to indicate spatial distribution of HSP30, or lack thereof, throughout cells. Cells

that were given a 33ºC heat pretreatment followed by a thermal challenge at 37ºC, showed numerous linear actin bundles transversing the entire cell, even extending into areas of cell-cell contact, and abundant HSP30 throughout the cytoplasm, slightly more concentrated in the perinuclear region surrounding an intact nucleus (Fig. 20, A). The image also showed the ends of actin fibers terminating near the nucleus (Fig. 20, B). In contrast, the KNK437-treated cells, given a 33ºC heat pretreatment followed by a thermal challenge at 37ºC, did not display any intact stress fibers spanning the entire length of the cell and no HSP30 was detectable (Fig. 20, C). The few partially intact stress fibers located in the perinuclear region were punctuated with actin aggregates (Fig 20, C and D). The cellular periphery was devoid of both well defined sites of substrate adhesion and of microspikes, with the formation of ruffled edges around the cell's circumference (Fig. 20, C). The smaller cell in the bottom corner shows that its entire actin cytoskeleton has collapsed around the nucleus (Fig. 20, C and D). Figure 21 examined the effect of a 33ºC pretreatment on a 1 h thermal challenge at 37ºC in the presence of KNK437. KNK437-treated cells given a 33ºC pretreatment displayed numerous actin-based microspikes (as indicated by arrows) of various lengths extending from the cell periphery to the substratum and to other cells. In comparison, KNK437-treated cells not exposed to a 33ºC pretreatment displayed global ruffling of actin at membrane edges instead of microspikes.

Several follow up experiments were conducted to evaluate the effect of the 2 h recovery period between the mild heat pretreatment at 33ºC and the subsequent thermal challenge at 37ºC. Figure 22 shows distinct differences in actin structures and HSP30 distribution when cells are given a recovery period (Fig. 22, A and B) before the thermal

challenge or not (Fig. 22, C and D). In comparison to cells given a recovery period, cells *immediately* challenged at 37ºC (after an initial pretreatment at 33ºC) show collapsed actin stress fibers surrounding cytoplasmic HSP30 (indicated by arrows in C and D), similar to the membrane blebs seen in quercetin-treated cells heat shocked for 4 h at 35ºC. Arrows in the top panel (A and B) show a wider actin protrusion from the cell periphery with cytoplasmic HSP30 in the centre, similar in appearance to a CLF or TNT. Figure 23 shows the same cell in the bottom panels of Figure 22 (C and D) wherein optical slices were merged into a 3-D image and rotated to a side view spanning the adherent side of the cell (indicated by arrows) through to the nucleus (blue).

Figure 24 shows the effect of a 1 h thermal challenge at 37ºC immediately following a 33ºC pretreatment, without a 2 h recovery period at 22ºC in the absence and presence of KNK437. In this experiment, cells remained in the 33ºC waterbath for 2 h, at which time the heat was increased to 37ºC and held there for 1 additional hour, followed by a 2 h recovery at 22ºC. Optical slices were taken through the cells, merged into a 3-channel, 3-D projected image, and rotated to show top (Fig. 24, A and C) and bottom (Fig. 24, B and D) views to indicate spatial distribution of HSP30, or lack thereof, throughout cells. In the absence of KNK437, the cells were completely devoid of microspikes but did contain membrane blebs at the cell periphery, and HSP30 was localized in the cytoplasm as well as within membrane blebs (Fig. 24, A and B). In contrast, the KNK437-treated cells given a 33ºC heat pretreatment followed immediately by a thermal challenge at 37ºC were covered with microspikes and aggregates of actin at the cell periphery (C and D). Arrows indicate actin in membrane blebs with localized HSP30 (Fig. 24, A and B), and microspikes in the absence of HSP30 (Fig. 24, C and D).

Figure 7. Effect of HSR inhibitors on the heat shock-induced accumulation of *hsp30, hsp47, hsp70, hsc70,* and *ef1α* mRNAs in A6 cells. A6 cells were exposed to 100 μM quercetin or KNK437 dissolved in 0.1% DMSO (vehicle) or vehicle alone for 6 h at 22°C prior to a heat shock of 33°C for 1 h. The cells were then harvested and total RNA was isolated. **A.** Total RNA (3 - 10 μg) was analyzed by northern hybridization using *hsp30, hsp47, hsp70, hsc70* and *ef1α* antisense riboprobes. A representative reversible blot stain is shown in the bottom panel to confirm equal loading and quality of transfer. C and H represent control (22°C) and heat shock (33°C) conditions, respectively.

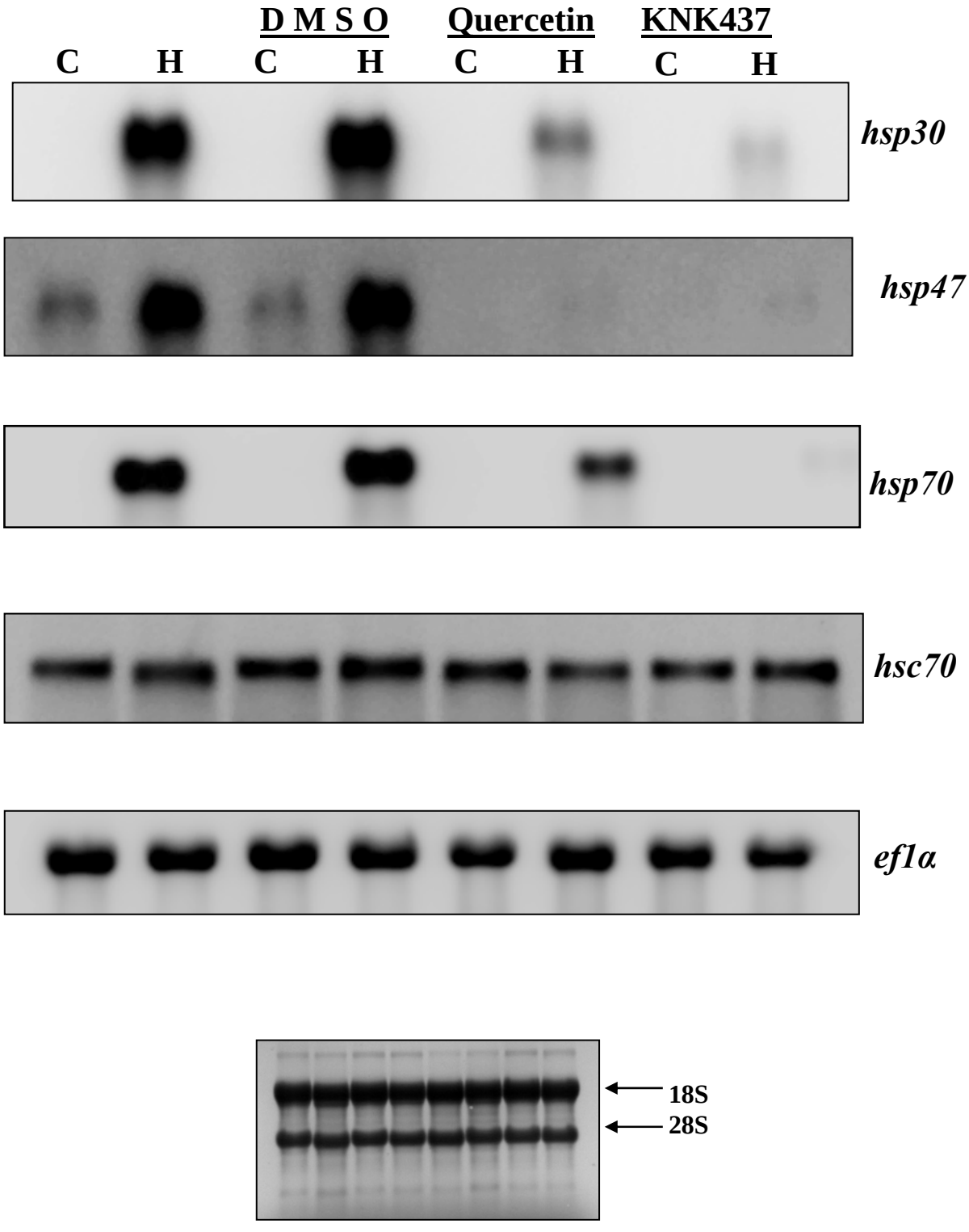
DMSO
Quercetin
KNK437
C
H
C
H
C
H
C
H
hsp30
hsp47
hsp70
hsc70
ef1α
18S
28S

Figure 8. Effect of HSR inhibitors on the heat shock-induced accumulation of *hsp30, hsp47, hsp70* (8A), and *hsc70* and *ef1α* (8B) mRNAs in A6 cells. ImageJ (1.24o) software was used for densitometric analysis of mRNA bands on northern blot images. Control (open bars) and heat shock (solid bars) treatment data were expressed as a percentage of the maximum hybridization within each blot and then graphed as mean +/- standard error. Significant differences are annotated between untreated cells at 22ºC and 33ºC (*, $P < 0.001$) and between DMSO-treated cells and HSR inhibitor-treated cells at 33ºC (**, $P < 0.001$).

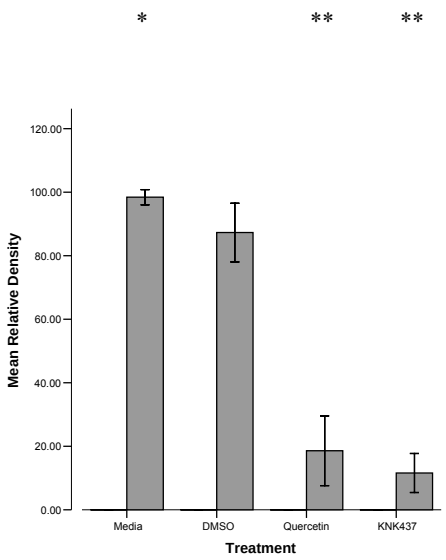

hsp30

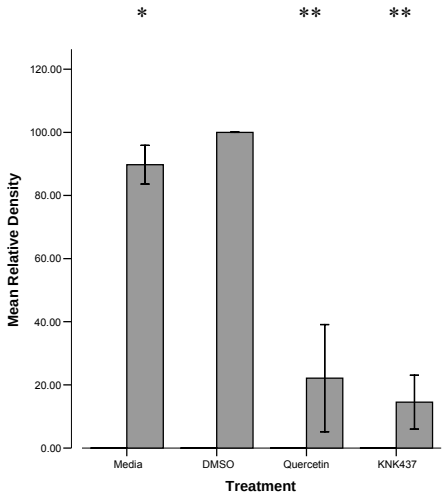

hsp70

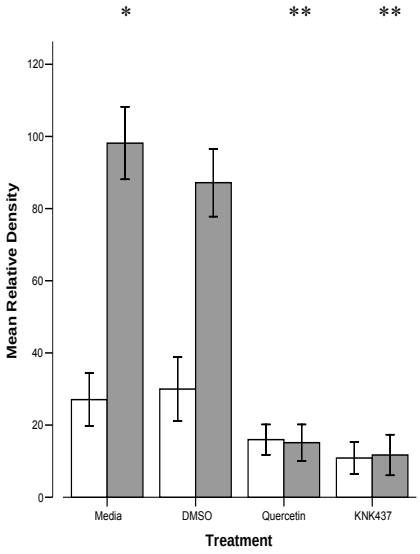

hsp47

8A

* ** **

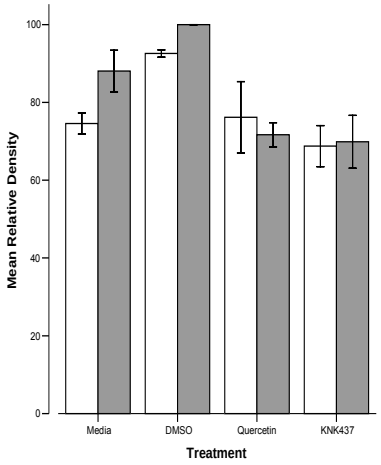

hsc70

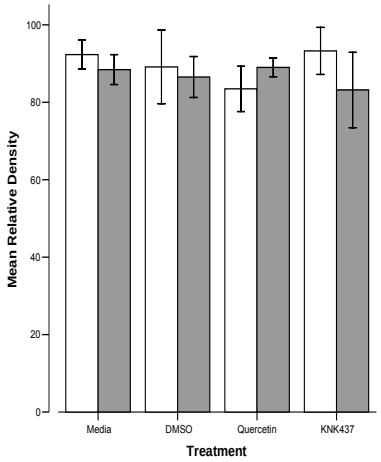

ef1α

8B

Figure 9. Effect of HSR inhibitors on the heat shock-induced accumulation of HSP30 and actin in A6 cells. A6 cells were exposed to 100 μM quercetin or KNK437 dissolved in 0.1% DMSO (vehicle) or vehicle alone for 6 h at 22^{o}C prior to a 2 h 33^{o}C heat shock and a 2 h recovery at 22^{o}C. Cells were then harvested and total protein was isolated. Total protein (10 - 40 μg) was analyzed by immunoblotting using HSP30 and actin antibodies. A Ponceau-S reversible blot stain is shown in the bottom panel to confirm equal loading and quality of transfer. C and H represent control (22^{o}C) and heat shock (33^{o}C) conditions, respectively.

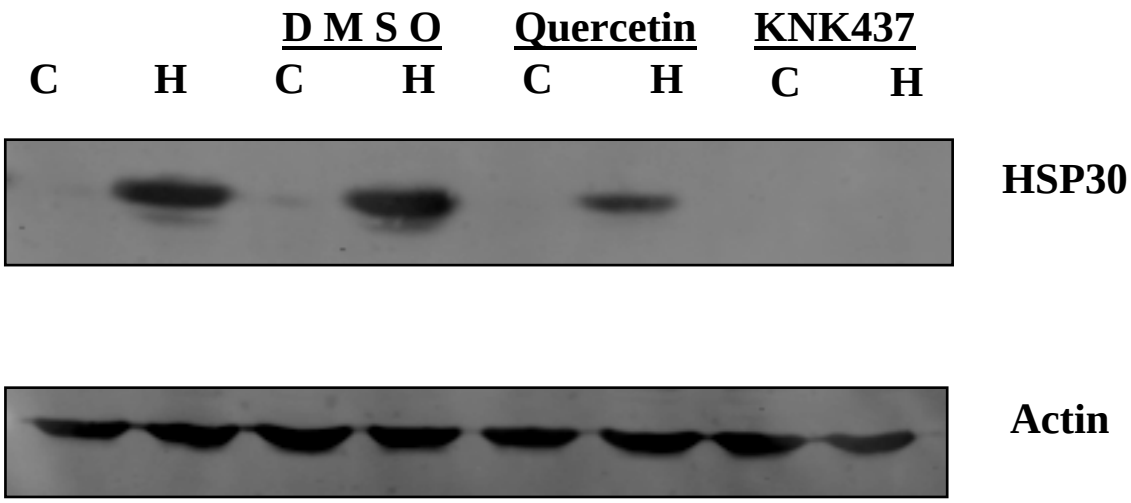
D M S O
Quercetin
KNK437
C
H
C
H
C
H
C
H
HSP30
Actin

Figure 10. Effect of HSR inhibitors on the heat shock-induced accumulation of HSP30 and actin in A6 cells. ImageJ (1.24o) software was used for densitometric analysis of HSP30 and actin protein bands on immunoblot images. Control (open bars) and heat shock (solid bars) treatment data were expressed as a percentage of the maximum binding within each blot then graphed as mean +/- standard error. Significant differences annotated between untreated cells at 22ºC and 33ºC (*, $P < 0.001$) and between DMSO-treated cells and HSR inhibitor-treated cells at 33ºC (**, $P < 0.001$).

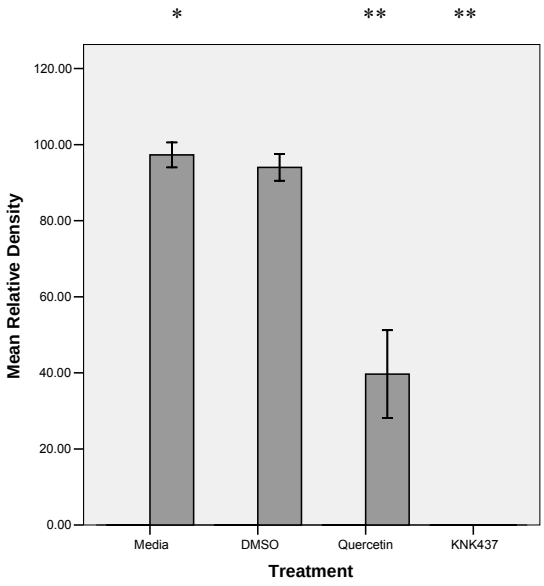
*
**
**
120.00
100.00
80.00
60.00
40.00
20.00
0.00
Mean Relative Density
Media
DMSO
Quercetin
KNK437
Treatment

HSP30

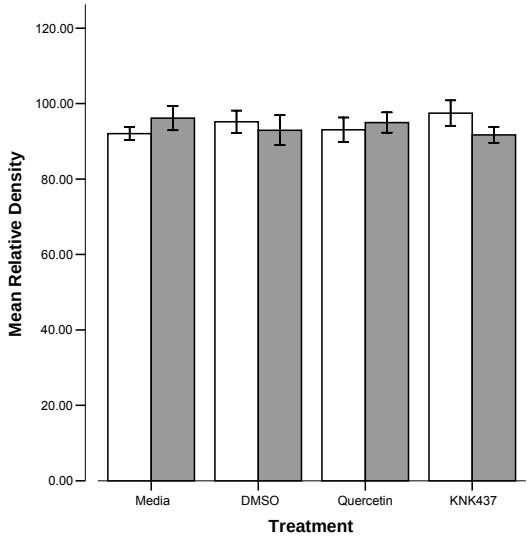
120.00
100.00
80.00
60.00
40.00
20.00
0.00
Mean Relative Density
Media
DMSO
Quercetin
KNK437
Treatment

Actin

Figure 11. The effect of HSR inhibitors, quercetin and KNK437, at 22ºC on HSP30 and F-actin localization in *Xenopus* A6 cells using LSCM. A6 cells were grown on glass coverslips in L-15 media alone (A-C) or with 0.1% DMSO as a vehicle (D-F) for 100 μM quercetin (G-I) or 100 μM KNK437 (J-L) at 22ºC. Actin was directly detected by staining with TRITC (red). HSP30 was indirectly detected with an anti-HSP30 primary antibody and FITC secondary antibody conjugate (green). As expected, images did not indicate detectable levels of HSP30 for cells maintained at 22ºC. From left to right, columns indicate fluorescence detection channels for HSP30 and actin, and a second, separate example of actin staining. Control conditions (A-C) show intact actin stress fibers and arrows indicate well defined and separated sites of substrate adhesion at the cell periphery. Exposure to DMSO (D-F), quercetin (G-I), or KNK437 (J-L) did not show an observable effect on actin stress fibers in cells maintained at 22ºC.

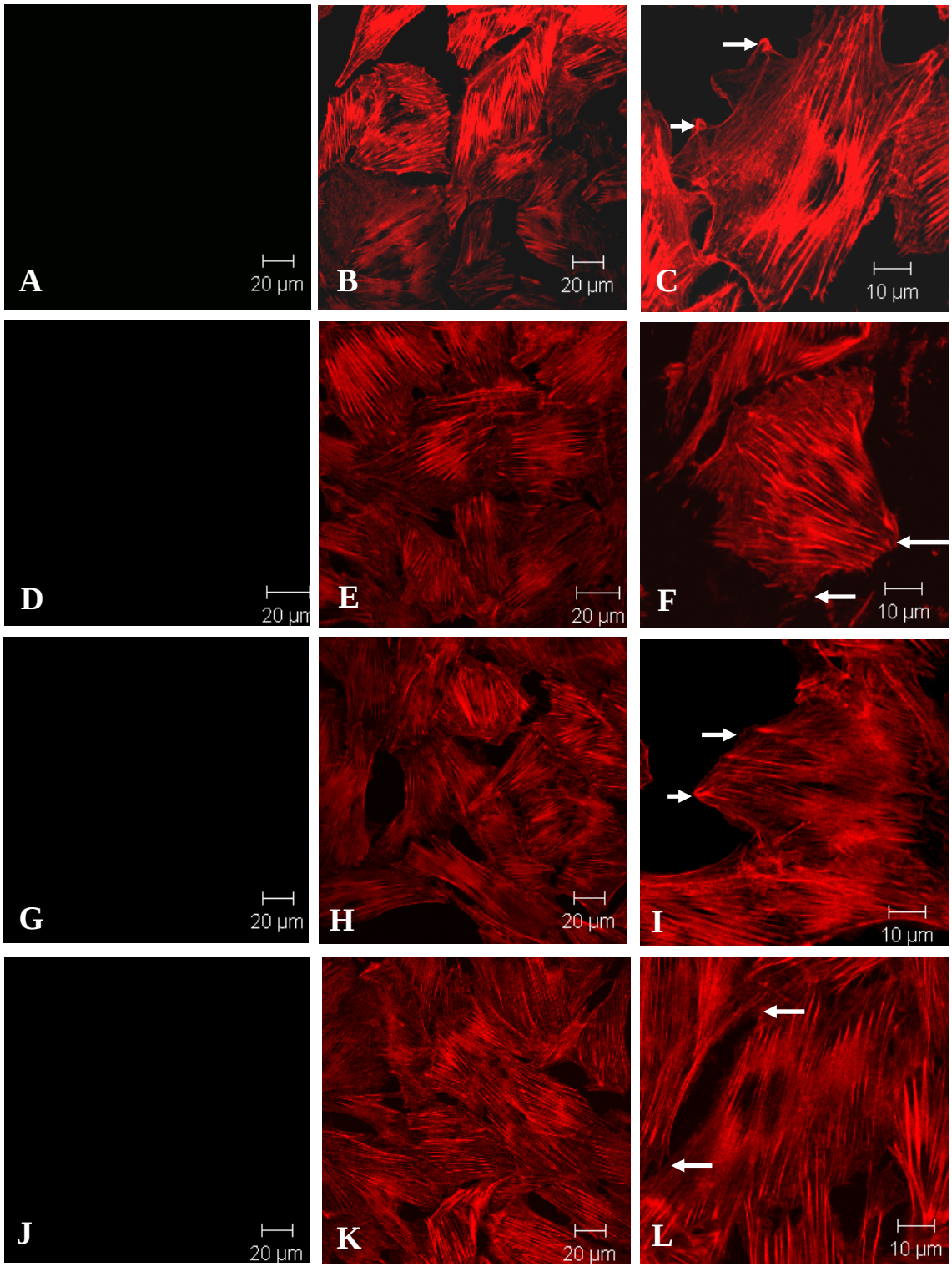
A
20 µm
B
20 µm
C
10 µm
D
20 µm
E
20 µm
F
10 µm
G
20 µm
H
20 µm
I
10 µm
J
20 µm
K
20 µm
L
10 µm

Figure 12. The effect of 2 h heat shock at 33ºC on HSP30 and F-actin localization in *Xenopus* A6 cells using LSCM. A6 cells were grown on glass coverslips in L-15 media alone (A-C and G-I) or with 0.1% DMSO (D-F and J-L) at 22ºC (A-F) and or heat shocked for 2 h at 33ºC (G-L) followed by a 2 h recovery period at 22ºC. Actin was directly detected by staining with TRITC (red). HSP30 was indirectly detected with an anti-HSP30 primary antibody and FITC secondary antibody conjugate (green). From left to right, columns indicate fluorescence detection channels for HSP30, actin, and merged images respectively. In comparison to cells maintained at 22ºC (A-F), cells heat shocked at 33ºC showed detectable levels of HSP30 throughout the cytoplasm (G, I, J, L).

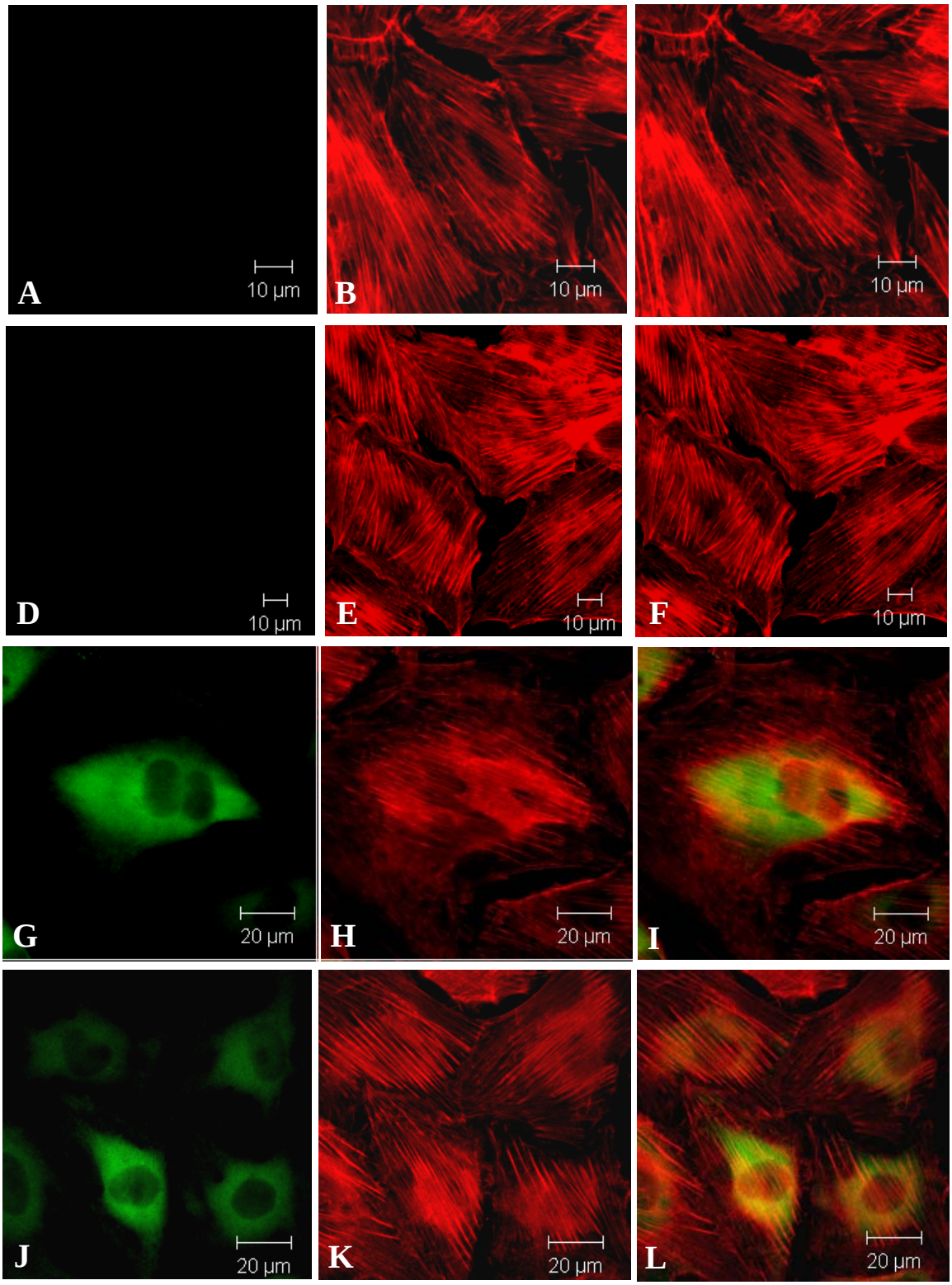
A
10 µm
B
10 µm
10 µm
D
10 µm
E
10 µm
F
10 µm
G
20 µm
H
20 µm
I
20 µm
J
20 µm
K
20 µm
L
20 µm

Figure 13. The effect of HSR inhibitors during a 2 h heat shock at 33ºC on HSP30 and F-actin localization in *Xenopus* A6 cells using LSCM. A6 cells were grown on glass coverslips in L-15 media with 0.1% DMSO as a vehicle and either 100 μM quercetin (A-C and G-I) or 100 μM KNK437 (D-F and J-L) at 22ºC (A-F) or heat shocked for 2 h at 33ºC (G-L) followed by a 2 h recovery period at 22ºC. Actin was directly detected by staining with TRITC (red). HSP30 was indirectly detected with an anti-HSP30 primary antibody and FITC secondary antibody conjugate (green). From left to right, columns indicate fluorescence detection channels for HSP30, actin, and merged images respectively. In 1-10% of cells treated with KNK437, slight disruptions in actin stress fibers and possible aggregation of actin at the cell periphery were observed (arrows).

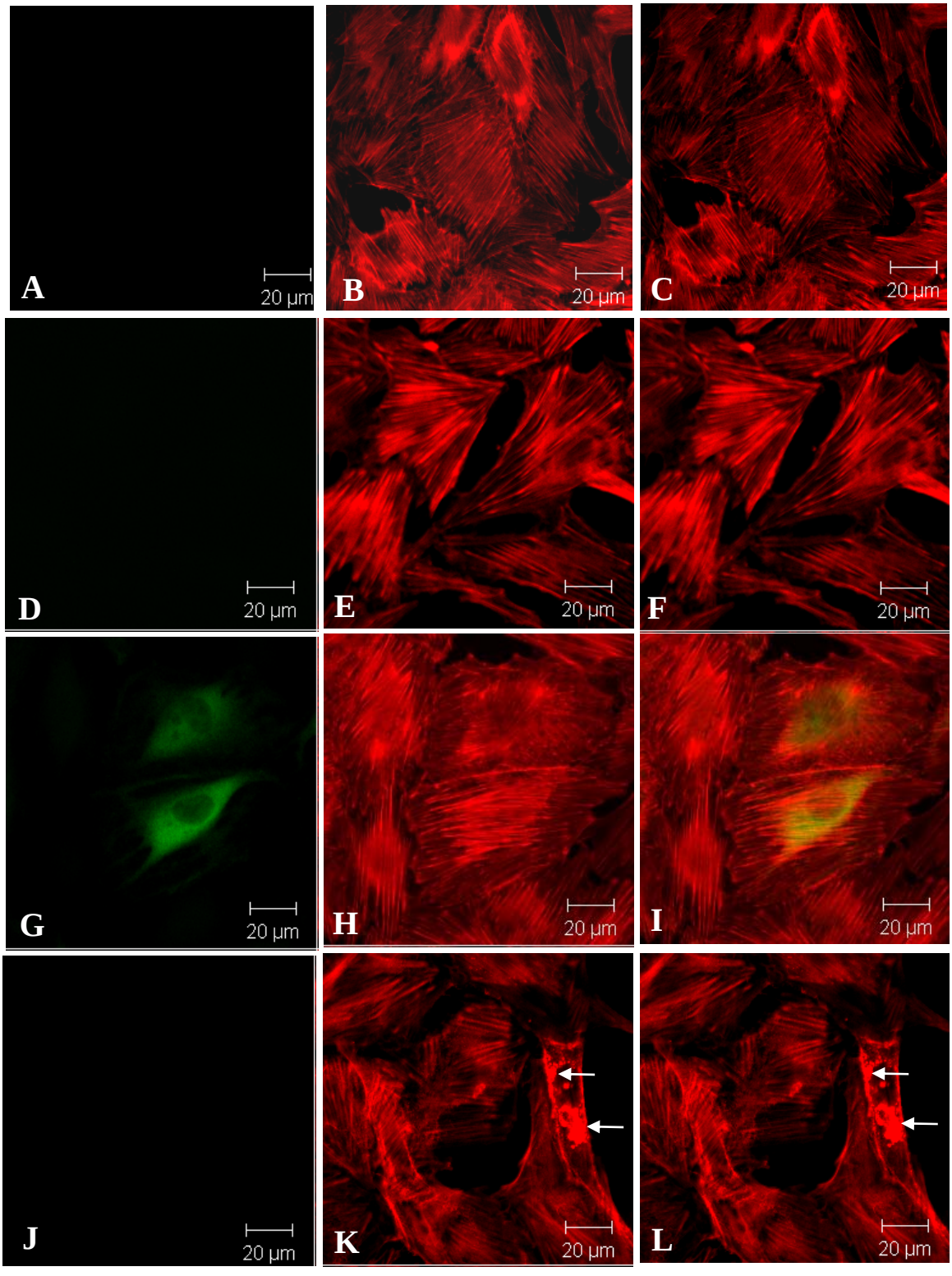
A
20 µm
B
20 µm
C
20 µm
D
20 µm
E
20 µm
F
20 µm
G
20 µm
H
20 µm
I
20 µm
J
20 µm
K
20 µm
L
20 µm

Figure 14. The effect of HSR inhibitors during a 2 h heat shock at 35ºC on HSP30 and F-actin localization in *Xenopus* A6 cells using LSCM. A6 cells were grown at 22ºC on glass coverslips in L-15 media with 0.1% DMSO as a vehicle (A-L) and 100 μM quercetin (G-I) or 100 μM KNK437 (J-L). Cells were heat shocked for 2 h at 35ºC (D-L), followed by a 2 h recovery period at 22ºC. Actin was directly detected by staining with TRITC (red) whereas HSP30 was indirectly detected with an anti-HSP30 primary antibody and FITC secondary antibody conjugate (green). From left to right, columns indicate fluorescence detection channels for HSP30, actin, and merged images respectively.

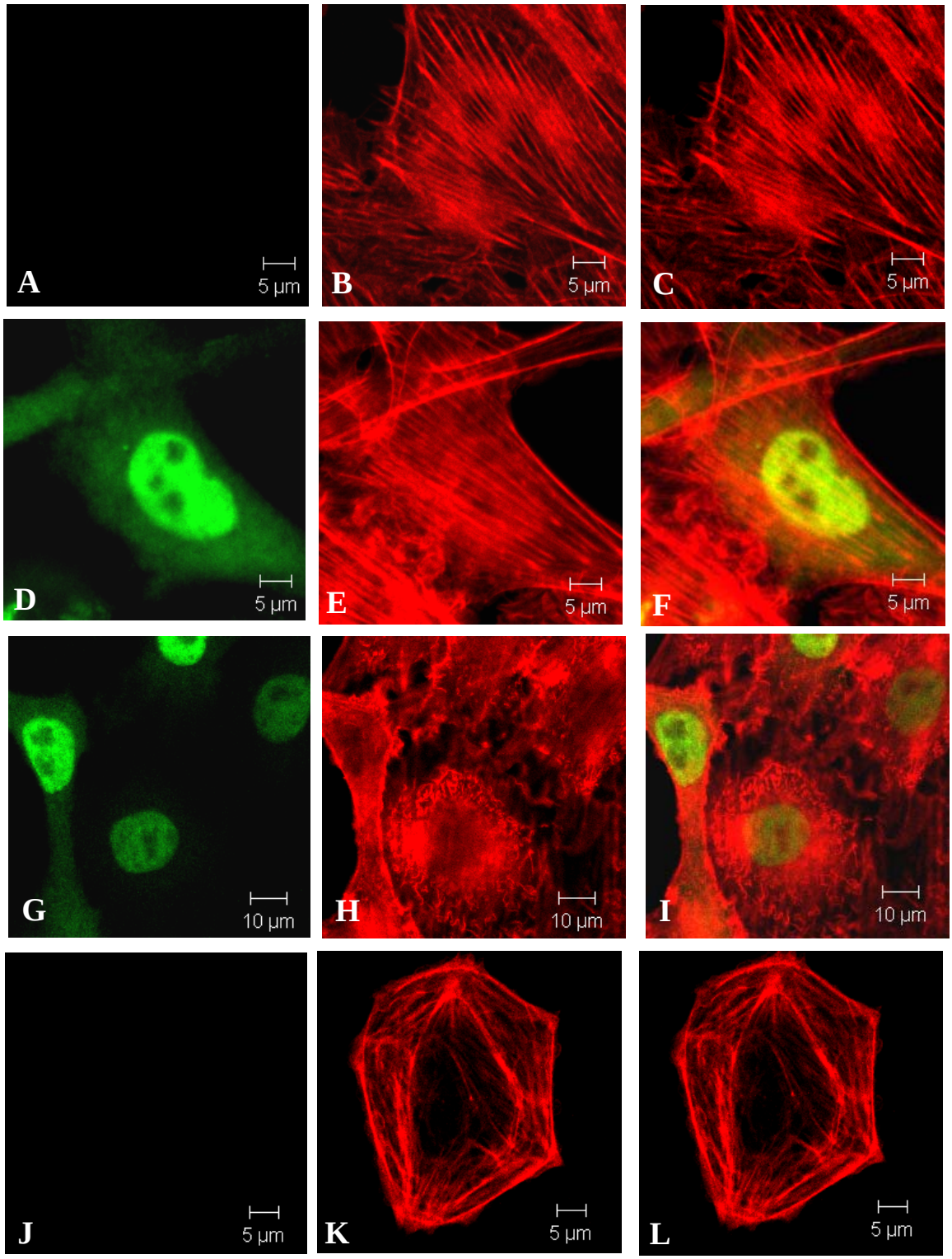
A
5 µm
B
5 µm
C
5 µm
D
5 µm
E
5 µm
F
5 µm
G
10 µm
H
10 µm
I
10 µm
J
5 µm
K
5 µm
L
5 µm

Figure 15. **The effect of HSR inhibitors during a 4 h heat shock at 35ºC on HSP30 and F-actin localization in *Xenopus* A6 cells using LSCM.** A6 cells were grown at 22ºC on glass coverslips in L-15 media with 0.1% DMSO as a vehicle (A-L) and 100 μM quercetin (G-I) or 100 μM KNK437 (J-L). Cells were heat shocked (D-L) for 4 h at 35ºC followed by a 2 h recovery period at 22ºC. Actin was directly detected by staining with TRITC (red). HSP30 was indirectly detected with an anti-HSP30 primary antibody and FITC secondary antibody conjugate (green). From left to right, columns indicate fluorescence detection channels for HSP30, actin, and merged images respectively. Cells treated with quercetin showed changes in the actin cytoskeleton marked by the appearance of membrane blebs at the cellular periphery (G-I, arrows), whereas cells treated with KNK437 showed aggregates of actin at the periphery with the appearance of numerous microspikes (K-L, arrows).

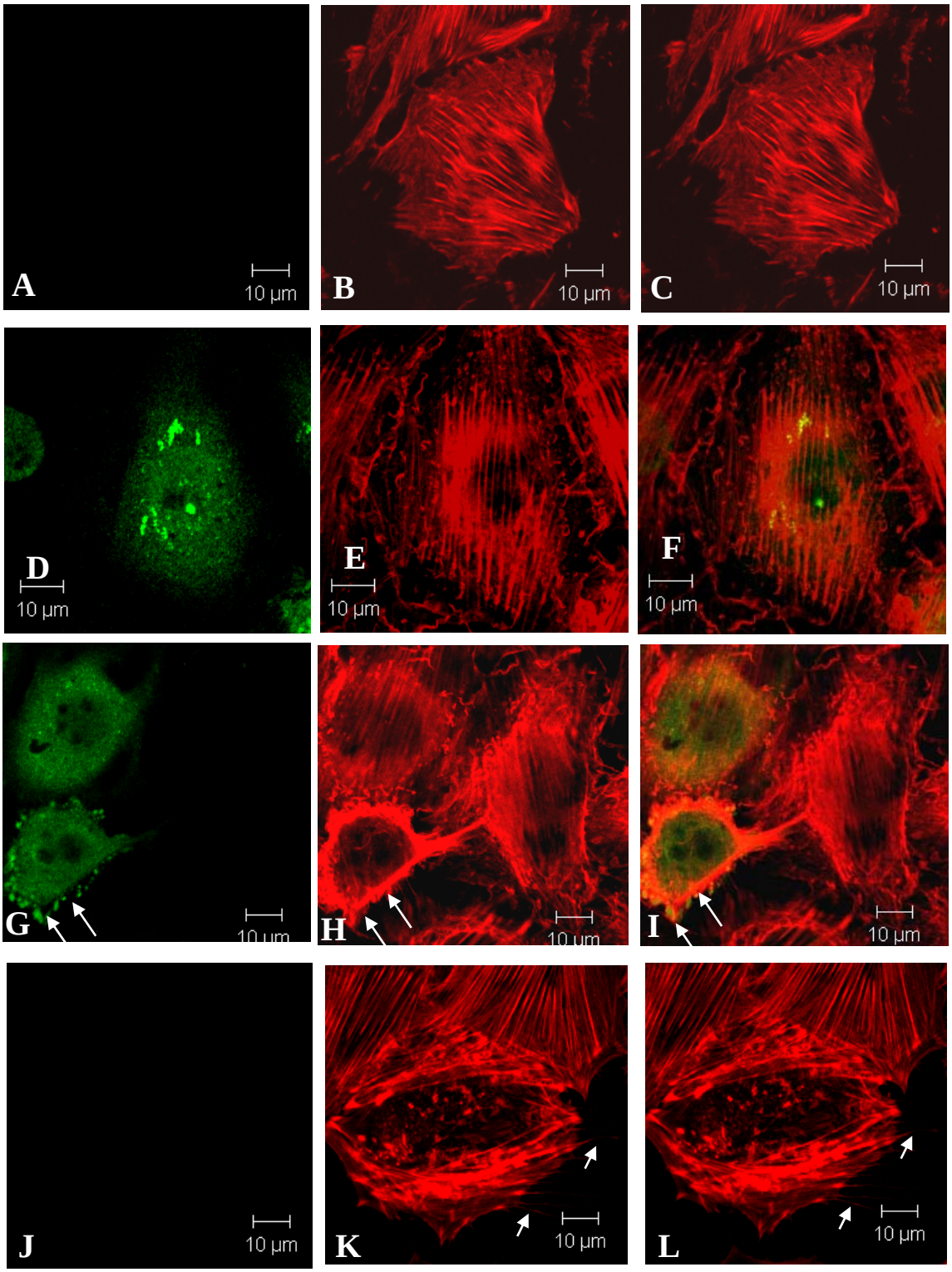
A
10 µm
B
10 µm
C
10 µm
D
10 µm
E
10 µm
F
10 µm
G
10 µm
H
10 µm
I
10 µm
J
10 µm
K
10 µm
L
10 µm

Figure 16. The effect of quercetin during a 4 h heat shock at 35ºC on HSP30 and F-actin localization in *Xenopus* A6 cells using LSCM. A6 cells were grown at 22ºC on glass coverslips in L-15 media with 0.1% DMSO as vehicle (A-F) and 100 μM quercetin (D-F). Cells were heat shocked for 4 h at 35ºC followed by a 2 h recovery period at 22ºC. Actin was directly detected by staining with TRITC (red). HSP30 was indirectly detected with an anti-HSP30 primary antibody and FITC secondary antibody conjugate (green). Optical slices were taken through cells, merged into a 3-channel, 3-D projected image, and rotated to show the bottom (A-C) and top (D-F) views. Arrows indicate the presence of a distinct pattern of HSP30 accumulation in cells exposed to quercetin only.

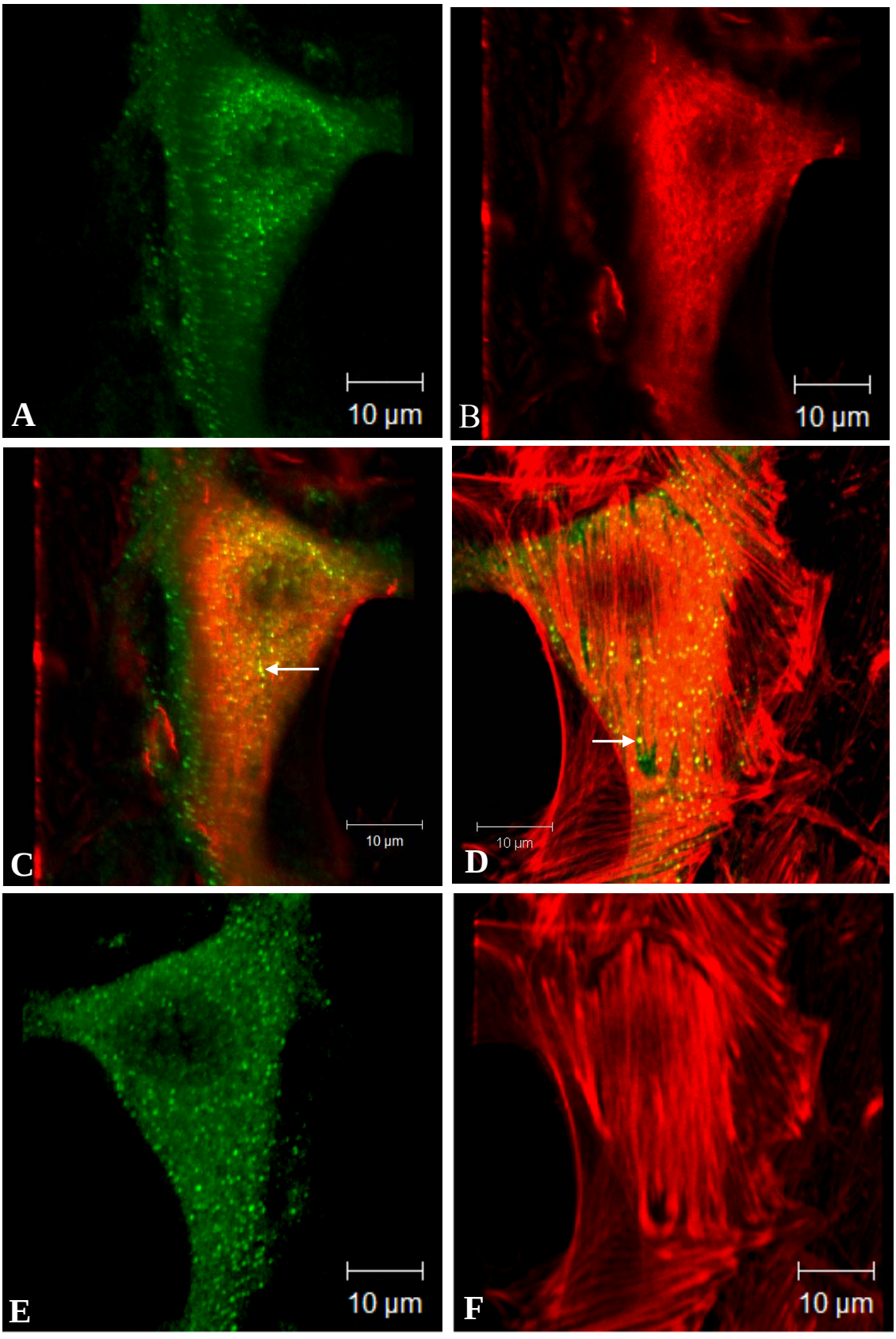
A
10 µm
B
10 µm
C
10 µm
D
10 µm
E
10 µm
F
10 µm

Figure 17. The emergence of long actin-based protrusions during a 2 h heat shock at 33ºC in *Xenopus* A6 cells using LSCM. A6 cells were grown at 22ºC on glass coverslips in L-15 media with 0.1% DMSO as a vehicle and 100 µM quercetin. Cells were heat shocked for 2 h at 33ºC, followed by a 2 h recovery period at 22ºC. Actin and the nucleus were directly detected by staining with TRITC (red) and DAPI (blue) respectively. HSP30 was indirectly detected with an anti-HSP30 primary antibody and FITC secondary antibody conjugate (green). Top and bottom images show elongated actin-based fibers extending from each end of the same cell towards other congregated cells.

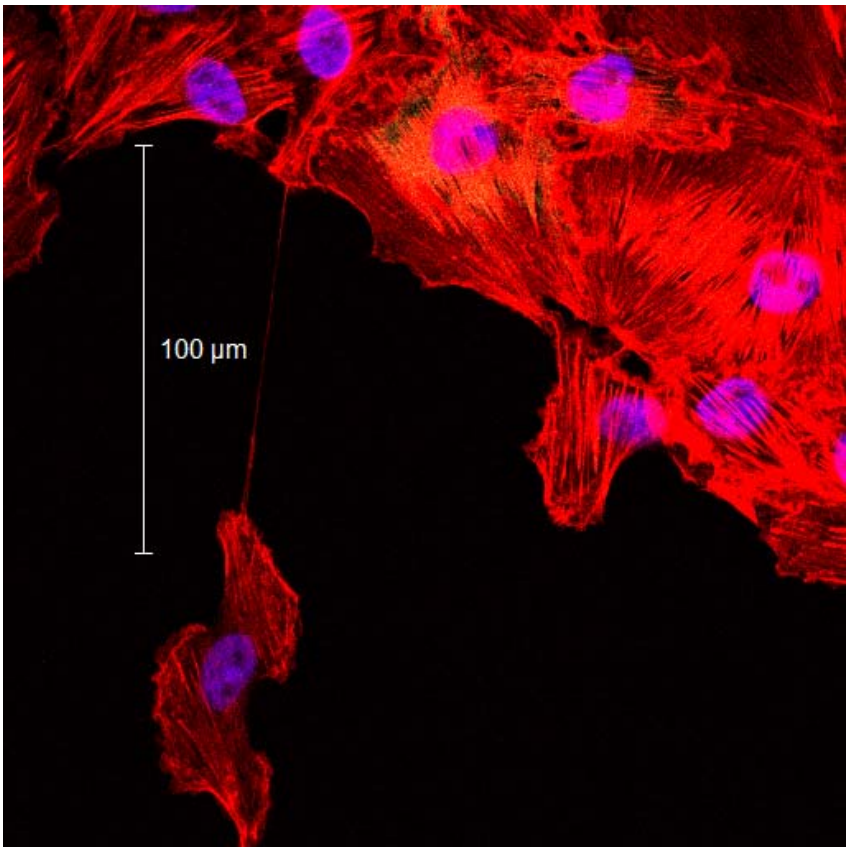
100 µm

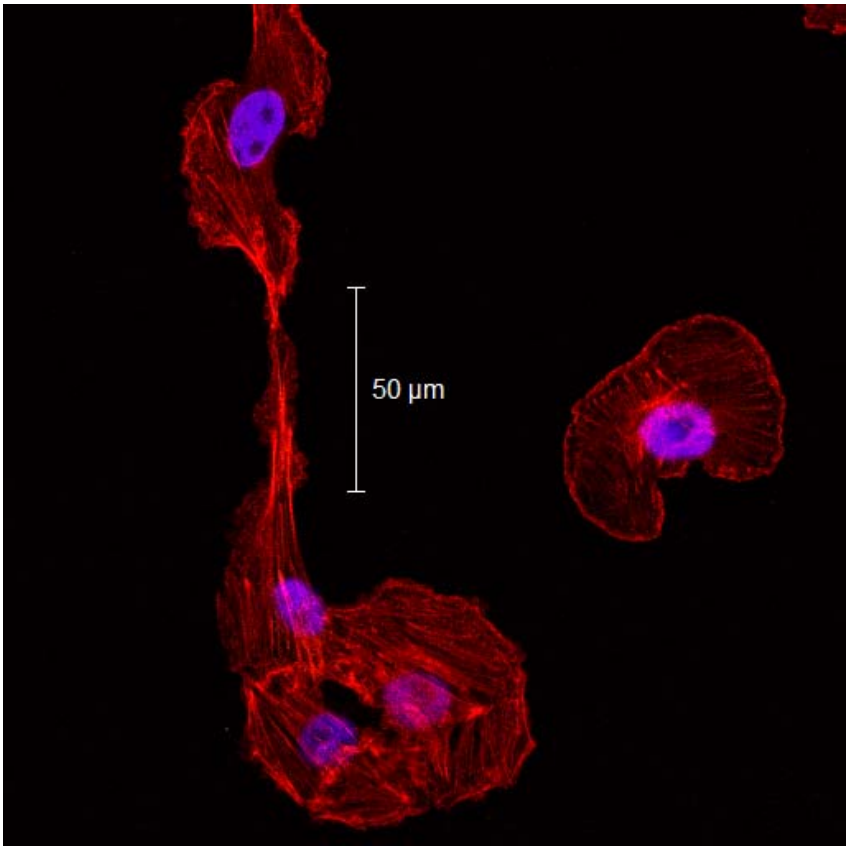
50 µm

Figure 18. The effect of a 1 h thermal challenge at 37ºC, with and without a prior 2 h heat shock at 33ºC, on HSP30 and F-actin localization in *Xenopus* A6 cells using LSCM. A6 cells were grown at 22ºC on glass coverslips in L-15 media with 0.1% DMSO as a vehicle (A-P). Control cells (A-D) were maintained at 22ºC for up to 14 h in DMSO. Cells were heat shocked for 2 h at 33ºC, followed by a 2 h recovery at 22ºC, then immediately fixed (E-H) or then further heat shocked for 1 h at 37ºC followed by a 2 h recovery period at 22ºC (I-L). Cells without a prior heat shock exposure at 33ºC were directly challenged for 1 h at 37ºC, followed by a 2 h recovery at 22ºC (M-P). Actin and the nucleus were directly detected by staining with TRITC (red) and DAPI (blue) respectively. HSP30 was indirectly detected with an anti-HSP30 primary antibody and FITC secondary antibody conjugate (green). From left to right, columns indicate fluorescence detection channels for HSP30, actin, nucleus, and merged images respectively. At 37ºC, the appearance of microspikes was evident (L and P, arrows). In comparison to cells given a 33ºC pretreatment, cells directly challenged 1 h at 37ºC showed a marked decrease in HSP30, which was located predominantly at the cellular periphery with actin (M-P).

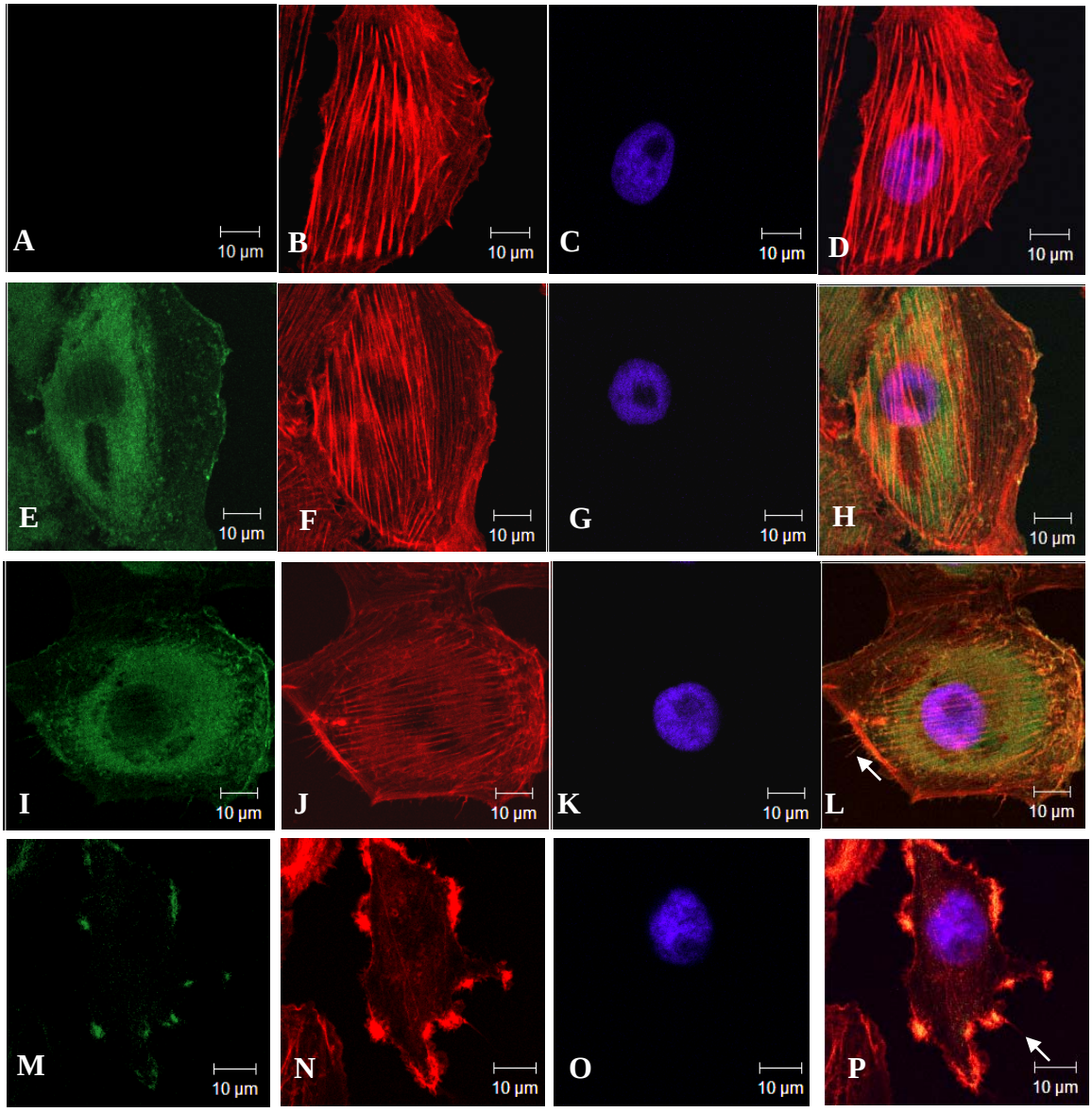
A
10 µm
B
10 µm
C
10 µm
D
10 µm
E
10 µm
F
10 µm
G
10 µm
H
10 µm
I
10 µm
J
10 µm
K
10 µm
L
10 µm
M
10 µm
N
10 µm
O
10 µm
P
10 µm

Figure 19. The effect of KNK437 during a 1 h thermal challenge at 37ºC, with and without a prior 2 h heat shock at 33ºC, on HSP30 and F-actin localization in *Xenopus* A6 cells using LSCM. A6 cells were grown at 22ºC on glass coverslips in L-15 media with 100 μM KNK437 in 0.1% DMSO (A-P). Control cells (A-D) were maintained at 22ºC for up to 14 h in DMSO. Cells were heat shocked for 2 h at 33ºC, followed by a 2 h recovery at 22ºC, then immediately fixed (E-H) or further then heat shocked for 1 h at 37ºC followed by a 2 h recovery period at 22ºC (I-L). Cells without a prior heat shock exposure at 33ºC were directly challenged for 1 h at 37ºC, followed by a 2 h recovery at 22ºC (M-P). Actin and the nucleus were directly detected by staining with TRITC (red) and DAPI (blue) respectively. HSP30 was indirectly detected with an anti-HSP30 primary antibody and FITC secondary antibody conjugate (green). From left to right, columns indicate fluorescence detection channels for HSP30, actin, nucleus, and merged images respectively. Cells heat shocked for 2 h at 33ºC showed intact stress fibers spanning cells, but at the cellular periphery displayed ruffled edges in areas of cell-cell contact (E-H, arrows). Cells further heat shocked for 1 h at 37ºC showed increased ruffling at edges accompanied by aggregates of disrupted actin fibers (I-L, arrows). Cells directly challenged for 1 h at 37ºC showed virtually no intact stress fibers after having degenerated into aggregates (M-P).

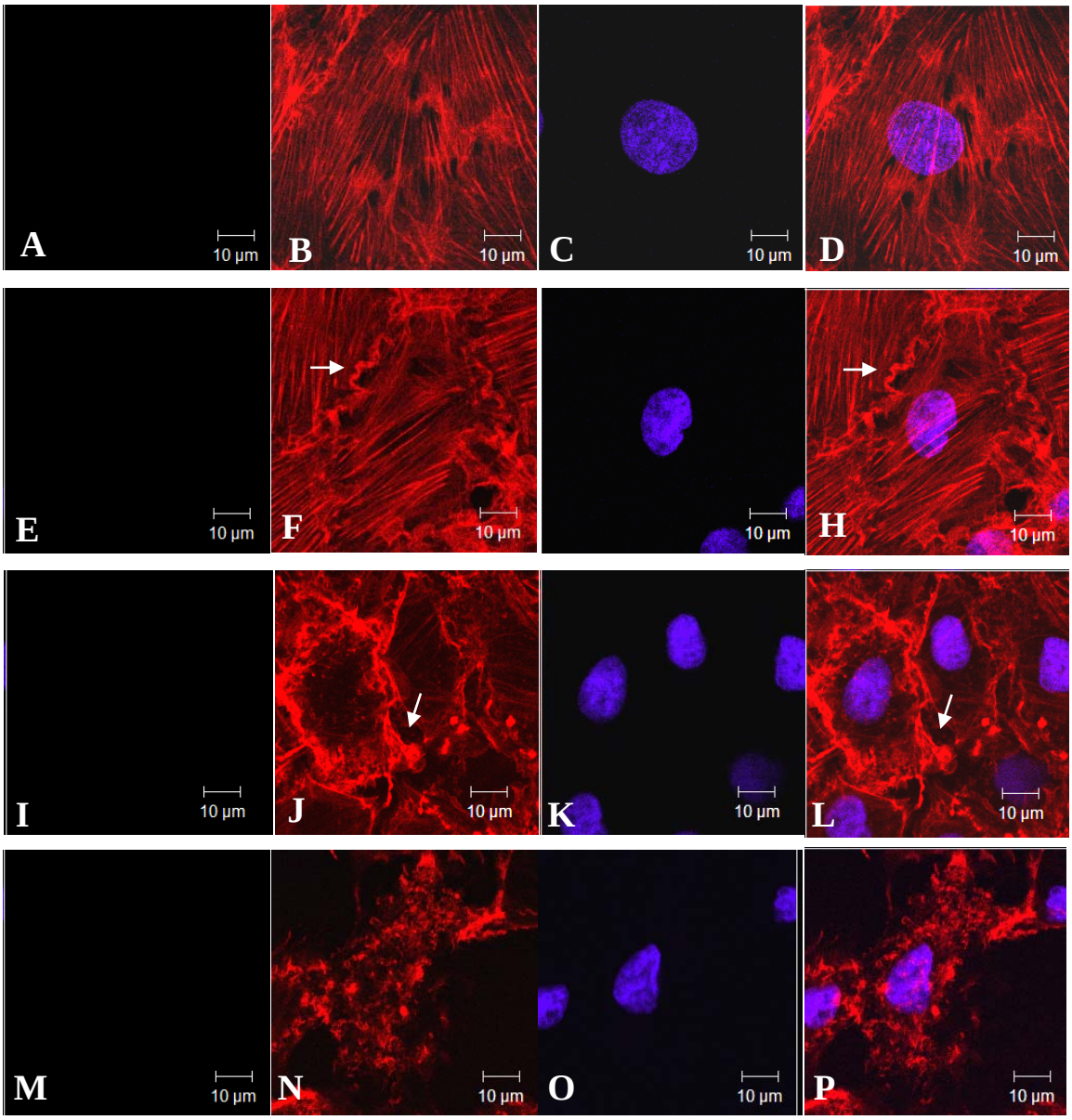
A
10 µm
B
10 µm
C
10 µm
D
10 µm
E
10 µm
F
10 µm
10 µm
H
10 µm
I
10 µm
J
10 µm
K
10 µm
L
10 µm
M
10 µm
N
10 µm
O
10 µm
P
10 µm

Figure 20. The effect of a 1 h thermal challenge at 37ºC, with a prior 2 h heat shock at 33ºC, on HSP30 and F-actin localization in *Xenopus* A6 cells using LSCM. A6 cells were grown at 22ºC on glass coverslips in L-15 media with 0.1% DMSO (A-D) and 100 μM KNK437 (C-D). Cells were heat shocked for 2 h at 33ºC, followed by a 2 h recovery at 22ºC, then further heat shocked for 1 h at 37ºC, followed by a 2 h recovery period at 22ºC. Actin and the nucleus were directly detected by staining with TRITC (red) and DAPI (blue) respectively. HSP30 was indirectly detected with an anti-HSP30 primary antibody and FITC secondary antibody conjugate (green). Optical slices were taken through the cells, merged into a 3-channel, 3-D projected image, and rotated to show top (A and C) and bottom (B and D) views to indicate distribution of HSP30 throughout cells.

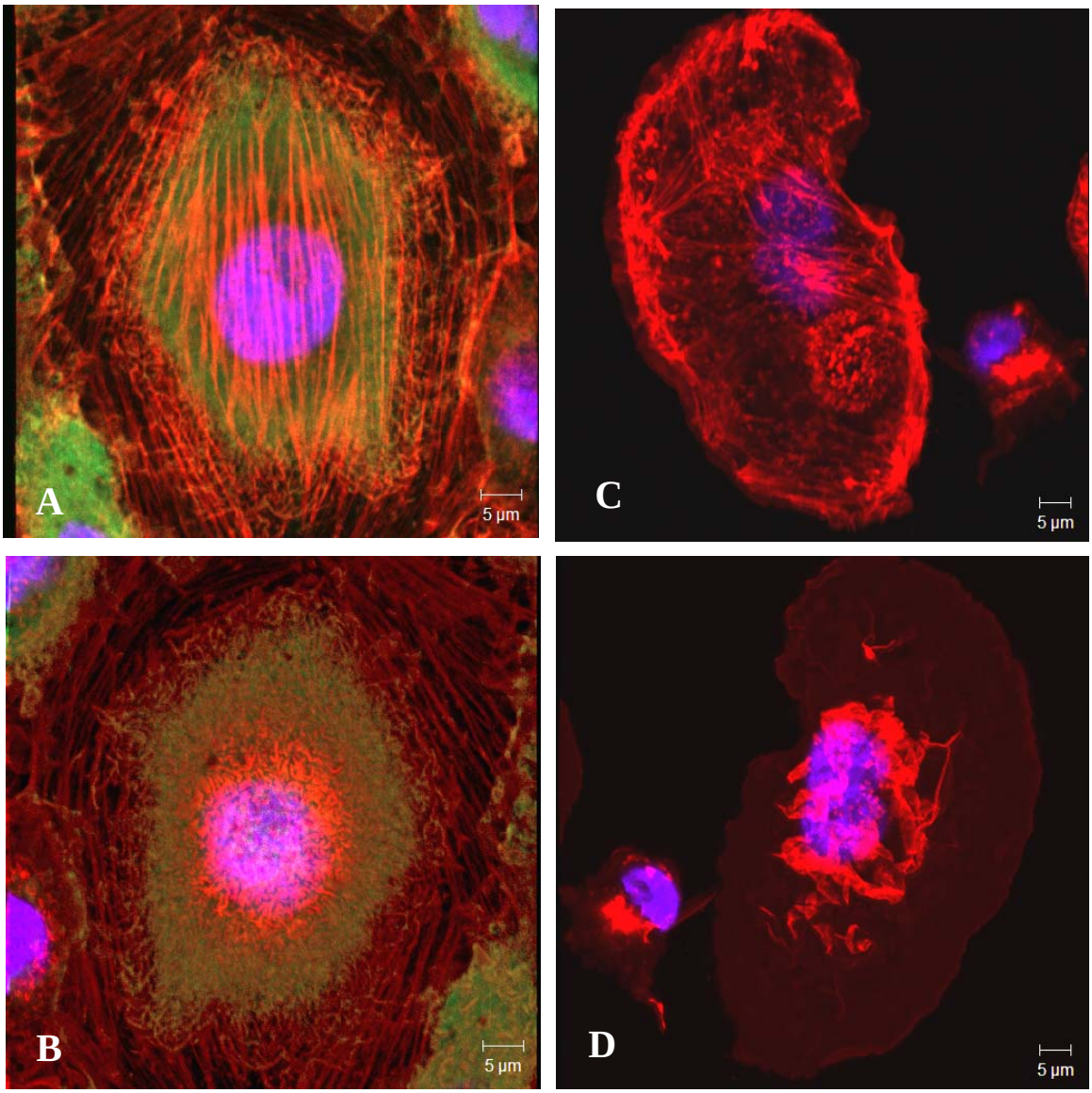
A
5 µm
C
5 µm
B
5 µm
D
5 µm

Figure 21. The effect of a 1 h thermal challenge at 37ºC, with (top) and without (bottom) a prior 2 h heat shock at 33ºC, on HSP30 and F-actin localization in *Xenopus* A6 cells treated with KNK437 using LSCM. A6 cells were grown at 22ºC on glass coverslips in L-15 media with 0.1% DMSO as vehicle and 100 μM KNK437. Cells were heat shocked at 33ºC for 2 h, followed by a recovery period of 2 h at 22ºC, then challenged for 1 h at 37ºC, followed by a 2 h recovery at 22ºC. Actin and the nucleus were directly detected by staining with TRITC (red) and DAPI (blue) respectively. HSP30 was indirectly detected with an anti-HSP30 primary antibody and FITC secondary antibody conjugate (green). Arrows show F-actin microspikes, possibly indicating regions of increased substrate contact (top) in comparison to non-adherent ruffled edges (bottom).

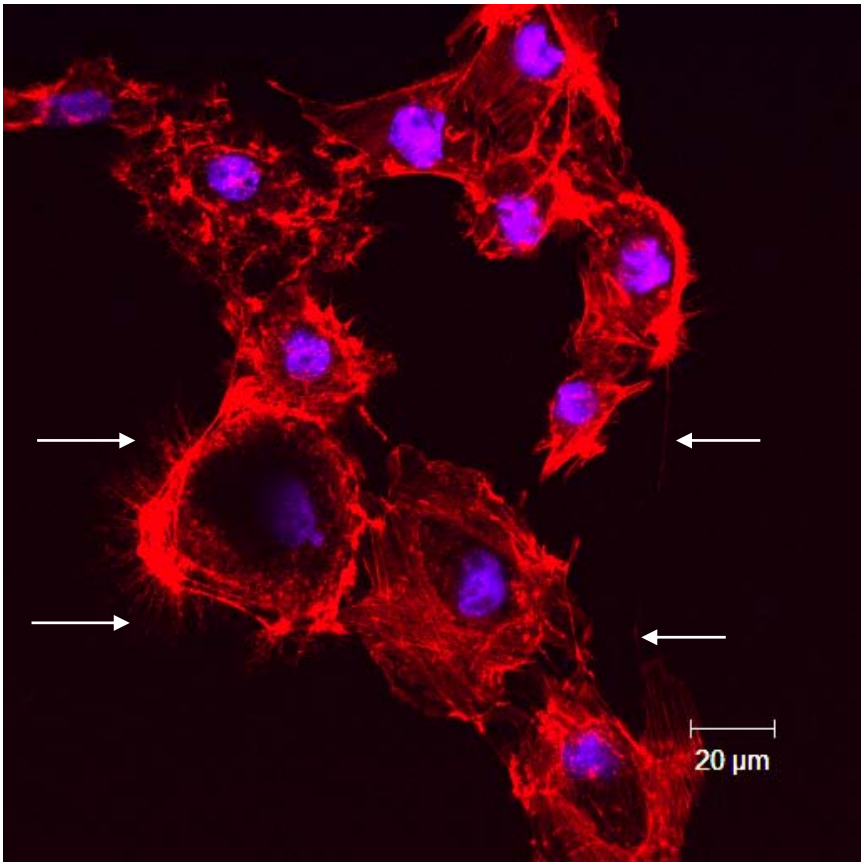
20 µm

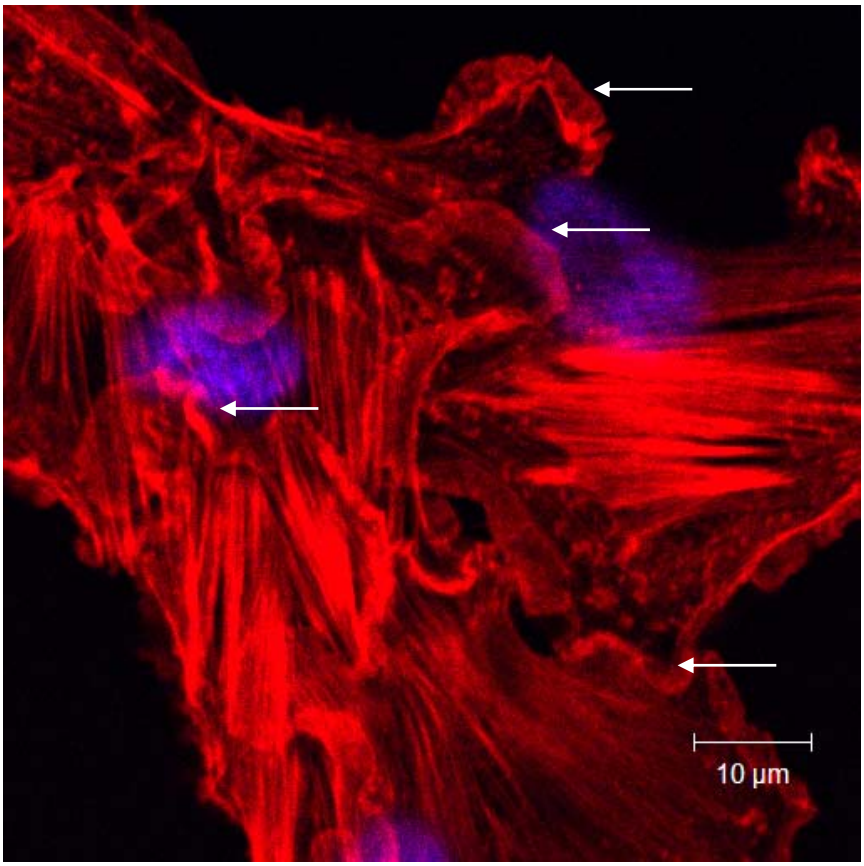
10 µm

Figure 22. The effect of a 1 h thermal challenge at 37ºC, with (top) and without (bottom) a prior 2 h recovery at 22ºC (after heat shock pretreatment at 33ºC) on HSP30 and F-actin localization in *Xenopus* A6 cells using LSCM. A6 cells were grown at 22ºC on glass coverslips in L-15 media. Cells were heat shocked at 33ºC for 2 h, with (top) and without (bottom) a recovery period of 2 h at 22ºC, then challenged for 1 h at 37ºC, followed by a 2 h recovery at 22ºC. Actin and the nucleus were directly detected by staining with TRITC (red) and DAPI (blue) respectively. HSP30 was indirectly detected with an anti-HSP30 primary antibody and FITC secondary antibody conjugate (green). Top panel shows view at the plasma membrane (A) and just below (B) with arrows indicate F-actin cytoskeletal extensions with HSP30. Bottom panel shows view at the plasma membrane (C) and just below (D) with arrows indicate membrane blebs with collapsed actin bundles surrounding cytoplasmic HSP30. Arrows in the top panels (A and B) show a wider actin protrusion from the cell periphery with cytoplasmic HSP30 in the centre.

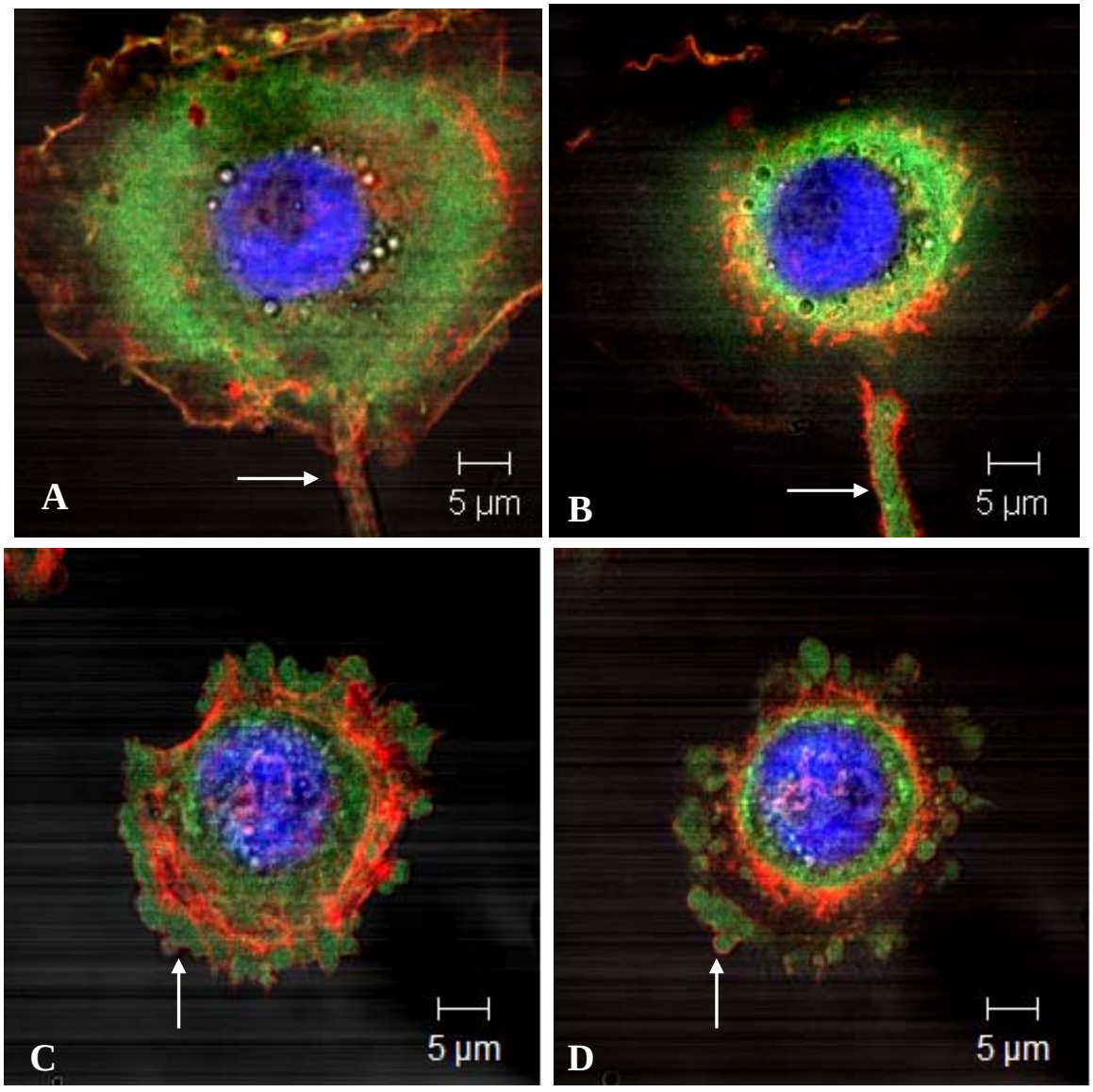
A
5 µm
B
5 µm
C
5 µm
D
5 µm

Figure 23. The effect of a 1 h thermal challenge at 37ºC without a prior 2 h recovery at 22ºC (after heat shock pretreatment at 33ºC) on HSP30 and F-actin localization in *Xenopus* A6 cells using LSCM. A6 cells were grown at 22ºC on glass coverslips in L-15 media. Cells were heat shocked at 33ºC for 2 h, without a recovery period of 2 h at 22ºC, then challenged for 1 h at 37ºC, followed by a 2 h recovery at 22ºC. Actin and the nucleus were directly detected by staining with TRITC (red) and DAPI (blue) respectively. HSP30 was indirectly detected with an anti-HSP30 primary antibody and FITC secondary antibody conjugate (green). Optical slices were taken through the cells, merged into a 3-channel, 3-D projected image, and rotated to show side view spanning the adherent side of the cell (indicated by arrows) through to the nucleus (blue).

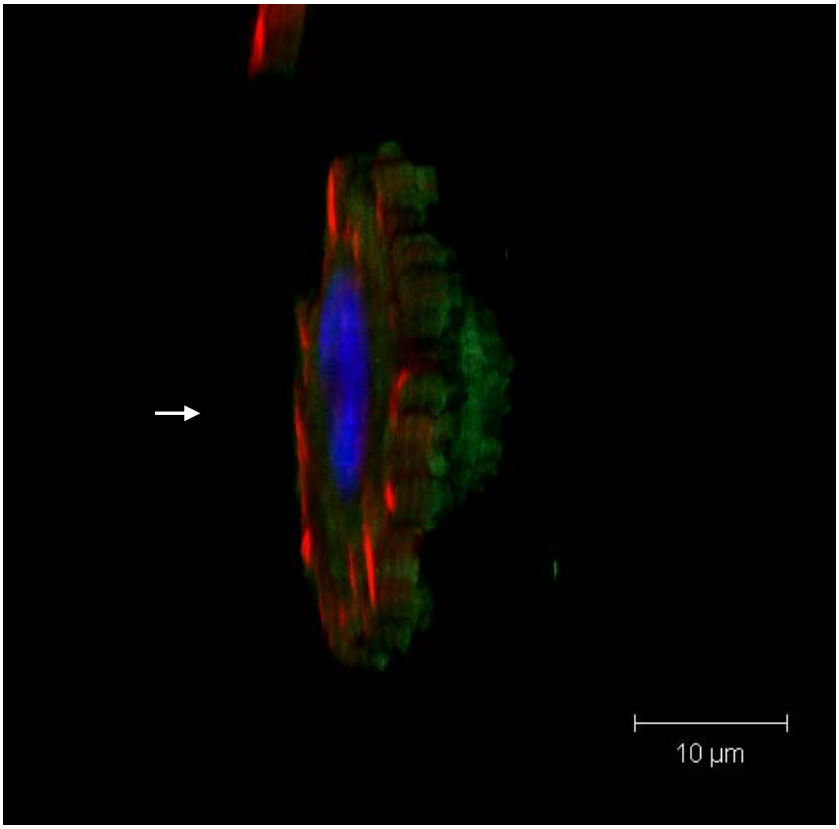
10 µm

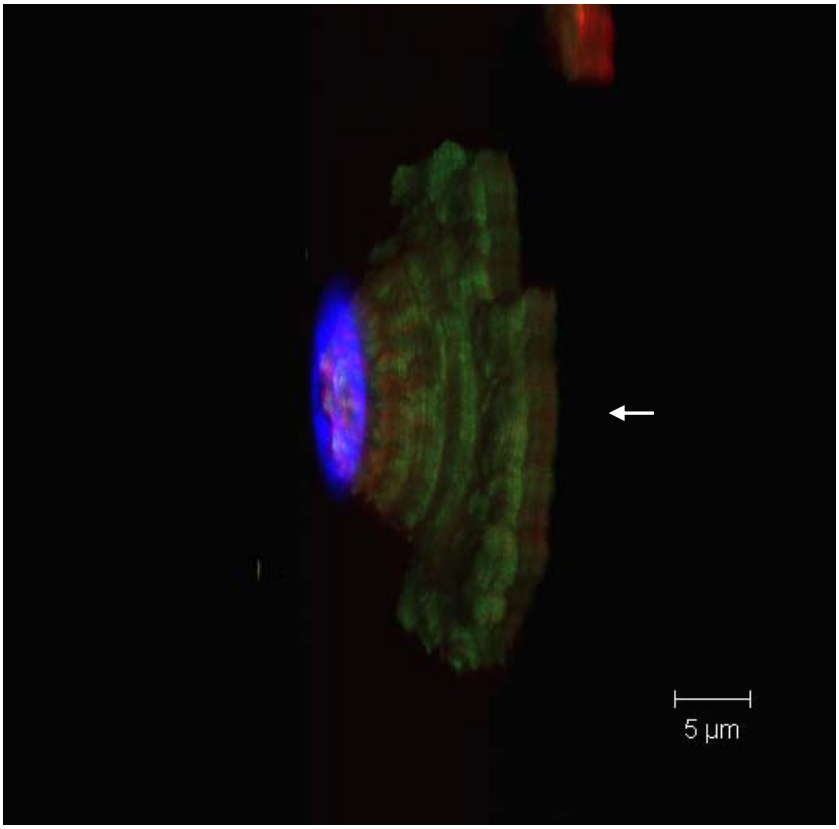
5 µm

Figure 24. The effect of a 1 h thermal challenge at 37ºC, with a prior 2 h heat shock at 33ºC, on HSP30 and F-actin localization in *Xenopus* A6 cells treated with or without KNK437 using LSCM. A6 cells were grown at 22ºC on glass coverslips in L-15 media with 0.1% DMSO as vehicle (A and B) and 100 μM KNK437 (C and D). Cells were heat shocked at 33ºC for 2 h then *immediately* challenged for 1 h at 37ºC, followed by a 2 h recovery at 22ºC. Actin and the nucleus were directly detected by staining with TRITC (red) and DAPI (blue) respectively. HSP30 was indirectly detected with an anti-HSP30 primary antibody and FITC secondary antibody conjugate (green). A stack of optical slices was taken through cells, individual channels and slices were merged into 3-D images, and rotated to view the top (A and C) and bottom (B and D). Arrows show actin in membrane blebs with localized HSP30 (A and B) and actin microspikes in the absence of HSP30.

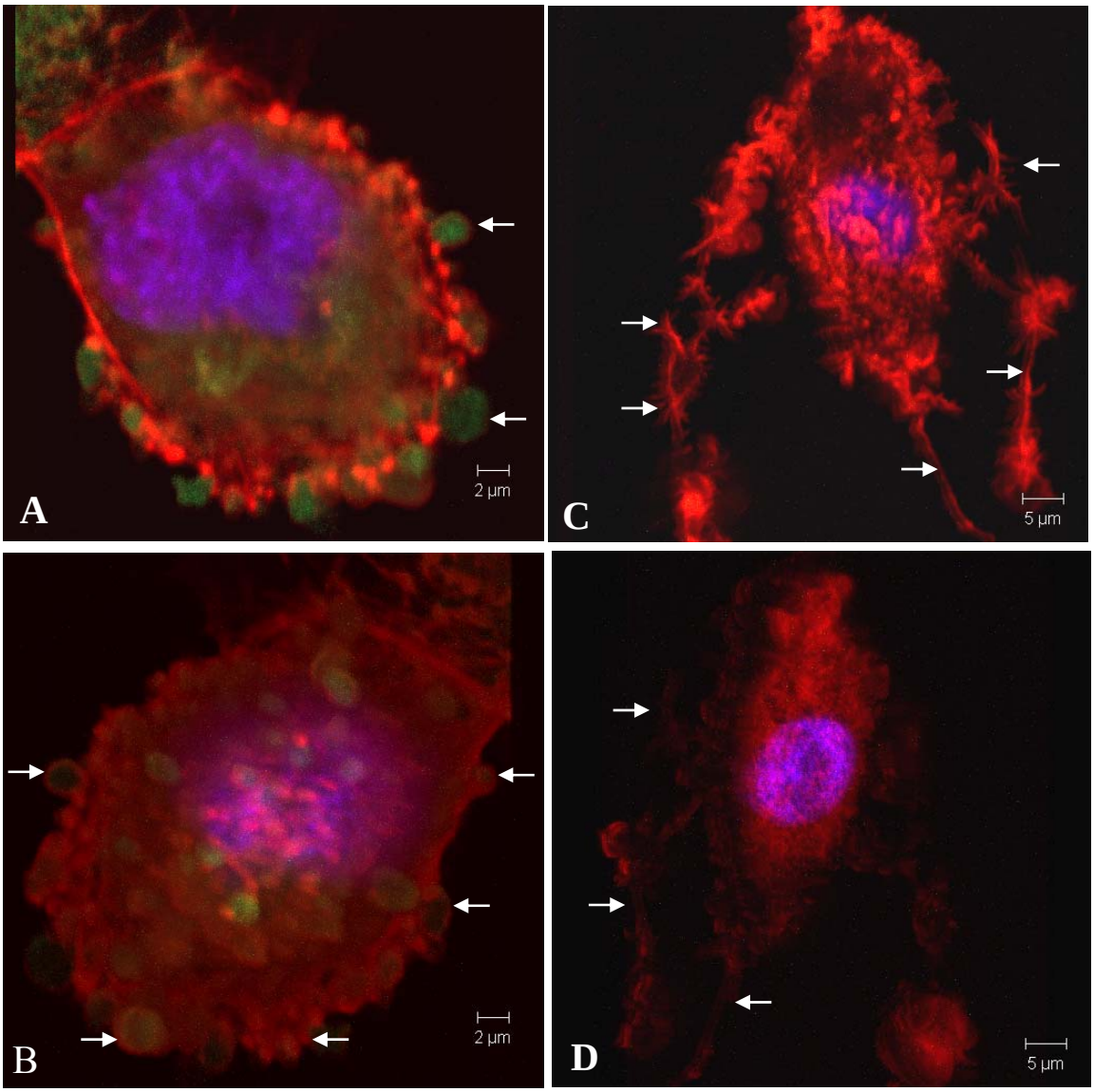
A
2 µm
C
5 µm
B
2 µm
D
5 µm

5. Discussion

The present study has compared for the first time the effect of two HSR inhibitors, quercetin and KNK437, on heat shock protein gene expression in *Xenopus* A6 cells. This is the first study examining quercetin and KNK437 in a non-mammalian system, demonstrating HSR inhibition in poikilotherms comparable to inhibition in rat (Yao *et al,* 2006), mouse (Kabakov *et al.,* 2006), guinea pig (Oksala *et al.,* 2004), monkey (Jakubowicz-Gil et al., 2002), and human systems (Hansen, 1997; Wu and Yu, 2000; Debes *et al.,* 2003). Northern blot and densitometric analysis showed that cells treated with either quercetin or KNK437 decreased the heat shock-induced accumulation of *hsp70, hsp47,* and *hsp30* mRNAs. Additionally, constitutive levels of *hsp47* and *hsc70* mRNAs were reduced. Considering that KNK437 appears to be specific for HSF inhibition, these findings may suggest that HSF activity is involved in the constitutive expression of these *hsp* genes under non-stress conditions. In comparison, neither quercetin nor KNK437 affected the relative levels of constitutively expressed *ef1α* mRNAs under control or heat shock conditions. Western blot and densitometric analysis in this study showed that under heat shock conditions, exposure to quercetin or KNK437 significantly decreased the accumulation of HSP30, and that KNK437 was more effective in doing so than quercetin. In comparison, relative levels of F-actin were not significantly affected by either heat shock or exposure to DMSO, quercetin, or KNK437.

These findings suggest that one mechanism by which quercetin and KNK437 inhibit the HSR in *Xenopus* is through the inhibition of HSF activity. Export of RNA from the nucleus to the cytoplasm is explicitly regulated upon heat shock and other stresses (Saavedra *et al*., 1997). RNAs accumulate in the nucleus but only mRNAs

encoding HSPs are adeptly exported to the cytoplasm (Rollenhagen *et al*., 2004). Changes in the chaperone proteins associated with mRNAs in the nucleus during stress work to export HSP mRNAs at the expense of retaining other mRNAs. This may reflect a need to compensate for the acute increase in molar mass of these mRNAs in the nucleus in response to *hsp* gene activation via HSF-HSE binding and redirection of RNA polymerase complexes to *hsp* gene loci (Bond, 2006). In mammalian systems, quercetin has been found to inhibit the synthesis of HSPs and other important factors by interfering specifically with HSF DNA-binding activity (Hosokawa *et al.,* 1992; Nagai *et al.,* 1995; Hansen 1997). Studies of KNK437, showing that it also inhibits the synthesis of HSPs, suggest that its effects may be more specific to inhibiting the HSR than quercetin, which affects many other important factors in the cell, such as protein kinases (Yokota *et al.,* 2000; Koishi *et al.,* 2001). Specifically, KNK437 inhibited the heat-shock induced synthesis of HSP72 and HSP27 (Sakurai *et al*., 2005). The fact that Sakurai *et al.* (2005) did not observe a change in the mobility shift of HSF-1 by KNK437 suggests that its mechanism of action is not dependent upon HSF-1 transactivation, leaving the possibility that it interferes with HSF DNA-binding competence in a manner similar to quercetin. The results of the present study also showed that quercetin and KNK437 inhibit heat-shock induced *hsp* mRNA accumulation, which may be a consequence of interfering with HSF DNA-binding competence. Concomitantly, pretreatments of cells to conditions which induce HSPs protect both mRNA splicing and nuclear export complexes, preserving their function upon subsequent exposure to a thermal stress challenge (Rollenhagen *et al*., 2004).

Results of the present study also suggest that KNK437 inhibits the acquisition of thermotolerance in poikilotherms, similar to observations in mammalian systems (Yokota *et al.,* 2000; Koishi *et al.,* 2001; Nonaka *et al.,* 2003a/b; Ohnishi *et al.,* 2004; Sakurai *et al.,* 2005). The accumulation of HSP30 was used primarily to monitor the HSR in A6 cells, with immunocytochemistry and LSCM revealing several morphological effects of heat shock and the HSR inhibitors on actin cytoskeletal components. For example, whereas *Xenopus* A6 cells maintained at 22ºC showed intact actin stress fibers and distinct substrate contacts at the cellular periphery, cells exposed to the HSR inhibitors during a 2 h heat shock at 33ºC, showed detectable levels of HSP30 only throughout the cytoplasm of some cells treated with quercetin, and no HSP30 in cells treated with KNK437. Although stress fibers were intact after exposure to both HSR inhibitors at 33ºC, a slight disruption in actin stress fibers and some aggregation of actin at the cell periphery was observed in a minority of cells exposed to KNK437, but not quercetin. Increasing heat shock temperatures to 35ºC resulted in HSP30 predominantly localizing in the nuclear region of cells after 2 h, followed by relocation back to the cytoplasm after 4 h. This finding is congruent with studies showing sHSPs are primarily cytoplasmic upon heat shock, with enhanced accumulation in nuclear and perinuclear regions in both mammalian cells (e.g., Chinese hamster, Lavoie *et al.,* 1993) and non-mammalian cells (e.g., chicken, Katoh *et al.,* 2004; and frog, Gellalchew and Heikkila, 2005).

Interestingly, after 4 h at 35ºC in the presence of DMSO alone or quercetin, cytoplasmic HSP30 was marked by a punctuated pattern of aggregation, particularly in membrane blebs at the cellular periphery, where it appeared in association with collapsed actin bundles. However, under the same conditions in the presence of KNK437, the

cellular periphery was marked by the appearance of numerous actin microspikes, particularly in areas where the cell did not have stabilizing cell-to-cell contacts. In general, membrane blebs occurred predominantly in heat shocked cells treated with either DMSO alone or quercetin, and hence varying degrees of s*hsp* expression, whereas microspikes appeared to emerge from heat shocked cells treated with KNK437. In support of these findings, Mounier and Arrigo (2000) postulated that the cytoskeleton is sheltered from collapse when small oligomers of phosphorylated sHSPs cover actin filaments in a protective coating. Mounier and Arrigo (2000) suggested a direct actin-sHSP interaction, proposing two potential mechanisms: 1) when present as nonphosphoylated monomers, sHSPs act as actin-binding proteins, capping microfilaments, or 2) when organized into small, phosphorylated oligomers, sHSPs stabilize and protect microfilaments. The latter suggestion would seem to be supported by the appearance of actin stress fibers having collapsed encapsulating cytoplasm in membrane blebs only in the associated presence of HSP30, and any other HSPs present (but not identified). It could be speculated that, under stressful conditions, F-actin is preferentially nucleated at the cellular periphery to produce protrusions from the cell to form stabilizing contacts with both the substratum and neighbouring cells. However, under conditions wherein sHSPs accumulate in the cytoplasm, small oligomers of sHSPs may coalesce, not to stabilize and protect intact actin micofilaments, but to prevent the aggregation of heat-denatured F-actin which, having fragmented into short sticky oligomers, would otherwise form aggregates that could emesh, and thus disrupt, intact microfilaments (Pivovarova *et al*., 2005). In A6 cells, sHSPs, in particular HSP30, are known to form supermolecular aggregates upon heat shock (Ohan et al., 1998).

The contrasting appearance of membrane blebs and microspikes seen in the present study under heat shock and recovery conditions, depending upon the presence or absence of only one HSR inhibitor, KNK437, could also be explained in terms of interactions between the plasma membrane and cytoskeleton. Membrane-cytoskeleton adhesion is dynamically altered by major changes in cellular volume, including changes in temperature (Gervais *et al.,* 2003) and osmotic pressure (Morris and Homann, 2001). For example, temperature increases cause an increase in intestinal epithelial tight junction permeability (Dokladny *et al.,* 2006) which may induce swelling of the cell, requiring increases in the plasma membrane area of up to 10% (Morris and Homann, 2001). However, upon return to non-stressed conditions, if the cell volume shrinks to less than the original volume, excess membrane can be shed as external vesicles or invaginate into the cytoskeleton in regions that are still connected to the exterior of the cell, forming large vacuole-like dilations (VLDs) (Dai *et al.,* 1998; Morris and Homann, 2001). It is possible that the membrane blebs seen in this study formed under rapid increases in temperature which, having stretched the plasma membrane tightly over the cytoskeleton, caused blebs or VLDs upon return to control conditions during subsequent recovery periods. This possibility is supported by observations in the present study of membrane bleb formation under a) more intense and prolonged heat shock (e.g., 4 h at 35ºC) in comparison to milder heat shock conditions (e.g., 2 h at 33ºC); b) when cells are not given a recovery period at 22ºC in between mild heat shock and thermal challenge at 37ºC; and c) in the presence of HSP30 (as accumulated in the presence and absence of DMSO and quercetin) but not in the presence of KNK437.

Recent research also suggests that cell protrusions, such as the microspikes and possible CLFs or TNTs seen in this study, are an important mechanism for cell-to-cell communication wherein the exchange of information occurs via the direct membrane continuity of connected cells (Rustom *et al.,* 2004). Actin-based filopodial extensions, similar to the ones observed in this study, establish TNT connections when membrane fusion occurs; either between the tip of the protrusion and the planar plasma membrane of the target cell, or between the tips of two cell protrusions directed towards each other. TNT connections, which may span distances of over a 100 μm, are extremely sensitive to mechanical and shear stresses (Castro *et al.,* 2005). In the present study, numerous cell-to-cell actin-based connections were observed under heat shock conditions, particularly in the presence of the HSR inhibitor KNK437. This suggests that, in addition to attempts to form stabilizing contacts with the substratum upon heat stress, cells may form F-actin based protrusions in an endeavour to form contacts with other cells.

In contrast to observations on the formation of TNTs, studies of cells exposed to drugs such as latrunculin-B, which disrupt actin polymerization, show protrusion removal and arrest in organelle transfer at the cellular periphery (Rustom *et al.,* 2004). In the present study, under heat shock and in the presence of the HSR inhibitor KNK437, actin-based protrusions increased, suggesting an alternative method of coping with heat stress when s*hsp* gene expression is effectively shut-off. Under heat shock conditions, exposure to quercetin did not completely eliminate *hsp30* gene expression, resulting in an increase in membrane blebs at the cellular periphery, in comparison to the numerous microspikes observed in the presence of KNK437. Considering the overwhelming evidence in the literature suggesting over a dozen different biological effects of quercetin upon cellular

mechanics, and evidence of the exclusive efficiency of KNK437 over quercetin in inhibiting the HSR shown in this study, it would be prudent to continue to evaluate cellular responses to stress in the presence of the more specific HSR inhibitor, KNK437. Studies of cells exposed to KNK437 instead of quercetin may reveal further significant differences in cellular mechanics under heat shock conditions.

This is also the first study to examine the effects of KNK437 on F-actin dynamics during mild heat shock and a subsequent thermal stress challenge. In the presence of KNK437, cells given a 2 h heat pretreatment at 33ºC followed by a thermal challenge for 1 h at 37ºC, showed numerous ruffled membrane edges accompanied by aggregates of disrupted actin fibers. In comparison, cells directly challenged for 1 h at 37ºC, showed a marked decrease in HSP30, which was located predominantly at the cellular periphery in conjunction with actin aggregates in clusters of possible focal contacts. These cells showed virtually no intact stress fibers spanning cells and no coherent cell-to-cell connections. A 3-D analysis of cells given a 1 h thermal challenge at 37ºC (after a prior 2 h heat shock at 33ºC) in the absence of KNK437, showed numerous linear actin bundles transversing the entire cell, even extending into areas of cell-cell contact, and abundant HSP30 concentrated in the perinuclear region surrounding an intact nucleus. However, in the presence of KNK437, there was a significant emergence of membrane ruffles indicating global instability of cellular adhesion.

In a follow up experiment, comparing the effect of a 1 h thermal challenge at 37ºC *immediately* following a 33ºC pretreatment (e.g., no intervening recovery at 22ºC), in the absence and presence of KNK437, revealed a possible effect of a 2 h recovery at 22ºC prior to a thermal challenge. In the presence of KNK437, cells were covered with

microspikes and aggregates of actin at the cell periphery. In the absence of KNK437, cells were completely devoid of microspikes, instead showing massive membrane blebs around the cell periphery where actin bundles had collapsed around the cytoplasm, surrounding localized HSP30. In cells expressing *hsp30* and other *hsp* genes, the absence of a 2 h recovery at 22ºC may have prevented the elongation of actin cytoskeletal extensions, in the form of microspikes, into the extracellular matrix or towards creating stable contacts with other cells, a finding which is consistent with current studies on HSP production and function in severely stressed cells. In comparison to mildly stressed cells, where HSPs are synthesized during stress and function to protect macromolecular structures from disruption, severely stressed cells must wait for a return to normal growth conditions to resume HSP synthesis and repair of cellular machinery (Bond, 2006). For example, in studies of the role of HSP27 in actin stress fiber and focal adhesion formation after heat shock, Schneider *et al.* (1998) reported a significant effect of giving cells a recovery period after heat shock or not. Although heat shocked cells, which were immediately fixed and labeled showed focal adhesion and stress fiber disruption, cells given a recovery period of 2 h showed reformation of both (Schneider *et al.,* 1998). In conjunction with the results of this study, this suggests that eliminating the recovery period after the thermal challenge (and / or the heat pretreatment) would possibly produce an even more pronounced difference in F-actin cytoskeletal structure than has been observed in the literature as of yet.

Research showing various adhesion-mediated signaling mechanisms to converge at the actin cytoskeleton, thus affecting cellular physiology (Ridley and Hall, 1994), is becoming more crucial in understanding later evidence that cell adhesion, or the absence

of secure attachment to the substratum, can regulate entry into the cell cycle or apoptosis (Wilson *et al.,* 1995; Gilmore and Romer, 1996; Frisch *et al.,* 1996). For example, actin stress fiber formation has been shown to pave the way for the formation of focal adhesions (Bockholt and Burridge, 1993; Haimovich *et al.,* 1993; Seufferlein and Rozengurt, 1994; Burridge and Chrzanowska-Wodnicka, 1996). However, Schneider et al (1998) were the first to report on the effects of heat stress-mediated cytoskeletal changes after experimentally inducing changes in the structure and function of stress fibers and focal adhesions. Future experiments comparing the effects of inhibiting the HSR with KNK437 and the effects of recovery on actin stress fibers and the formation of focal and cell-to-cell contacts should include labeling of proteins known to associate with the cytoskeleton and plasma membrane to evaluate focal adhesions more specifically. For example, employing a fluorescent antibody-conjugate to paxillin, alpha-actinin, vinculin or profilin (Miyamoto *et al.,* 1995; Schulter *et al.,* 1997).

Confirmation that KNK437 inhibits the HSR by preventing HSF DNA-binding activity should be confirmed via DNA mobility shift assay. Antirequisite experiments should also investigate other stressors known to act synergistically with heat shock, such as sodium arsenite, comparing the effects of quercetin and KNK437 on the HSR. Exposing cultured cells to quercetin, which inhibits HSF activation, may eliminate the role of *hsp* gene transcription, but possibly promote the expression of other survival signalling pathways. Antithetically, an increase in levels of apoptosis may be induced by the addition of quercetin. KNK437, which appears to have a more direct and pronounced effect on the HSR, should be an interesting inhibitor to compare with quercetin. For example, the effects of inhibiting HSF activity on the developmental regulation of heat

shock proteins could be assessed via whole mount *in situ* hybridization of *Xenopus* early embryos exposed to the HSR inhibitor KNK437. It is anticipated that exposure to KNK437 will greatly reduce the levels of mRNAs encoding for inducible HSPSs and protooncogenes, leading to reduced thermotolerance and temporal and spatial increases in levels of apoptosis in embryos. As this study has demonstrated, KNK437, which is the more specific and efficient HSR inhibitor, will be an important inhibitor to compare with the well-documented quercetin for future investigations.

References

Abdulle, R., Mohindra, A., Fernando, P., Heikkila, J.J. 2002. *Xenopus* small heat shock proteins, Hsp30C and Hsp30D, maintain heat- and chemically denatured luciferase in a folding-competent state. Cell Stress Chaperones, 7: 6-16.

Abravaya, K., Myers, M.P., Murphy, S.P., and Morimoto, R.I. 1992. The human heat shock protein hsp70 interacts with HSF, the transcription factor that regulates heat shock protein transcription. *Genes in Development*, **6**: 1153-1164.

Alberts, A., Johnson, A., Lewis, J., Raff, M., Roberts, K., and Walter, P. 2002. *Molecular Biology of the Cell,* Fourth Edition. Garland Science, New York. Pp. 907-982.

Ali, A., Bharadwaj, S., O'Carroll, and Ovsenek, N. 1998. Hsp90 interacts with and regulates the activity of heat shock factor 1 in *Xenopus* oocytes. *Molecular and Cellular Biology*, **18**: 4949-4960.

Ali, A., Krone, P.H., Pearson, D.S., and Heikkila, J.J. 1996a. Evaluation of stress-inducible hsp90 gene expression as a potential molecular biomarker in *Xenopus laevis. Cell Stress Chaperones,* **1**: 62-69.

Ali, A., Salter-Cid, L., Flajnik, M. F., and Heikkila, J.J. 1996b. Isolation and characterization of a cDNA encoding a *Xenopus* 70-kDa heat shock cognate protein, Hsc70.1. *Comparative Biochemistry and Physiology*, **113B**: 681-697.

Arrigo, A-P., Suhan, J.P., and Welch, W.J. 1988. Dynamic changes in the structure and intracellular locale of the mammalian low-molecular-weight heat shock protein. *Molecular and Cellular Biology*, **8:** 5059-5071.

Ben-Ze'ev, A., and Amsterdam, A. 1986. Regulation of cytoskeletal proteins involved in cell contact formation during differentiation of granulose cells on extracellular matrix. *Proceedings of the National Academy of Sciences USA,* **83**, 2894-2898.

Bharadwaj, S., Ali, A., and Ovsenek, N. 1999. Multiple components of the hsp90 chaperone complex function in regulation of heat shock factor 1 *in vivo*. *Molecular and Cellular Biology*, **19**: 8033-8041.

Bienz, M. 1984a. Developmental control of the heat shock response in *Xenopus*. *Proceedings of the National Academy of Science USA*, **81**: 3138-3134.

Bienz, M. 1984b. *Xenopus* hsp70 genes are constitutively expressed in injected oocytes. *EMBO Journal,* **3:** 2477-2483.

Bockholt, S., and Burridge, K. 1993. Cell spreading on extracellular matrix proteins induces tyrosine phosphorylation of tensin. *Journal of Biology and Chemistry*, **268**: 1465-14567.

Bond, U. 2006. Stressed out! Effects of environmental stress on mRNA metabolism. *Federation of European Microbiological Societies*, **6**: 160-170.

Briant, D., Ohan, N., and Heikkila, J.J. 1997. Effect of herbimycin A on HSP30 and HSP70 heat shock protein gene expression in *Xenopus* cultured cells. *Biochemistry and Cell Biology*, **75**: 777-782.

Bryantsev, A.L., Loktionova, S.A., Ilyinskaya, O.P., Tararak, E.M., Kampinga, H.H., and Kabakov, A.E. Distribution, phosphorylation, and activities of Hsp25 in heat-stressed H9c2 myoblasts: a functional link to cytoprotection. *Cell Stress Chaperones,* **7:** 146-155.

Burridge, K., and Chrzanowska-Wodnicka, M. 1996. Focal adhesions, contractility, and

signaling. *Annual Review of Cell Biology*, **12**: 463-519.

Castro, M.A., Grieneisen, V.A., de Almeida, R.M. 2005. Disruption and de novo formation of nanotubular extensions in SW620 colon carcinoma cell line during cell division. *Cell Biology International,* **29**: 929-31.

Cervera, M., Dreyfus, G., and Penman, S. 1981. Messenger RNA is translated when associated with the cytoskeletal framework in normal and SV40 infected HeLa cells. *Cell*, **23**, 113-120.

Chen SY, Bhargava A, Mastroberardino L, Meijer OC, Wang J, Buse P, Firestone GL, Verrey F, Pearce D. 1999. Epithelial sodium channel regulated by aldosterone-induced protein sgk. *Proceedings of the National Academy of Science USA,* **96**: 2514-2519.

Clark, E. A., and Brugge, J.S. 1995. Integrins and signal transduction pathways: The road taken. *Science*, **14**: 233-239.

Conklin, C.M., Bechberger, J.F., McFabe, D., Guthrie, N., Kurowska, E.M., and Naus, C.C. 2006. Genistein and quercetin increase connexin43 and suppress growth of breast cancer cells. *Carcinogenesis,* Jun 15; [Epub ahead of print]

Coss, R.A.., and Linnemans, W.A.M.1996. The effects of hyperthermia on the cytoskeleton: A review. *International Journal of Hyperthermia*, **12**, 173-196.

Creagh, E. M., Sheehan, D., and Cotter, T.G. 2000. Heat shock proteins – modulators of apoptosis in tumour cells. *Leukemia*, **14**: 1161-1173.

Csokay, B., Prajda, N., Weber, G., and Olah, E. 1997. Molecular mechanisms in the antiproliferative action of quercetin. *Life Sciences*, **60**: 2157-2163.

Dai, J., Sheetz, M.P., Wan, X., and Morris, C.E. 1998. Membrane tension in swelling and

shrinking molluscan neurons. *Journal of Neuroscience,* **18:** 6681-6692.

Dajas, F., Rivera-Megret, F., Blasina, F., Arredondo, F., Abin-Carriquiry, J.A., Costa, G., Echeverry, C., Lafon, L., Heizen, H., Ferreira, M., and Morquio, A. 2003a. Neuroprotection by flavonoids. *Brazilian Journal of Medical and Biological Research, 36:* 1613-1620.

Dajas, F., Rivera, F., Blasina, F., Arredondo, F., Echeverry, C., Lafon, L., Morquio, A. and Heizen, H. 2003b. Cell culture protection an in vivo neuroprotective capacity of flavonoids. *Neurotoxicity Research, 5:* 377-384.

Darasch, S., Mosser, D.D., Bols, N.C., and Heikkila, J.J. 1988. Heat shock gene expression in *Xenopus laevis* A6 cells in response to heat shock and sodium arsenite treatments. *Biochemistry and Cell Biology,* **66**: 862-870.

Debes, A., Oerding, M., Willers, R., Gobel, U., and Wessalowski, R. 2003. Sensitization of human Ewing's tumor cells to chemotherapy and heat treatment by the bioflavonoid quercetin. *Anticancer Research,* **23**: 3359-3366.

Demontis, F. 2004. Nanotubes make big science. *Public Library of Science: Biology*, **2**; 896-897.

Dokladny, K., Moseley, P.L., and Ma, T.Y. 2006. Physiologically relevant increase in temperature causes an increase in intestinal epithelial tight junction permeability. *American Journal of Physiology and Gastrointestinal Liver Physiology,* **290:** G204-G212.

Elia, G. and Santoro, G. 1994. Regulation of heat shock protein synthesis by quercetin in human erythroleukaemia cells. *Biochemistry Journal*, **300**: 201-209.

Fernando, P., Abdulle, R., Mohindra, A., Guillemette, J.G., Heikkila, J.J. 2002. Mutation

or deletion of the C-terminal tailaffets the function and structure of *Xenopus laevis* small heat shock protein, hsp30. *Comparative Biochemistry and Physiology B: Biochemistry and Molecular Biology*, **133**: 95-133.

Fernando, P. and Heikkila, J.J. 2000. Functional characterization of *Xenopus* small heat shock protein, Hsp30C: the carboxyl end is required for stability and chaperone activity. *Cell Stress Chaperones*, 5; 148- 59.

Fernando, P., Megeney, L.A., and Heikkila, J.J. 2003. Phosphorylation-dependent structural alterations in the small hsp30 chaperone are associated with cellular recovery. *Experimental Cell Research,* **286**: 175-185.

Frisch, S., Vuori, K., Ruoslahti, E., and Chan-Hui, P.Y. 1996. Control of adhesion-dependent cell survival by focal adhesion kinase. *Journal of Cell Biology*, **134**: 793-799.

Fujita, M., Nagai, M., Murata, Kawakami, K., Irino, S., Takahara, J. 1997. Synergistic cytotoxic effect of quercetin and heat treatment in a lymphoid cell line (OZ) with low Hsp70 expression. *Leukemia Research*, **21**; 139-145.

Fulton, A. 1984. *The cytoskeleton: Cellular architecture and choreography*. Chapman and Hall: New York.

Galisteo, M., Garcia-Saura, MF., Jimenez, R.,m Villar, I.C., Zarzuelo, A., Vargas, F., and Duarte, J. 2004. Effects of chronic quercetin treatment on antioxidant defence system and oxidative status of deoxycorticosterone acetate-salt-hypertensive rats. *Molecular and Cellular Biochemistry*, 259: 91-99.

Geiger, B. 1983. Membrane-cytoskeleton interaction. *Biochimica et Biophysica Acta.,* **737**, 305-341.

Gellalchew, M. and Heikkila, J.J. 2005. Intracellular localization of *Xenopus* small heat shock protein, HSP30, in A6 kidney epithelial cells. *Cell Biology International,* **29**: 221-227.

Gervais, P., Martinez de Maranon, I., Evrard, C., Ferret, E., Moundanga, S. 2003. Cell volume changes during rapid temperature shifts. *Journal of Biotechnology*, **102**: 269-279.

Gilmore, A.P., and Romer, L.H. 1996. Inhibition of FAK signaling in focal adhesions decreases cell motility and proliferation. *Molecular Biology of the Cell*, **7**: 1209-1224.

Gingrich, J.C., Davis, D.R., and Nguyen,Q. 2000. Multiplex detection and quantitation of proteins on western blots using fluorescent probes. *Biotechniques,* 29: 636-642.

Goldenberg, C. J., Luo, Y., Fenna, M., Baler, R., Weinmann, R., and Voellmy, R. 1988. Purified human factor activates heat shock promoter in a HeLa cell-free transcription system. *Journal of Biology and Chemistry*, **263**: 19734-19739.

Goodson, M.L., Hong, Y., Rogers, R., Matunis, M.J., Park-Sarge, O-K., Sarge, K.D. 2001. Sumo-1 modification regulates the DNA binding activity of heat shock transcription factor 2, a promyelocytic leukemia nuclear body associated transcription factor. *Journal of Biology and Chemistry*, **276**: 18513-18518.

Gordon, S., Bharadwaj, S., Hnatov, A., Ali, A., and Ovsenek, N. 1997. Distinct stress-inducible and developmentally regulated heat shock transcription factors in *Xenopus* oocytes. *Developmental Biology*, **181**: 47-63.

Gumbiner, B. 1987. Structure, biochemistry, and assembly of epithelial tight junctions. *American Journal of Physiology*, **253**: C749-C758.

Haimovich, B., Lipfert, L., Brugge, J.S., and Shattil, S.J. 1993. Tyrosine phosphorylation and cytoskeletal reorganization in platelets are triggered by interaction of intergrin receptors with their immobilized ligands. *Journal of Biology and Chemistry*, **268:** 15868-15877.

Hamilton, A.M. and Heikkila, J.J. 2006. Examination of the stress-induced expression of the collagen binding heat shock protein, hsp47, in *Xenopus laevis* cultured cells and embryos. *Comparative Biochemistry and Physiology. Part A, Molecular and Integrative Physiology,* **143**: 133-141.

Hansen, R.K., Oesterreich, S., Lemieux, P., Sarge, K.D., and Fuqua, S.A. W. 1997. Quercetin inhibits heat shock protein induction but not heat shock factor DNA-binding in human breast carcinoma cells. *Biochemical and Biophysical Research Communications*, **239**: 851-857.

Heikkila, J.J., Kloc, M., Bury, J., Schultz, G.A., and Browder, L.W. 1985. Acquisition of the heat shock response and thermotolerance during early development of *Xenopus laevis. Developmental Biology*, **107**: 483-489.

Heikkila, J.J., Krone, P.H., and Ovsenek, N. 1991. Regulation of heat shock gene expression during Xenopus development. *In* "Heat shock development" (Hightower, L. and Nover, L., Eds.), pp. 120-137, Springer-Verlag, New York.

Heikkila, J.J., Ohan, N., Tam., Y., and Ali, A. 1997. Heat shock protein gene expression during *Xenopus* development. *Cellular and Molecular Life Sciences*, **53**: 114-121.

Heikkinen, H.L., Lelewellyn, S.A., and Barnes, C.A. 2003. Initiation-mediated mRNA decay in yeast affects heat shock mRNAs and works through decapping and 5' to 3' hydrolysis. *Nucleic Acids Research,* **31**: 4006-4016.

Hietakangas, V., Ahlskog, J.K., Jakobsson, A.M., Hellesuo, M., Sahlberg, N.M., Holmberg, C.I., Mikhailov, A., Palvimo, J.J., Pirkkala, L., and Sistonen, L. 2003. Phosphorylation of serine 303 is a prerequisite for the stress-inducible SUMO modification of heat shock factor 1. *Molecular and Cellular Biology*, **23**: 2953-2968.

Hilgarth, R.S., Murphy, L.A., O'Connor, C.M., Clark, J.A., Park-Sarge, O-K, and Sarge, K. D. 2004. Identification of *Xenopus* heat shock transcription factor-2: conserved role of sumolyation in regulating deoxyribonucleic acid-binding activity of heat shock transcription factor-2 proteins. *Cell Stress and Chaperones*, **9**: 214-220.

Holbrook, N.J., and Udelsman, R. 1994. Heat shock gene expression in response to physiologic stress and aging. In *The Biology of Heat Shock Proteins and Molecular Chaperones*, (ed. R.I. Morimoto, Tissières, T., and Georgopoulos, C.), p. 577-594. Cold Spring Harbor Laboratory Press, Cold Spring Harbor, New York.

Holmberg, C.I., Hietakangas, V., Mikhailov, A., Rantanen, J.O., Kallio, M., Meinander, A., Hellman, J., Morrice, N., MacKintosh, C., Morimoto, R.I., Eriksson, J.E., and Sistonen, L. 2001. Phosphorylation of serine 230 promotes inducible transcriptional activity of heat shock factor 1. *EMBO Journal*, **20**: 3800-3810.

Hosokawa, N., Hirayoshi, K., Kudo, H., Takechi, H., Aoike, A., Kawai, K., Nagata, K. 1992. Inhibition of heat shock factor in vivo and in vitro by flavonoids. *Molecular and Cellular Biology*, **12**: 3490-3498.

Hu, Y., and Mivechi, N. F. 2003. HSF-1 interacts with Ral-binding protein 1 in a stress-responsive, multiprotein complex with hsp90 in vivo. *The Journal of Biological Chemistry*, **278**: 17299-17306.

Huot, J., Houle, F., Spitz, D.R., and Landry, J. 1996. Hsp27 phosphorylation-mediated resistance against actin fragmentation and cell death induced by oxidative stress. *Cancer Research,* **56:** 273-279.

Huot, J., Houle, F., Rousseau, S., Deschesnes, R. G., Shah, G. M. and Landry, J. 1998. SAPK2/p38-dependent F-actin reorganization regulates early membrane blebbing during stress-induced apoptosis. *Journal of Cell Biology,* **143:** 1361-1373.

Inouye, S., Katsuki, K., Izu, H., Fujimoto, M., Sugahara, K., Yamada, S., Shinkai, Y., Oka, Y., Katoh, Y., and Nakai, A. 2003. Activation of heat shock genes is not necessary for protection by heat shock transcription factor 1 against cell death due to a single exposure to high temperatures. *Molecular and Cell Biology,* **23**: 5882-5895.

Jakubowicz-Gil, J., Rzymowska, J., and Gawron, A. 2002.Quercetin, apoptosis, heat shock. *Biochemical Pharmacology*, **62**: 1591-1595.

Jakubowicz-Gil, J., Rzymowska, J., Paduch, R., and Gawron, A. 2002. The effect of quercetin on the expression of heat shock proteins and apoptosis induction in monkey kidney cell line GMK. *Folia Histochemistry and Cytobiology*, **40**: 137-8.

Jockusch, B.M., Bubeck, P., Giehl, K., Kroemker, M., Moschner, J., Rothkegal, M., Rudiger, M., Schluter, K., Stanke, G., and Winkler, J. 1995. The molecular architecture of focal adhesions. *Annual Review of Cell and Developmental Biology,* **11**: 379-416.

Jolly, C. and Morimoto, R.I. 2000. Role of heat shock response and molecular chaperones in oncogenesis and cell death. *Journal of the National Cancer Institute*, **92**: 1564-1572.

Juliano, R.L., and Haskill, S. 1993. Signal transduction from the extracellular matrix. The *Journal of Cell Biology,* **20**, 577-585.

Kabakov, A.E., Malyutina, Y.V., and Latchman, D.S. 2006. Hsf1-mediated stress response can transiently enhance cellular thermoresistance. *Radiation Research*, **165:** 410-23.

Katoh, Y., Fujimoto, M., Nakamura, K., Inouye, S., Sugahara, K., Izu, H., Nakai, A. 2004. Hsp25, a member of the Hsp30 family, promotes inclusion formation in response to stress. *FEBS Letter*, 565: 28-32.

Katschinski, D.M. 2004. On heat and cells and proteins. *News in Physiological Sciences*, **19**: 11-15.

Karn, H., Ovsenek, N., and Heikkila, J. J. 1992. Examination of the DNA sequence-specific binding properties of heat shock transcription factor in *Xenopus* embryos. *Biochemistry and Cell Biology*, **70**: 1006-1013.

Kline, M.P., and Morimoto, R.I. 1997. Repression of the heat shock factor 1 transcriptional activation domain is modulated by constitutive phosphorylation. *Molecular and Cellular Biology,* **17**: 2107-2115.

Knauf, U., Newton, E.M., Kyriakis, J., and Kingston, R.E. 1996. Repression of human heat shock factor 1 activity at control temperature by phosphorylation. *Genes and Development,* **10**: 2782-2793.

Koh, T.J., and Escobedo, J. 2004. Cytoskeletal disruption and small heat shock protein

translocation immediately after lengthening contraction. *American Journal of Physiology and Cellular Physiology*, **286:** C713-C722.

Koishi, M., Hosokawa, N., Sato, M., Nakai, A., Hirayoshi, K., Hiraoka, M., Abe, M., and Nagata, K. 1992. Quercetin, an inhibitor of heat shock protein synthesis, inhibits the acquisition of thermotolerance in a human colon carcinoma cell line. *Japanese Journal of Cancer Research*, **83**; 1216-1222.

Koishi, M., Yokota, S., Mae, T., Nishimura, N., Kanamori, S., Horii, N., Shibuya, K., Sasai, K., and Hiraoka, M. 2001. The effects of KNK437, a novel inhibitor of heat shock protein synthesis, on the acquisition of thermotolerance in a murine transplantable tumor in vivo. *Clinical Cancer Research,* **7**, 215-219.

Krone, P.H., Snow, A., Ali, A., Pasternak, J.J., and Heikkila, J.J. 1992. Comparison of the regulatory regions of the *Xenopus laevis* small heat-shock protein encoding gene family. *Gene*, **110**: 159-166.

Laing, P., and MacCrae, T. H. 1997. Molecular chaperones and the cytoskeleton. *Journal of Cell Science,* **110**: 1431-1440.

Landry, J. and Chretien, P. 1983. Relationship between hyperthermia-induced heat-shock proteins and thermotolerance in Morris hepatoma cells. *Canadian Journal of Cell Biology,* **61:** 428-437.

Landry, J., Chretien, P., Lambert, H., Hickey, E., and Weber, L. A. 1989. Heat shock resistance conferred by expression of the human Hsp27 gene in rodent cells. *The Journal of Cell Biology*, **109:** 7-15.

Landry, J., Chretien, P., Laszlo, A., and Lambert, H. 1991. Phosphorylation of Hsp27 during development and decay of thermotolerance in Chinese hamster cells.

Journal of Cell Physiology, **147**: 93-101.

Landsberger, N., Ranjan, M., Almouzni, G., Stump, D., and Wolffe, A. P. 1995. The heat shock response in *Xenopus* oocytes, embryos, and somatic cells: A regulatory role for chromatin. *Developmental Biology*, **170**: 62-74.

Lang, L., Miskovic, D., Fernando, P., and Heikkila, J.J. 1999. Spatial pattern of constitutive and heat shock-induced expression of the small heat shock protein gene family, Hsp30, in *Xenopus laevis* tailbud embryos. *Developmental Genetics*, **25**: 265-374.

Lang, L., Miskovic, D., Lo, M., and Heikkila, J.J. 2000. Stress-induced, tissue-specific enrichment of hsp70 mRNA accumulation in *Xenopus laevis* embryos. *Cell Stress and Chaperones,* **5**: 36-44.

Larson, J.S., Shuetz, T.J., and Kingston, R.E. 1988. Activation in vitro of sequence-specific DNA binding by a human regulatory factor. *Nature*, **335**: 373-375.

Lavoie, J.N., Gingras-Breton, G., Tanguay, R.M., and Landry, J. 1993. Induction of Chinese hamster hsp27 gene expression in mouse cells confers resistance to heat shock. *The Journal of Biological Chemistry*, **268:** 3420-3429.

Lavoie, J.N., Lambert, H., Hickey, E., Weber, L.A., and Landry, J. 1995. Modulation of cellular thermoresistance and actin filament stability accompanies phosphorylatio-induced changes in the oligomeric structure of heat shock protein 27, *Molecular and Cellular Biology*, **15**: 505-516.

Linder, S., and Aepfelbacher, M. 2003. Podosomes: adhesion hot-spots of invasive cells. *TRENDS in Cell Biology*, **13**: 376-385.

Linder, S., and Kopp, P. 2005. Podosomes at glance. *Journal of Cell Science*, **118**: 2079-

2082.

Lindquist, S., and Craig, E.A. 1988. The heat shock proteins. *Annual Review of Genetics,* **22**: 31-677.

Lis, J.T., Xiao, H., and Perisic, O. 1990. Modular units of heat shock regulatory regions: Structure and function. In In *Stress Proteins in Biology and Medicine.* (ed. R.I. Morimoto et al.), p.411-442. Cold Spring Harbor Laboratory Press, Cold Spring Harbor, New York.

Lis, J.T. 1991. Transcriptional activation of *Drosophila* heat shock genes. In Maresca, B., and Lindquist, S. (eds), *Heat Shock*. Springer-Verlag, New York. 3-8.

Locke, M. and Noble, E.G. 2002. *Exercise and the Stress Response: The Role of Stress Proteins.* p. 18. CRC Press LLC, Boca Raton, Florida.

Loktionova, S.A. and Kabakov, A.E. 1998. Protein phosphatase inhibitors and heat preconditioning prevent Hsp27 dephosphorylation, F-actin disruption and deterioration of morphology in ATP-depeleted endothelial cells. *FEBS Letters,* **433:** 294-300.

Macario, A.J., Conway de Macario, E. 2005. Sick chaperones, cellular stress, and disease. *New England Journal of Medicine*, **353**: 1489-1501.

Martinez-Balbas, M. A., Dey, A., Rabindran, S.K., Ozato, K., and Wu, C. 1995. Displacement of sequence-specific transcription factors from mitotic chromatin. *Cell*, **83**: 29-38.

Mercier, P.A., Foksa, J., Ovsenek, N., and Westwood, J. T. 1997. *Xenopus* heat shock factor 1 is a nuclear protein before heat stress. *Journal of Biological Chemistry*, 272: 14147-14151.

Miskovic, D. and Heikkila, J.J. 1999. Constitutive and stress-inducible expression of the endoplasmic reticulum heat shock protein 70 gene family member, immunoglobulin-binding protein (BiP), during *Xenopus laevis* early development. *Developmental Genetics*, **25**: 31-39.

Miskovic, D., Salter-Cid, L., Ohan, N., Flajnik, M., Heikkila, J. J. 1997. Isolation and characterization of a cDNA encoding a *Xenopus* immunoglobulin binding protein, BiP (Grp78). *Comparative Biochemistry and Physiology. Part B*, *Biochemistry and Molecular Biology,* **116:** 227-234.

Miaymoto, S., Teramoto, H., Coso, O.A., Gutkind, J.S., Burbelo, P.D., Akiyama, S.K., and Yamada, K.M. 1995. Integrin function: molecular hierarchies of cytoskeletal and signaling molecules. *Journal of Cell Biology*, **131**: 791-805.

Morimoto, R.I., Jurivich, D.A., Kroeger, P.E., Mathur, S.K., Murphy, S.P., Nakai, A., Sarge, K., Abravaya, K., and Sistonen, L.T. 1994. Regulation of heat shock gene transcription by a family of heat shock factors. In *The Biology of Heat Shock Proteins and Molecular Chaperones*, (ed. R.I. Morimoto, Tissières, T., and Georgopoulos, C.), p. 417-455. Cold Spring Harbor Laboratory Press, Cold Spring Harbor, New York.

Morris, C.E., and Homann, U. 2001. Cell surface area regulation and membrane tension. *Journal of Membrane Biology*, **179**: 79-102.

Mosser, D.D., Theodorakis, N.G., and Morimoto, R.I. 1988. Coordinate changes in heat shock element-binding activity and hsp70 gene transcription rates in human cells. *Molecular and Cellular Biology*, **8**: 4736-4744.

Mosser, D.D., Kotzbauer, P.T., Sarge, K.D., and Morimoto, R.I. 1990. *In vitro* activation

of heat shock transcription factor DNA-binding by calcium and biochemical conditions that affect protein conformation. *Proceedings of the National Academy of Sciences*, **87**: 3748-3752.

Mounier, N., and Arrigo, A.P. 2000. Actin cytoskeleton and small heat shock proteins: how do they interact? *Cell Stress Chaperones*, **7**: 167-176.

Muller, M., Gauley, J., and Heikkila, J.J. 2004. Hydrogen peroxide induces heat shock protein and *proto-oncogene* mRNA accumulation in *Xenopus laevis* A6 kidney epithelial cells. *Canadian Journal of Physiology and Pharmacology*, **82**: 523-529.

Nagai, N., Nakai, A., and Nagata, K. 1995. Quercetin suppresses heat shock response by down regulation of HSF1. *Biochemical and Biophysical Research Communications*, **208**: 1099-1105.

Nair, MP., Mahajan, S., Reynolds, J.L., Aalinkeel, R., Nair, H., Schwartz, S.A., and Kandaswami, C. 2006. The flavonoid quercetin inhibits proinflammatory cytokine (tumor necrosis factor alpha) gene expression in normal peripheral blood mononuclear cells via modulation of the NF-kappa beta system. *Clinical Vaccine Immunology,* **13**: 319-328.

Nakai, A. and Morimoto, R.I. 1993. Characterization of a novel chicken heat shock transcription factor, heat shock factor 3, suggests a new regulatory pathway. *Molecular and Cellular Biology*, **13**: 1983-1997.

Nakai, A., Tanabe, M., Kawazoe, Y., Inazawa, J., Morimoto, R.I., and Nagata, K. 1997. HSF4, a new member of the human heat shock factor family which lacks properties of a transcriptional activator. *Molecular and Cellular Biology,* **17**: 469-481.

Nicholl, W.S., Boshoff, A., Ludewig, M.H., Hennessy, F., Jung, G.L., and Blatch, G.L. 2006. Approaches to the isolation and characterization of molecular chaperones. *Protein Expression and Purification,* **46:** 1-15.

Nonaka, T., Akimoto, T., Mitsuhashi, N., Tamaki, Y., and Nakano, T. 2003a. Changes in the number of HSF1 positive granules in the nucleus reflects heat shock semiquantitatively. *Cancer Letters, 202*, **89**-100.

Nonaka, T., Akimoto, T., Mitsuhashi, N., Tamaki, Y., Yokota, S., and Nakano, T. 2003b. Changes in the localization of heat shock protein 72 correlated with development of thermotolerance in human esophageal cancer cell line. *Anticancer Research,* **23**, 4677-87.

Ohan, N. and Heikkila, J.J. 1995. Involvement of differential gene expression and mRNA stability in the developmental regulation of the Hsp 30 gene family in heat-shocked *Xenopus laevis* embryos. *Developmental Genetics*, **17**: 176-184.

Ohan, N.W., Tam, Y., Fernando, P., and Heikkila, J.J. 1998a. Characterization of a novel group of basic small heat shock proteins in *Xenopus laevis* A6 kidney epithelial cells. *Biochemistry and Cell Biology*, **76**: 665- 671.

Ohan, N.W., Tam, Y., and Heikkila, J.J. 1998b. Heat shock-induced assembly of Hsp30 family members into high molecular aggregates in *Xenopus laevis* cultured cells. *Comparative Biochemisrty and Physiology B: Molecular Biology,* **119**: 381-389.

Ohnishi, K., Takahashi, A., Yokota, S., and Ohnishi, T. 2004. Effects of a heat shock protein inhibitor KNK437 on heat sensitivity and heat tolerance in human squamous cell carcinoma cell lines differing in p53 status. *International Journal of Radiation Biology,* **80**, 607-614.

Ohtsuka, K., Masuda, A., Nakai, A., and Nagata, K. 1990. A novel 40-kDa protein induced by heat shock and other stresses in mammalian and avian cells. *Biochemical and Biophysical Research Communications*, **166**: 642-647.

Oksala, N., Alhava, E., and Paimela, H. 2004. Heat shock preconditioning and eicosanoid pathways modulate caspase 3-like activity in superficially injured isolated guinea pig gastric mucosa. *European Surgical Research*, **36**: 67-73.

Orosz, A., Wisniewski, J., and Wu, C. 1996. Regulation of Drosophila heat shock factor trimerization: global sequence requirements and independence of nuclear localization. *Molecular and Cellular Biology*, **16**: 7018-7030.

Ovsenek, N. and Heikkila, J.J. 1990. DNA sequence-specific binding activity of the heat-shock transcription factor is heat inducible before the midblastula transition of early *Xenopus* development. *Development*, **110**: 427-433.

Parsell, D.A., and Lindquist, S. 1993. The function of heat shock proteins in stress tolerance: Degradation and reactivation of the damaged proteins. *Annual Review of Genetics*, **27**: 437-496.

Perisic, O., Xiao, H., and Lis, J.T. 1989. Stable binding of *Drosophila* heat shock factor to head-to-head and tail-to-tail repeats of a conserved 5 bp recognition unit. *Cell* **59:** 797-806.

Phang, D., Joyce, E. M., and Heikkila, J. J. 1999. Heat shock-induced acquisition of thermotolerance at the levels of cell survival and translation in *Xenopus* A6 kidney epithelial cells. *Biochemistry and Cell Biology*, **77**: 141-151.

Pivovarova, A.V., Mikhailova, V.V., Chernik, I.S., Chebotareva, N.A., Levitsky, D.I.,

and Gusev, N.B. 2005. Effects of small heat shock proteins on the thermal denaturation and aggregation of F-actin. *Biochemical and Biophysical Research Communications,* **331:** 1548-1553.

Rafferty, K. A. 1968. Mass culture of amphibian cells: Methods and observations concerning stability of cell type. In *Biology of Amphibian Tumour,* (ed. M. Mizell), p. 52-81.

Rafferty, K. A. and Sherwin, R.W. 1969. The length of secondary chromosomal constrictions in normal individuals and in a nucleolar mutant of *Xenopus laevis*. *Cytogenetics*, **8**: 427-438.

Ridley, A.J., and Hall, A. 1994. Signal transduction pathways regulating rho-mediated stress fiber formation: Requirement for a tyrosine kinase. *EMBO Journal*, **13:** 2600-2610.

Rollenhagen, C., Hodge, C.A., and Cole, C.N. 2004. The nuclear pore complex and the DEAD box protein Rat8p/Dbp5p have nonessential features which appear to facilitate mRNA export following heat shock. *Molecular and Cellular Biology*, **24**: 4869-4879.

Rustom, A., Saffrich, R., Markovic, I., Walther, P., and Gerdes, H.-H. 2004. Nanotubular highways for intercellular transport. *Science,* **303**, 1007-1010.

Saavedra, C.A., Hammell, C.M., Heath, C.V., and Cole, C.N. 1997. Yeast heat shock mRNAs are exported through a distinct pathway defined by Rip1p. *Genes and Development,* **11:** 2845-2856.

Sakurai, H., Kitamoto, Y., Saitoh, J., Nonaka, T., Ishikawa, H., Kiyohara H, Shioya, M., Fukushima, M., Akimoto, T., Hasegawa, M., Nakano, T. 2005. Attenuation of

chronic thermotolerance by KNK437, a benzylidene lactam compound, enhances thermal radiosensitization in mild temperature hyperthermia combined with low dose-rate irradiation. *International Journal of Radiation Biology,* **81**: 711-718.

Sandqvist, A. and Sisttonen, L. 2004. Nuclear stress granules: the awakening of a sleeping beauty. *Journal of Cell Biology*, **164:** 15-17.

Sarge, K.D., Zimarino, V., Holm, K., Wu, C., and Morimoto, R.I. 1991. Cloning and characterization of two mouse heat shock factors with distinct inducible and constitutive DNA-binding ability. *Genes and Development*, **5:** 1902-1911.

Schneider, G.B., Hamano, H., and Cooper, L.F. 1998. *In vivo* evaluation of hsp27 as an inhibitor of actin polymerization: hsp27 inhibits stress fiber and focal adhesion formation after heat shock. *Journal of Cellular Physiology*, **177:** 575-584.

Schuetz, T.J., Sheldon, L., Tempst, P., Kingston, R.E. 1991. Isolation of a cDNA for HSF2: evidence for two heat shock factor genes in humans. *Proceedings of the National Academy of Sciences USA*, **88**: 6911-6915.

Schulter, K., Jockusch, B.M., and Rothkegel, M. 1997. Profilins as regulators of actin dynamics. *Biochimica et Biophysica Acta*, 1359: 97-109.

Schwartz, M. A., Schaller, M.D., and Ginsberg, M.H. 1995. Integrins: Emerging paradigms of signal transduction. *Annual Review of Cell and Developmental Biology*, 11: 549-599.

Seufferlein, T., and Rozengurt, E. 1994. Sphingosine induces pp125FAK and paxillin tyrosine phosphorylation, actin stress fiber formation, and focal contact assembly in Swiss 3T3 cells. *Journal of Biology and Chemistry*, **269**: 27610-27617.

Shabtay, A. and Arad, Z. 2006. Reciprocal activation of HSF1 and HSF3 in brain and

blood tissues: is redundancy developmentally regulated? *American Journal of Physiology: Regulatory, integrative, and comparative physiology,* **291**: R566-72.

Shackelford, R.E. 2005. Pharmacologic manipulation of the ataxia-telangiectasia mutated gene product as an intervention in age-related disease. *Medical Hypotheses*, **65**: 363-369.

Sheetz, M. P., Sable, J. E., and Döbereiner, H.-G. 2006. Continuous membrane-cytoskeleton adhesion requires continuous accommodation to lipid and cytoskeleton dynamics. *Annual Review of Biophysics and Biomolecular Structure*, **35**: 417-434.

Sive, H.L., Granger, R.M., and Harland, R.M. 2000. *Early development of Xenopus laevis.* Cold Spring Harbour Laboratory Press, New York.

Spector, D.L., Goldman, R.D., and Leinwand, L.A. 1998. *Cells: A laboratory manual, Vol. 3: Subcellular localization of genes and their products.* Cold Spring Harbor Laboratory Press: New York.

Stump, D. G., Landsberger, N., and Wolffe, A..P. 1995. The cDNA encoding *Xenopus laevis* heat-shock factor 1 (XHSF1): nucleotide and deduced amino-acid sequences, and properties of the encoded protein. *Gene*, **160**: 207-211.

Tam, Y. and Heikkila, J.J. 1995. Identification of members of the hsp30 small heat shock protein family and characterization of their developmental regulation in heat-shocked *Xenopus laevis* embryos. *Developmental Genetics*, **17**: 331-339.

Tanikawa, J., Ichikawa-Iwata, E., Kanei-Ishii, C., and Shunsuke, I. 2001. Regulation of cMyb activity by tumor suppressor p53. *Blood Cells, Molecules, and Diseases,* **27:** 479-482.

Timpson, P., and Daly, R.J. 2005. Distinction at the leading edge of the cell. *BioEssays*, **27:** 349-342.

Thomas, G.P., Welch, W.J., Matthews, M.B., and Feramisco, J.R. 1982. Molecular and cellular effects of heat shock and related treatments of mammalian tissue culture cells. *Cold Spring Harbor Symposia on Quantitative Biology*, **46**: 985-996.

Van Why, S.K., Mann, A.S., Ardito, T., Thulin, G., Ferris, S., Macleod, M.A., Kashgarian, M., Siegel, N.J. 2003. Hsp27 associates with actin and limits injury in energy depleted renal epithelia. *Journal of the American Society of Nephrology,* **14:** 98-106.

Verrey, F., Kairouz, P., Schaerer, E., Fuentes P, Geering K, Rossier BC, Kraehenbuhl JP. 1989. *American Journal of Physiology*, **256**: F1034-F1043.

Wang, K. and Spector, A. 1996. α-Crystallin stabilizes actin filaments and prevents cytochalasin-induced depolymerization in a phosphorylation-dependent manner. *European Journal of Biochemistry*, **242:** 56-66.

Watson, K., Dunlop, G., and Cavicchioli, R. 1984. Mitochondrial and cytoplasmic protein syntheses are not required for heat shock acquisition of ethanol and thermotolerance in yeast. *Federation of European Biochemical Sciences (FEBS),* **172:** 299-302.

Wei, Y., Zhao, X., Kariya, Y., Fukata, H., Teshigawara, K., and Uchinda, A. 1994. Induction of apoptosis by quercetin: involvement of heat shock proteins. *Cancer Research*, **54**: 4952-4957.

Westwood, J.T., Clos, J., and Wu, C. 1991. Stress-induced oligomerization and chromosomal relocation of heat-shock factor. *Nature* **353:** 822-827.

Welch, W.J. 1990. The mammalian stress response: cell physiology and biochemistry of stress proteins. In In *Stress Proteins in Biology and Medicine.* (ed. R.I. Morimoto et al.), p.223-278. Cold Spring Harbor Laboratory Press, Cold Spring Harbor, New York.

Welch, W.J. and Suhan, J.P. 1985. Morphological study of the mammalian stress response: characterization of changes in cytoplasmic organelles, cytoskeleton, and nucleoli, and appearance of intranuclear actin filaments in rat fibroblasts after heat-shock treatment. *Journal of Cell Biology*, **101**: 1198-1211.

Wilson, L., Carrier, M.J., and Kellie, S. 1995. pp125FAK tyrosine kinase activity is not required for the assembly of F-actin stress fibers and focal adhesions in cultures mouse aortic smooth muscle cells. *Journal of Cell Science*, **108**: 2381-2391.

Wu, C. (1995). Heat shock transcription factors: structure and regulation. *Annual Review of Cell and Developmental Biology, 11*: 441-69.

Wu, C., Clos, J., Giorgi, G., Haroun, R.I., Kim, S.-J., Rabindran, S.K., Westwood, J.T., Wisniewski, J., and Yim, G. 1994. Structure and regulation of heat shock transcription factor. In *The Biology of Heat Shock Proteins and Molecular Chaperones*, (ed. R.I. Morimoto, Tissières, T., and Georgopoulos, C.), p. 395-416. Cold Spring Harbor Laboratory Press, Cold Spring Harbor, New York.

Wu, B.Y., and Yu, A.C. 2000. Quercetin inhibits c-fos, heat shock protein, and glial fibrillary acid protein expression in injured astrocytes. *Journal of Neuroscience Research,* **62**: 730-6.

Xiao, H., Perisic, O., and Lis, J.T. 1991. Cooperative binding of *Drosophila* heat shock factor to arrays of a conserved 5 bp unit. *Cell*, **64**: 585 – 593.

Yao, K., Rao, H., Wu, R., Tang, X., and Xu, W. 2006. Expression of Hsp70 and Hsp72 in lens epithelial cells in contused eye of rat modulated by thermoresistance or quercetin. *Molecular Vision*, **12:** 445-450.

Yokota, S., Kitahara, M., and Nagata, K. 2000. Benzylidene lactam compound, KNK437, a novel inhibitor of acquisition of thermotolerance and heat shock protein induction in human colon carcinoma cells. *Cancer Research,* **60,** 2942-2948.

Yoo, Y. S., Chung, C., Kim, J.K., and Chang, J.K. 2005. Perinuclear translocation of HSP27 in shear stress exposed human endothelial cells. *Biotechnology Letters*, **27:** 443-448.

Zamir, E., and Geiger, B. 2001. Molecular complexity and dynamics of cell-matrix adhesions. *Journal of Cell Science,* **114**: 3583-3590.

Zeiske W, Atia F, and Van Driessche W. 1998. Apical Cl- channels in A6 cells. *Journal of Membrane Biology*, **166**:169-78.

Zimarino, V., Wilson, S., and Wu, C. 1990. Antibody-mediated activation of *Drosophila* heat shock activator. *Nature,* **327**: 727-730.

Zimarino, V., and Wu, C. 1987. Induction of sequence-specific binding of *Drosophila* heat shock activator. *Nature* **327:** 727-730.

Zhu, Z., and Mivechi, N. 1999. Regulatory domain of human heat shock transcription factor-2 is not regulated by hemin or heat shock. *Journal of Cellular Biochemistry*, **73**: 56-69.

Zhu, D., Tan, K.S., Zhang, X., Sun, A.Y., Sun, G.Y., Lee, J.C. 2005. Hydrogen peroxide alters membrane and cytoskeleton properties and increases intercellular connections in astrocytes. *Journal of Cell Science*, **118**: 3695-3703.